

THE THERMODYNAMIC PROPERTIES OF THE LIQUID
MANGANESE-LEAD AND THE SOLID MANGANESE-IRON SYSTEMS

by

MARTIN WEINSTEIN

B. Metallurgical Engineering
Rensselaer Polytechnic Institute
1957

Submitted in partial Fulfillment of the
Requirements for the Degree of

MASTER OF SCIENCE

at the

MASSACHUSETTS INSTITUTE OF TECHNOLOGY

1959

Signature of Author
Department of Metallurgy
January, 1959

Signature of Professor in
Charge of Research

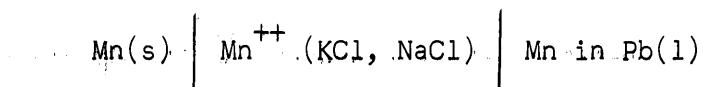
Signature of Chairman
Department Committee on
Graduate Students

.....
.....
.....
.....

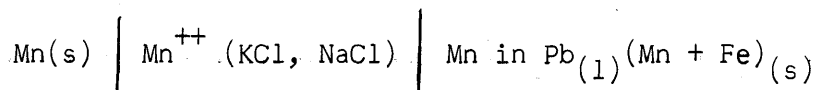
ABSTRACT

An electrode potential study was made to determine the thermodynamic properties of the liquid portion of the manganese-lead system between 800° and 1000°C, and the entire solid manganese-iron system between 750° and 850°C.

In the manganese-lead system the potential measured was between the liquid alloy, contained in a recrystallized alumina crucible, and a pure solid β -manganese casting. The electrolyte used was a eutectic mixture of potassium chloride and sodium chloride with a small trace of manganese chloride. The cell used was:



The method used in the manganese-iron study was slightly different. The solid iron-manganese alloy was immersed in a lead-manganese liquid bath and the potential between the lead-manganese liquid bath and a pure β -manganese casting was measured. The cell used was:



In the manganese-lead system the activities, the excess partial molar free energies of mixing, the partial molar heats of mixing, the partial molar free energies of mixing, the excess molar free energy of mixing, the molar heat of mixing, the excess molar entropy of mixing term, the molar free energy of mixing and the molar entropy of mixing term are reported. The estimated liquidus curve is also presented.

In the manganese-iron system the activities, the excess partial molar free energies of mixing, the partial molar free energies of mixing, the excess molar free energy of mixing and the molar free energy of mixing are reported.

The manganese-lead system shows positive deviation from Raoult's Law. The manganese-iron system shows negative deviation from Raoult's Law.

TABLE OF CONTENTS

<u>Chapter</u>		<u>Page No.</u>
	ABSTRACT	i
	LIST OF FIGURES	v
	LIST OF TABLES	vii
	ACKNOWLEDGEMENTS	viii
I	INTRODUCTION	1
	A. Electromotive Force Measurements	1
	B. Distribution Method	3
II	LITERATURE SURVEY	3
III	PURPOSE AND PLAN OF WORK	4
IV	APPARATUS AND MATERIALS	7
	A. Manganese-Lead Study	7
	1. Cell	7
	2. Cell furnace	7
	3. Vacuum and gas system	10
	4. Cell circuit	12
	B. Manganese-Iron Study	12
	1. Cell	12
	2. Alloy melting apparatus	16
	C. Materials	18
	1. Salts	18
	2. Metals	18
V	EXPERIMENTAL PROCEDURE	21
	A. Manganese-Lead Study	21
	1. Cell assembly	21
	B. Manganese-Iron Study	25
	1. Alloy production	25
	2. Cell assembly	28
VI	RESULTS	33
	A. Sources of Error	33
	1. Reversibility discussion	33
	2. General	35

<u>Chapter</u>		<u>Page No.</u>
	B. The Thermodynamic Properties of the Manganese-Lead System	38
	1. Plots and calculations	38
	2. Discussion of the manganese-lead system	53
	C. The Thermodynamic Properties of the Manganese-Iron System	55
	1. Plots and calculations	55
	2. Discussion of the manganese-iron system	63
VII	GENERAL DISCUSSION	74
VIII	CONCLUSIONS	76
IX	SUGGESTIONS FOR FURTHER STUDY	77
X	BIBLIOGRAPHY	78

Appendicies

I	EXPERIMENTAL DATA OF THE MANGANESE-LEAD SYSTEM	80
II	CALCULATED THERMODYNAMIC PROPERTIES OF THE MANGANESE-LEAD SYSTEM	81
III	CALCULATION OF AMOUNT AND COMPOSITION OF THE MANGANESE-LEAD BATH CHARGE	92
IV	CALCULATION OF THE FINAL COMPOSITION OF MANGANESE-IRON ALLOY AFTER DIFFUSION	94
V	EXPERIMENTAL DATA OF THE MANGANESE-IRON SYSTEM	96
VI	CALCULATED THERMODYNAMIC FUNCTIONS OF THE MANGANESE-IRON SYSTEM	97
VII	DATA AND CALCULATED ACTIVITIES FROM SOLID ELECTRODE CELL	104

LIST OF FIGURES

<u>Figure No.</u>		<u>Page No.</u>
1a	Cell Set-up (Pb-Mn Study)	8
1b	Lead Configuration	8
2	Cell Furnace	11
3	Vacuum and Gas System	13
4	Cell Circuit and Control Circuit	9
5	Alloy Melting Apparatus	14
6	Cell Set-up (Mn-Fe Study)	15
7	Crucible Assembly (Mn-Fe Study; $X_{\text{Mn}} = 0.8$)	17
8	Electrode Melting Apparatus	22
9	Electrolyte Transfer Tube	31
10	Sampling Apparatus	31
11	The Potential vs. Temperature Plot for the Manganese-Lead System	36
12	The Potential vs. Temperature Plot for the Manganese-Lead System	37
13	The Temperature Coefficient of Electro- motive Force for the Manganese-Lead System at 980°C	39
14	The Activity Coefficient Function of Manganese in the Manganese-Lead System at 980°C	40
15	The Free Energy Function of Manganese in the Manganese-Lead System at 980°C .	43
16	The Excess Partial Molar Free Energy of Mixing for Manganese and Lead in the Manganese-Lead System at 980°C	44

<u>Figure No.</u>		<u>Page No.</u>
17	The Partial Molar Free Energy of Mixing of Manganese and Lead in the Manganese-Lead System at 980°C	45
18	The Heat of Mixing Function of Manganese in the Manganese-Lead System at 980°C	46
19	The Partial Molar Heat of Mixing for Manganese and Lead in the Manganese-Lead System at 980°C	47
20	The Total Excess Molar Properties of the Manganese-Lead System at 980°C	49
21	The Total Molar Properties of the Manganese-Lead System at 980°C	50
22	The Activity of Manganese and Lead in the Manganese-Lead System at 980°C.....	51
23	The Activity of Manganese vs. X_{Mn} from 750° to 1000°C	52
24	Estimation of Portion of Liquidus Curve for the Manganese-Lead System	54
25	Diffusion Curve (emf vs. time) from Mn-Fe Study; $X_{Mn} = 0.365$	56
26	The Activity Coefficient Function of Manganese in the Manganese-Iron System in the Temperature Range 750°-850°C ...	57
27	The Activity Coefficient of Manganese in the Manganese-Iron System vs. X_{Mn} at 800°C (standard state $a_{\beta_{Mn}} = 1, a_{\gamma_{Fe}} = 1$)..	59
28	The Activity Coefficient of Manganese in the Manganese-Iron System at 800°C (standard state $a_{\beta_{Mn}} = 1, a_{\gamma_{Fe}} = 1$)	61
29	The Activity Coefficient Function of Manganese in the Manganese-Iron System at 800°C (standard state $a_{\beta_{Mn}} = 1, a_{\gamma_{Fe}} = 1$).	62

<u>Figure No.</u>		<u>Page No.</u>
30	The Excess Partial Molar Free Energy of Mixing of Manganese and Iron in The Manganese-Iron System at 800°C (standard state $a_{\beta_{Mn}} = 1, a_{\gamma_{Fe}} = 1$)	64
31	The Excess Partial Molar Free Energy of Mixing of Manganese and Iron in The Manganese-Iron System at 800°C (standard state $a_{\beta_{Mn}} = 1, a_{\gamma_{Fe}} = 1$)	65
32	The Partial Molar Free Energies of Mixing of Manganese and Iron in The Manganese-Iron System at 800°C (standard state $a_{\beta_{Mn}} = 1, a_{\gamma_{Fe}} = 1$)	66
33	The Partial Molar Free Energy of Mixing of Manganese and Iron in The Manganese-Iron System at 800°C (standard state $a_{\beta_{Mn}} = 1, a_{\alpha_{Fe}} = 1$)	67
34	The Total Excess Molar Free Energy of Mixing and the Total Molar Free Energy of Mixing of the Manganese-Iron System at 800°C (standard state $a_{\beta_{Mn}} = 1, a_{\gamma_{Fe}} = 1$).	68
35	The Total Excess Molar Free Energy of Mixing and the Total Molar Free Energy of Mixing of the Manganese-Iron System at 800°C ($a_{\beta_{Mn}} = 1, a_{\alpha_{Fe}} = 1$)	69
36	The Activity of Manganese and Iron in the Manganese-Iron System at 800°C (standard state $a_{\beta_{Mn}} = 1, a_{\gamma_{Fe}} = 1$)	70
37	The Activity of Manganese and Iron in the Manganese-Iron System at 800°C (standard state $a_{\beta_{Mn}} = 1, a_{\alpha_{Fe}} = 1$)	71
38	Schematic Manganese-Iron-Lead Ternary Phase Diagram	91

LIST OF TABLES

<u>Table No.</u>		<u>Page No.</u>
I	Impurities in Electrolyte Materials ...	19
II	Analyses of Metals	20

ACKNOWLEDGEMENTS

The author wishes to express his appreciation to:

Professor John F. Elliott, who acted as project supervisor and offered invaluable guidance and encouragement;
Mr. Frank Haynes, who offered much assistance in the solving of experimental problems;

Mr. Don Guernsey for chemical analysis of the electrodes, electrolytes and pure metals;

Mr. James Colgate and the Watertown Arsenal Staff for help in rolling the metal alloy coils;

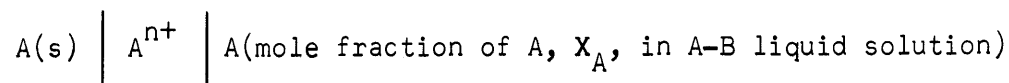
The United States Atomic Energy Commission, who sponsored this study under Contract AT(30-1)-1888;

Mr. Thomas C. Wilder for his unselfish help in the setting up of experiments.

I. INTRODUCTION

A. Electromotive Force Measurements

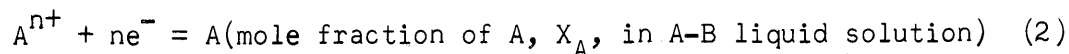
Electromotive force studies of liquid metal solutions are made by setting up a reversible cell of the type:



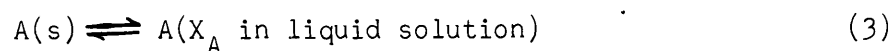
where A and B are metals of which A is the more electropositive and A^{n+} is an electrolyte containing ions of A of valence n. The reaction at the anode is:



The reaction at the cathode is:



The reaction in the cell is then,



The measured potential difference or electromotive force of such a reversible cell at a given temperature is a measure of the free energy change of the cell reaction. Experimentally, reversibility may be assumed if the weight of electrodes remains the same and if the electromotive force versus temperature are reproducible on both heating and cooling. Thus, if no work other than electrical work is done, the partial molar free energy of mixing of A for the cell reaction (3) can be given by

$$F_A^M = F_A - F_A^{\circ} = - n \int \mathcal{E} \quad (4)$$

where \bar{F}_A is the partial molar free energy of A in solution, F_A° is the molar free energy of pure liquid A, n is the valence of A in the electrolyte, \mathcal{E} is the reversible electromotive force and \mathcal{f} is the Faraday equivalent, (23,066 cal/volt). If the pure solid is selected as the standard state, the activity of A, (a_A), in the solution is given by

$$F_A^M = - n \mathcal{f} \mathcal{E} = RT \ln a_A \quad (5)$$

where R is the gas constant and T is the absolute temperature.

Thus, by making electromotive force measurements with a cell of the above type, using various mole fractions of the components, A and B, the activity of the more electropositive metal in each case can be determined over the entire composition range. Also, if the electromotive force values are obtained over a sufficiently wide temperature interval to establish the slope of the electromotive force versus temperature curve, $d\mathcal{E}/dT$, the enthalpy or heat content can be calculated from the Gibbs-Helmholtz equation:

$$H_A^E = - n \mathcal{f} \left[\mathcal{E} - T \frac{d\mathcal{E}}{dT} \right] \quad (6)$$

where H_A^E is the excess partial molar heat of mixing of A.

With the use of the Gibbs-Duhem equation and a graphical integration technique, similar properties may be obtained for the constituent B.

For a given binary metal system to be amenable to studies by electromotive force techniques, the free energy of formation per equivalent of the two metals must be far enough apart to give a potential measurement which can be assigned to the reaction being studied, an electrolyte containing only one kind of ion of the more

electropositive metal must be available, and a suitable vessel to withstand the high temperatures while under the particular pressure or vacuum must be available. Reactions between any of the experimental equipment and the metal system should be absent.

B. Distribution Method

When a substance is soluble in each of two immiscible liquids, it will distribute itself between the two phases. At equilibrium it will have the same activity in both phases. This concept has been applied to the distribution of manganese between iron and lead in the present study. The solubility of iron in lead is extremely low at the temperatures investigated.

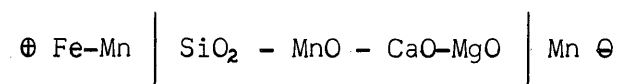
II. LITERATURE SURVEY

Taylor⁽¹⁾ was the first to use a concentration cell at elevated temperatures, (300° - 600°C), to study liquid, binary alloys.

Subsequently, many studies have been made on various liquid and solid metallic solutions. Summaries of many of these studies are reported by Chipman and Elliott,⁽²⁾ Wagner,⁽³⁾ and Kubaschewski and Evans.⁽⁴⁾

A survey of the published literature since 1900 showed that no previous work, other than the preliminary work of Harman,⁽⁵⁾ had been done on activity measurements in the manganese-lead system.

Sanbongi and Ohtani⁽⁶⁾ used an electrode potential measurement to determine the activity of manganese in liquid iron-manganese solutions. The electromotive force corresponding to a change in the manganese content in iron was measured by the use of the concentration cell,



The iron-manganese binary liquid solution at $1590^{\circ} \pm 5^{\circ}$ was found to be approximately ideal over the entire composition range. Iron-nickel and iron-cobalt binary solutions were also found to follow Raoult's Law.

McCabe⁽⁷⁾ determined activities in the solid manganese-iron system at 1232°K . He used the Knudsen effusion method to determine the vapor pressure of manganese over solid manganese-iron alloys. The solid manganese-iron system showed negative deviations from ideality. Further discussion of the results of this vapor pressure measurement is given in a subsequent section.

III. PURPOSE AND PLAN OF WORK

In order to increase the available thermodynamic data of liquid metal solutions, it was planned to make an electromotive force study of the liquid manganese-lead system. It was proposed to determine if accurate measurements could be made up to 1000°C . This had been investigated by Harman,⁽⁵⁾ but there was some possibility that reversibility was not achieved in all his cells and the manganese used was not highly pure.

The cell was to consist of four recrystallized alumina crucibles in a single alumina crucible. These would be housed in an 18 inch Vycor tube. The contact leads were to be tungsten. The high purity manganese buttons were to be suspended above the small crucibles. The electrolyte to be used consisted of a eutectic mixture of sodium chloride and potassium chloride, and 5 percent manganese chloride.

It was planned to use a resistance furnace with silocel packing in an aluminum jacket. Dry argon was to be passed continuously over the cell during its operation.

The cell potentials were to be measured with a Rubicon potentiometer, Catalog No. 2732.

The manganese buttons were proposed to be cast in small alumina crucibles. The melting would take place under an argon flush. A molybdenum susceptor was to be used in conjunction with an induction furnace.

To obtain the activity of manganese and iron in the solid manganese-iron system in the temperature range 750° - 850°C, a combination distribution and electromotive force measurement was to be set-up.

The manganese-iron alloys were to be melted under hydrogen and argon. Rods would be suctioned up from the melt in Vycor tubes by means of an aspirator bulb. These rods would then be rolled into thin strips which were to be coiled. These coils were then to be placed in an alumina crucible and manganese-lead alloys were to be melted over them. Tungsten leads and the same electrolyte proposed for the manganese-lead study were to be used.

It was proposed to measure the potential between the liquid manganese-lead bath and a solid pure β -manganese electrode. At equilibrium, this potential would give a measure of the activity of manganese in both the liquid manganese-lead bath and the solid manganese-iron alloy.

The data itself would be of value in the fields of diffusion,⁽⁸⁾ oxidation,⁽⁹⁾ nucleation⁽¹⁰⁾ and the martensite transformation.⁽¹¹⁾

The method, if successful, would increase the number of systems which could be investigated by electromotive force measurements. It was assumed that the manganese-lead liquid bath above the manganese-iron alloy would act as a barrier to the flow of iron, the less electropositive constituent of the electrolyte. This would eliminate, for the most part, the reaction between the ion of the more electropositive constituent, manganese, in the electrolyte and the less electropositive constituent, iron.

It was assumed that the problem of slow diffusion involved in electrode potential measurements which use solid alloys welded directly to contacts would also be eliminated. When balancing a potentiometer, a slight amount of current necessarily is drawn. This will cause an actual mass transfer of manganese. With a solid electrode, diffusion back to the equilibrium concentration will be slow so polarization may disrupt the reversibility of the cell. With a liquid solution electrode, however, the diffusion of manganese will be rapid and the equilibrium concentration will be reattained almost immediately.

IV. APPARATUS AND MATERIALS

A. Manganese - Lead Study

1. Cell

The cell assembly used is shown in Figure 1. It consisted of an 18 inch long, large Vycor tube, which was sealed with a water-cooled brass head. Four recrystallized alumina crucibles (F), which contained the liquid alloy electrodes, were placed into a larger alumina crucible (H). Above the small electrode crucibles, the two pure β - manganese buttons (E) were suspended. In the center of the four small alumina crucibles was placed a Vycor thermocouple protection tube (I) which contained the chromel-alumel thermocouple. Above this entire assembly, a large porcelain positioning crucible (D) was placed. The six contacts (C) were 0.036 inch diameter tungsten wires. The tungsten wires were encased in alumina protection tubes. The configuration, used for the contacts, (Figure 1-b), insured good contact between the liquid metal and the tungsten lead.

The brass head (A), had eight portholes with rubber tubing seals arranged in a circle for the six tungsten lead protection tubes and a gas inlet and outlet. A central hole and rubber seal was provided for the chromel-alumel thermocouple. The brass head had a water-cooled copper tube around its circumference.

2. Cell Furnace

A schematic drawing of the furnace used in this investigation is shown in Figure 2. The convoluted furnace tube (A),

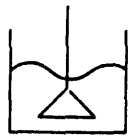
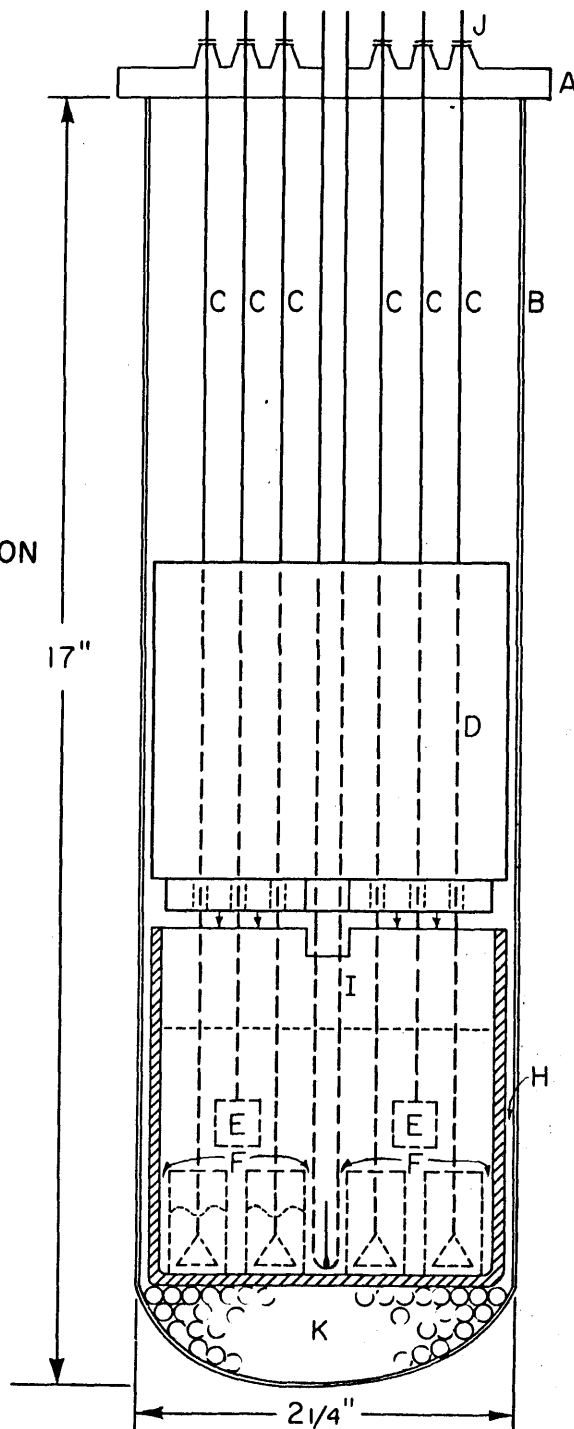


FIG. 1b
LEAD
CONFIGURATION



- A - Water Cooled Brass Furnace Head
- B - Vycor Furnace Tube
- C - Tungsten Lead with Alumina Protection Tube
- D - Porcelain Positioning Crucible
- E - Pure Manganese Buttons
- F - Alumina Electrode Crucibles (5/8" I.D. x 1")
- G - Electrolyte (KCl-NaCl-MnCl₂)
- H - Large Alumina Crucible (2" O.D. x 3")
- I - Vycor Thermocouple Protection Tube (7mm)
- J - Rubber Tube Seal with Pinch Clamp
- K - Alumina Beads

FIG. 1a CELL SET-UP (Pb-Mn STUDY)

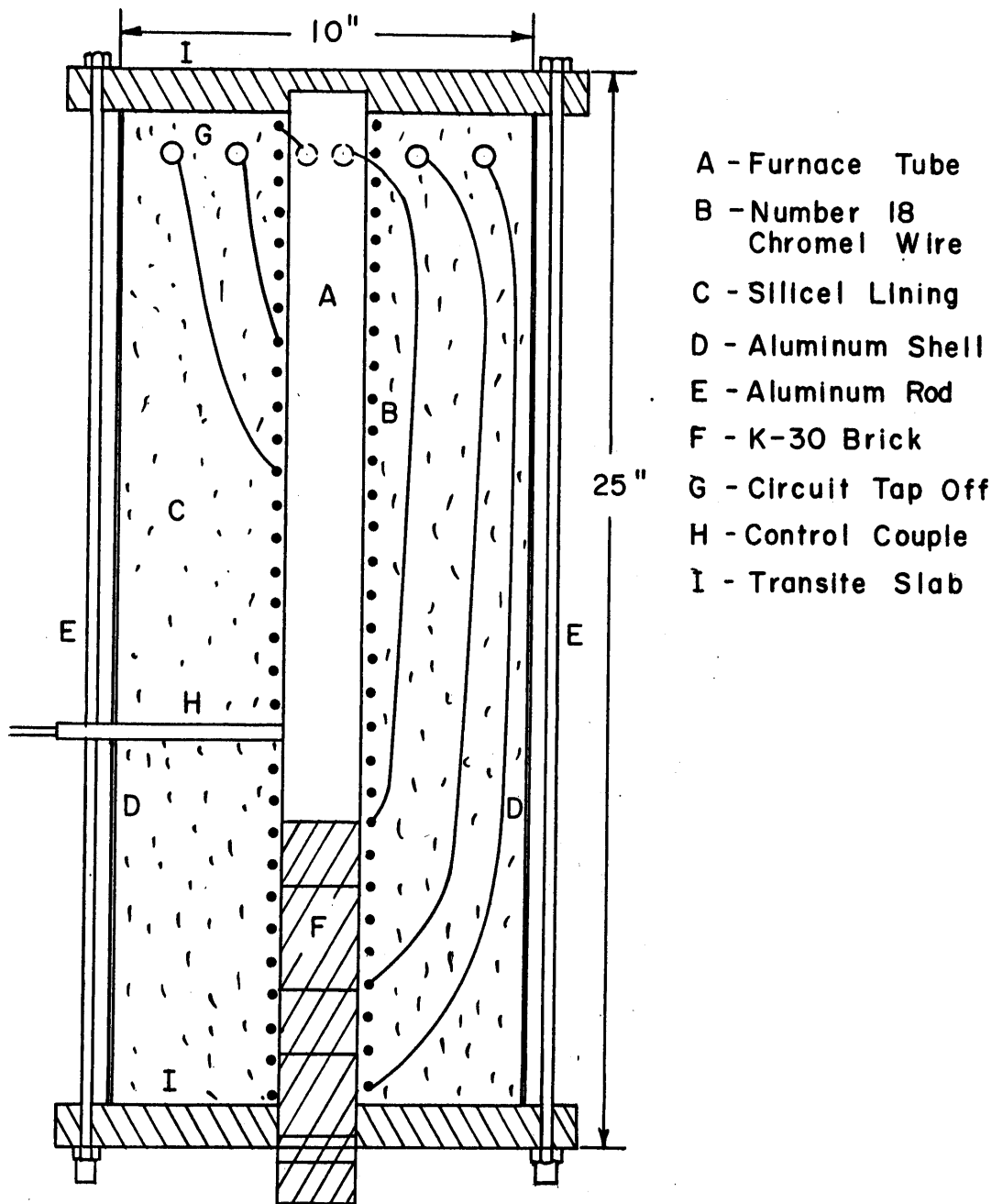


FIG. 2 CELL FURNACE

(Norton Company), which houses the cell was wound with number 18 chromel wire and had a total resistance of 30 ohms. Taps (G) were located at convenient intervals for control of the heat distribution. The space between the wound tube and the aluminum furnace shell was filled with silocel. Transite ends closed the furnace and held the furnace tube in position by means of grooves provided in the transite. The two transite ends were then connected by four aluminum tie rods. The assembly was allowed to rest vertically on the floor and was supported by angle iron feet attached to one end. The cell tube, when in the furnace, was held in position by K-30 brick (F).

Power was supplied to the furnace from a V20HM Variac, (General Radio), which was connected to a 115 volt source. Temperature control was obtained by having a Minneapolis Honeywell Controller, (Brown Electronik Indicator with Micro Switch Control, 0-1200°C), connected to the furnace circuit. The control couple (H) for this unit was located in the furnace as close as possible to the position where the crucibles in the cell were located.

3. Vacuum and Gas System

Figure 3 is a schematic diagram of the vacuum and gas system used. The argon used was the welding grade manufactured by Air Reduction Company. The copper gauze in the gas train was kept at 500°C by a small resistance furnace. Calcium chloride was used in the drying towers.

The vacuum was provided by a Duo Seal Vacuum Pump, (Welch Company). A manometer was used to measure the gas pressure

- A - Argon Tank
- B - Needle Valve
- C - Stopcock
- D - Bubbler
- E - Drying Tower
- F - Copper Furnace
- G - Manometer
- H - Cell Tube
- I - Vacuum Trap
- J - Vacuum Pump

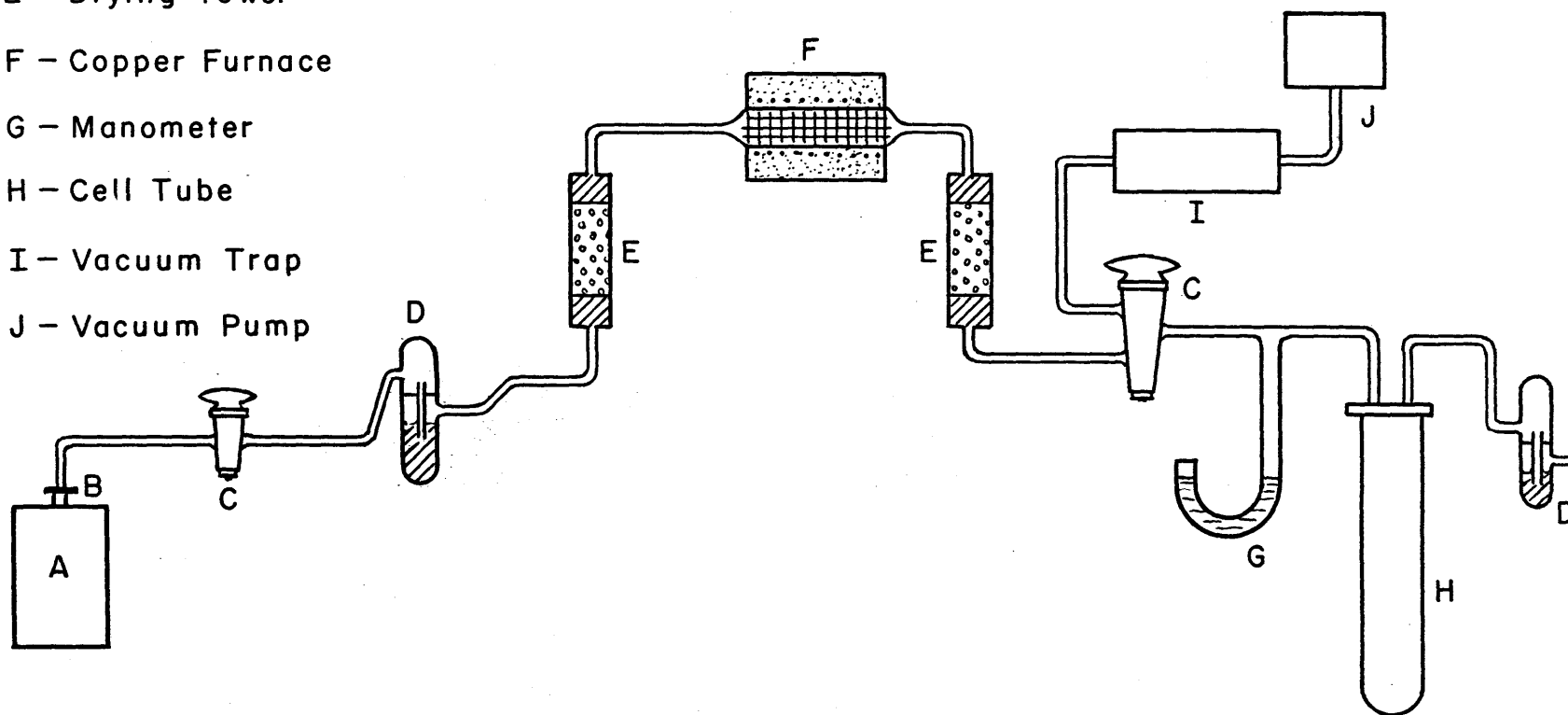


FIG. 3 VACUUM AND GAS SYSTEM

or vacuum in the system.

4. Cell Circuit

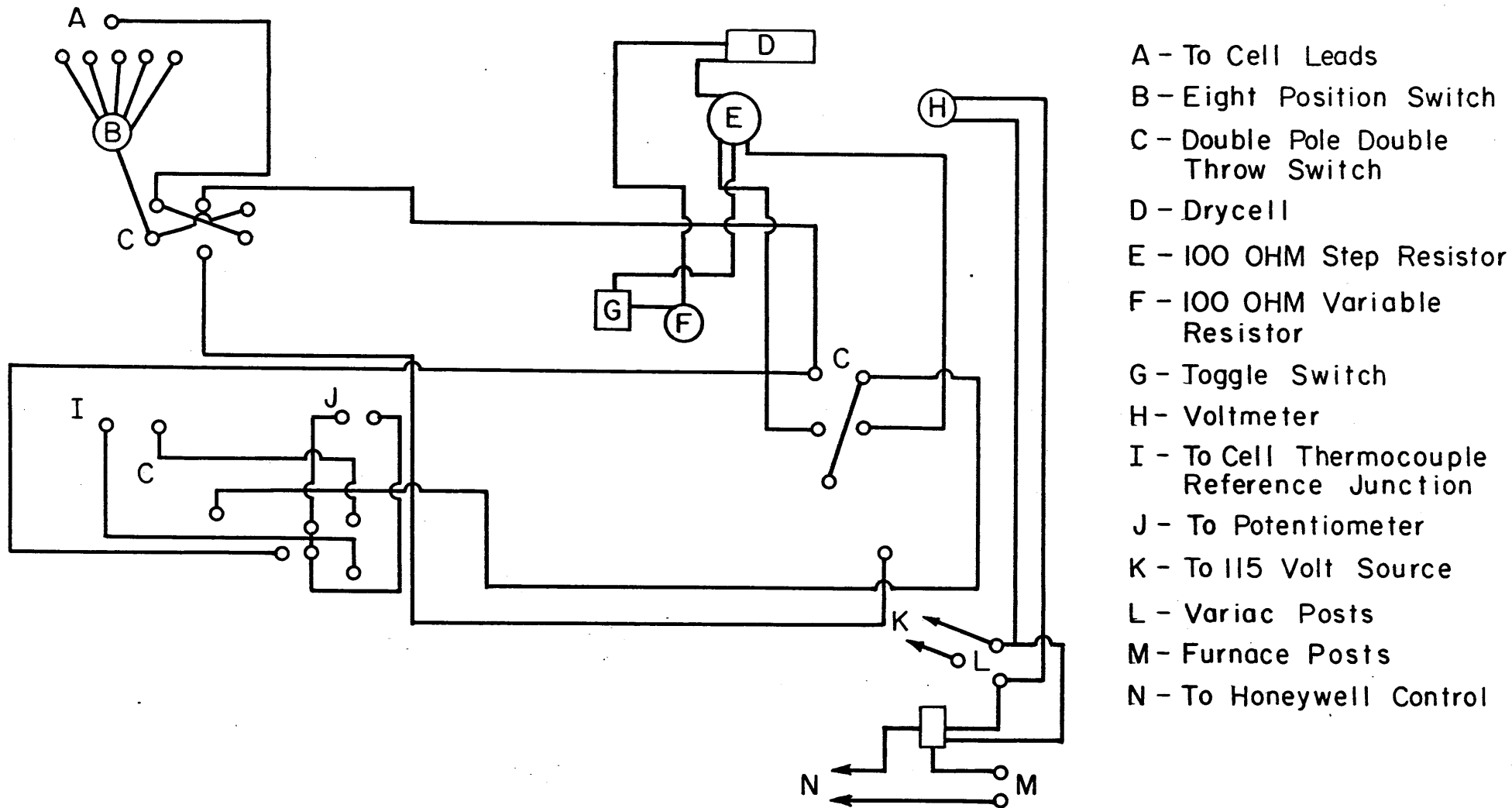
The circuit for measuring potentials of the cell electrodes and thermocouple is shown in Figure 4. The potentiometer used was a Rubicon, (Serial No. 907699). This circuit allowed the use of back potential when potentials rose over 140 millivolts. All wires in the circuit were copper except for the tungsten leads.

B. Manganese-Iron Study

1. Cell

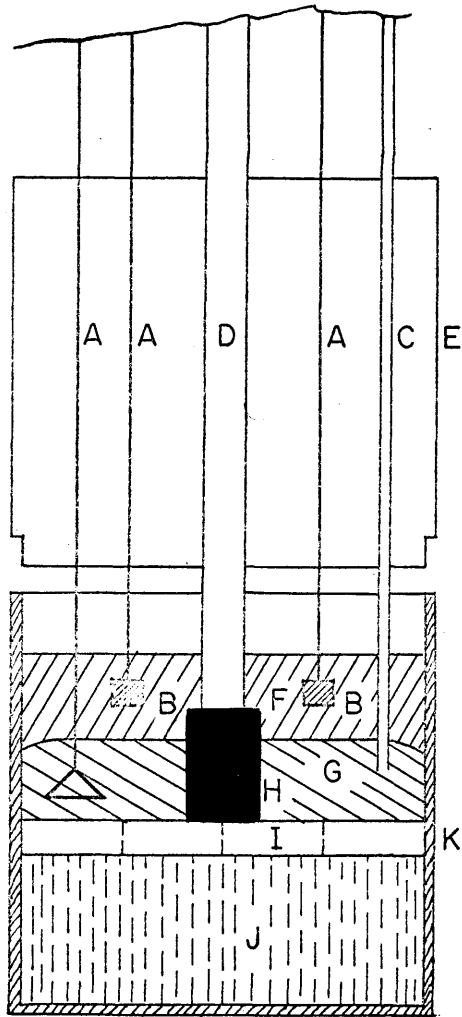
The cell assembly used in the composition range from 20 atomic percent manganese to 60 atomic percent manganese is shown in Figure 5. The large Vycor tube and the brass head were the same as were used in the manganese-lead study. The large alumina crucible, porcelain positioning crucible, tungsten leads, porcelain protection tubes, thermocouple and thermocouple protection tubes were also similar to the ones used in the manganese-lead study. The thermocouple protection tube (D) was placed into a small alumina crucible (H) which was subsequently placed on top of an alumina web (I). This assembly held the manganese-iron alloy coil (J) down below the electrolyte. A quartz quill Figure 10 (D) with a tuberculin syringe (A) was used as the sampling apparatus.

Since ductile coils could not be produced with the 80 atomic percent manganese-iron alloy, the cell crucible assembly shown in Figure 6 was used. Four small crucible set-ups as



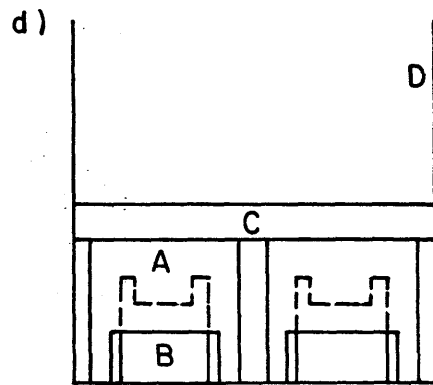
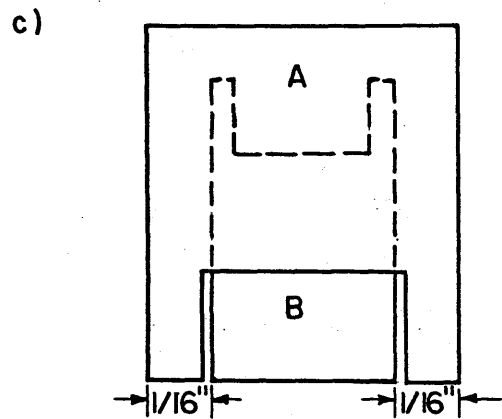
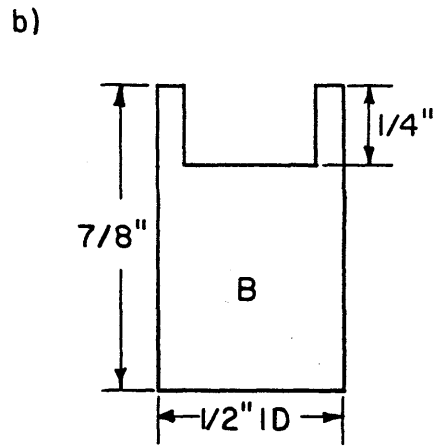
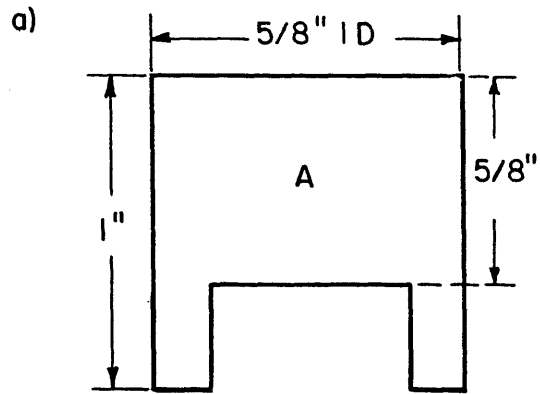
- A - To Cell Leads
- B - Eight Position Switch
- C - Double Pole Double Throw Switch
- D - Drycell
- E - 100 OHM Step Resistor
- F - 100 OHM Variable Resistor
- G - Toggle Switch
- H - Voltmeter
- I - To Cell Thermocouple Reference Junction
- J - To Potentiometer
- K - To 115 Volt Source
- L - Variac Posts
- M - Furnace Posts
- N - To Honeywell Control

FIG. 4 CELL CIRCUIT AND CONTROL CIRCUIT



- A - Tungsten Lead with Alumina Protection Tube
- B - Pure Manganese Button
- C - Quartz Sampling Tube
- D - Vyor Thermocouple Protection Tube
- E - Porcelain Positioning Crucible
- F - Electrolyte (KCl-NaCl-MnCl_2)
- G - Lead-Manganese Bath
- H - Small Alumina Crucible (1/2" ID x 7/8" long)
- I - Alumina Sheet
- J - Fe-Mn Coil
- K - Alumina Crucible (2" OD x 3")

FIG. 5 CELL SET-UP (Mn-Fe STUDY)



A,B,D- Alumina
Crucible
C- Alumina
Sheet

FIG. 6 CRUCIBLE ASSEMBLY (Mn-Fe Study; XMn=.8)

shown in Figure 6(c) were placed on the bottom of the large alumina crucible and an alumina web (C) was placed on the entire assembly. The manganese-iron alloy, in the form of a powder, was placed into the crucible shown in Figure 6(b). The rest of the cell set-up was entirely the same as used in the study of the other manganese-iron alloys.

The cell furnace, vacuum system, gas train, and cell circuit were the same as those used in the manganese-lead study.

2. Alloy Melting Apparatus

The manganese-iron alloy melting apparatus is shown in Figure 7. It consisted of a fused silica furnace tube (D) sealed with a water-cooled brass head (C). The head included an open-close valve which made possible the taking of a sample without opening the system to the atmosphere. A large alumina crucible (J) contained the melt. Around the crucible was a molybdenum susceptor (I) and around the susceptor was a K-30 brick protection cup. Above the alumina crucible was a K-30 brick cover with a porcelain tube (P) in its center. This porcelain tube acted as the entrance channel for the sampling tube. The lower surface of the cover had a thin layer of water glass (F) spread over it. The entire crucible assembly rested on a K-30 brick, an alundum sheet (K) and K-30 brick dust (L) in that order.

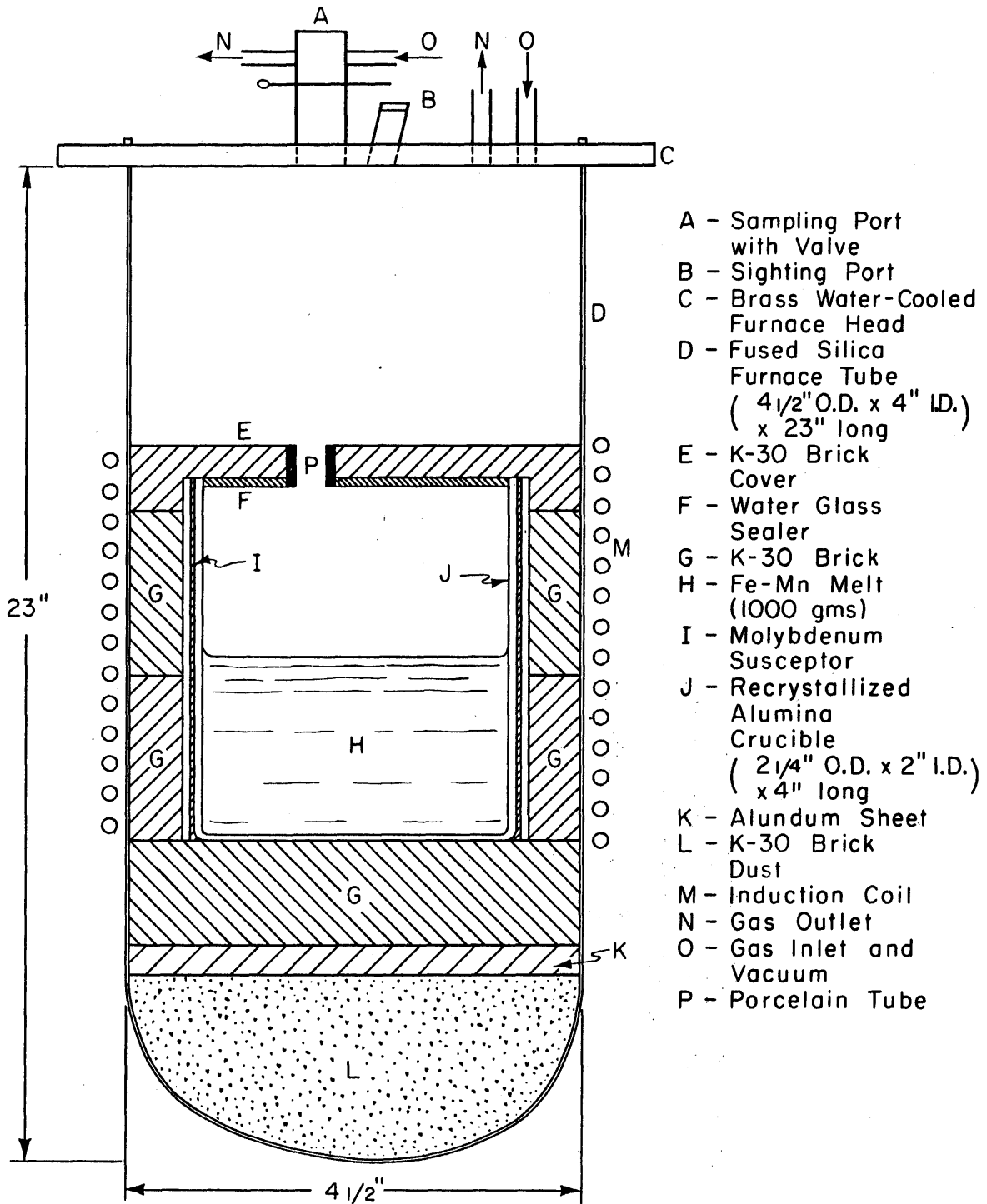


FIG. 7 ALLOY MELTING APPARATUS

B. Materials

1. Salts

The manganese chloride, potassium chloride and sodium chloride used in making up the electrolyte were all Mallinckrodt Analytical Reagent Grade. The lot analysis of each is given in Table I.

2. Metals

The manganese used was an electrolytic high-purity grade acquired from the Electromet Company. The manganese was pickled in nitric acid, washed in distilled water, washed with acetone and then dried. The lead used was supplied by American Smelting and Refining Company. The lead oxide film was removed with a wire brush before the lead was put into use. The iron used was electrolytic grade acquired from Plastic Metals Company. The iron was hydrogen reduced before being used. The analysis of each metal is given in Table II.

TABLE I

IMPURITIES IN ELECTROLYTE MATERIALS (LOT ANALYSES)

<u>Impurity</u>	<u>MnCl₂</u>	<u>NaCl</u>	<u>KCl</u>
Ba	-	0.001*	0.001*
Chlorate	-	0.001	0.001
Heavy Metals	0.0005*	0.0005	0.0005
Insoluble Matter	0.005	0.005	0.005
Iodide	-	0.002	0.002
Fe	0.0005	0.0003	0.0002
NO ₃	-	0.003	0.003
PO ₄	-	0.0005	0.0005

* All values are reported in weight percent.

TABLE II

ANALYSIS OF METALS (LOT ANALYSES)

<u>Impurity</u>	<u>Mn(99.9 + %)</u>	<u>Pb(99.99 + %)</u>	<u>Fe(99.84%)</u>
Al	-	-	0.002*
Bi	-	0.0008*	-
C	0.007*	-	0.018
Co	-	-	0.007
Cr	-	-	0.002
Cu	-	0.0003	0.008
Fe	0.01 or less	0.0002	-
Mn	-	-	0.002
Mo	-	-	0.002
Ni	-	-	0.008
O	-	-	0.008
P	-	-	0.002
S	-	-	0.004
Si	0.004	-	0.007
Sn	-	-	0.005
V	-	-	0.003

* All values in weight percent.

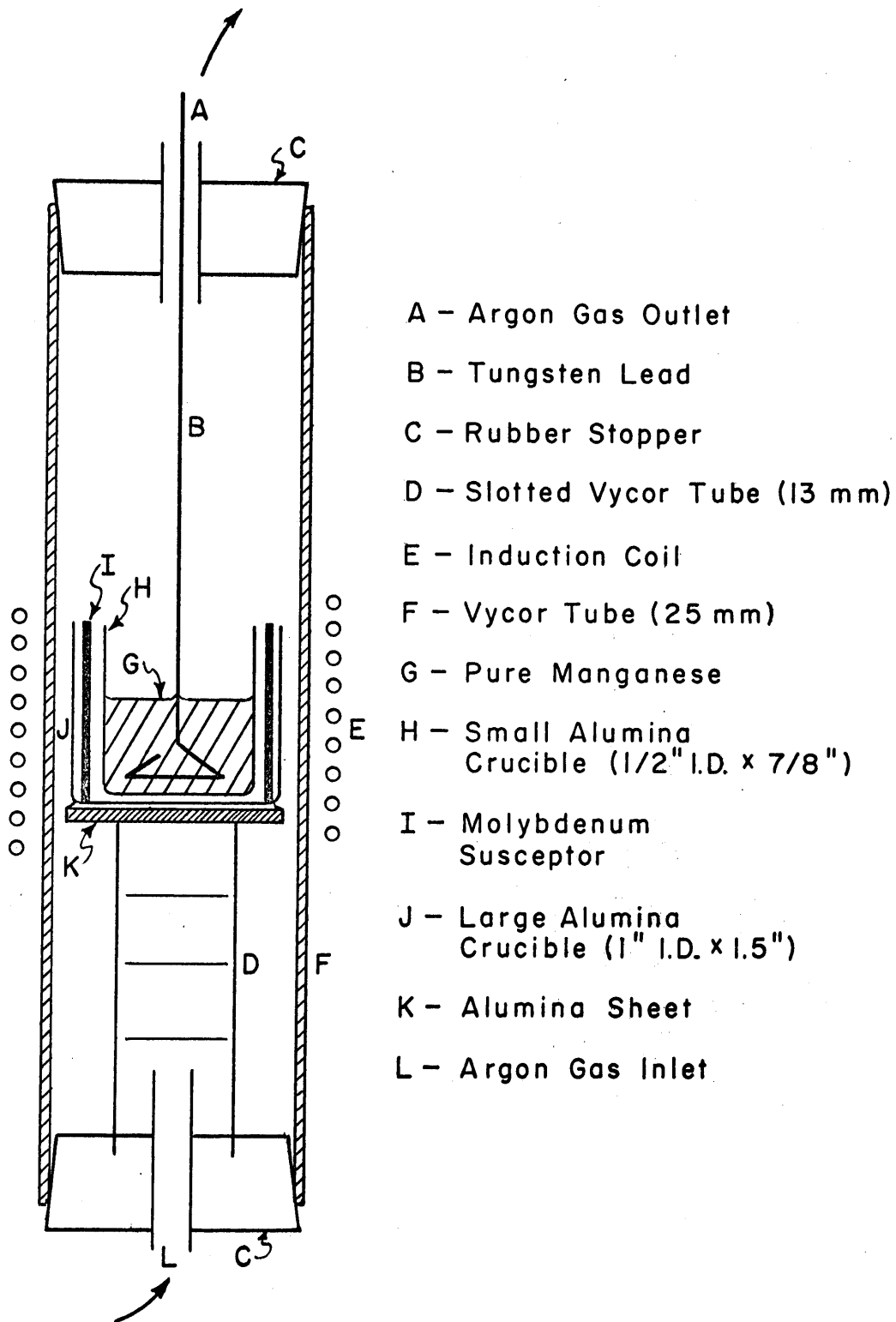
V. EXPERIMENTAL PROCEDURE

A. Manganese-Lead Study

1. Cell Assembly

Before a run all of the Vycor tubes, alumina crucibles, alumina protection tubes and other cell materials which would be in contact with the alloys and electrolyte were cleaned in nitric acid, distilled water and acetone. They were then placed into a drying oven at 140°C overnight. The tungsten leads were cleaned with emery paper and then washed with acetone before being bent into the configuration shown in Figure 1 - b.

Since manganese is solid in the temperature range under study, (750° - 1000°C), the apparatus in Figure 8 was used to cast solid manganese buttons around the tungsten leads. The manganese, after being pickled in nitric acid, washed in distilled water, and washed in acetone, was placed in the small alumina crucible (H). The alumina crucible was then placed inside the molybdenum susceptor (I) which was contained in the large alumina crucible (J). This crucible assembly was then placed into the Vycor tube which was set inside the induction coil. The tungsten lead (B) was then placed into the small crucible and the upper stopper (C) was set into place. The system was then flushed with argon for 10 minutes. Then the induction coil was activated. When the metal became molten the tungsten lead was pushed down into the melt. The



- A - Argon Gas Outlet
- B - Tungsten Lead
- C - Rubber Stopper
- D - Slotted Vycor Tube (13 mm)
- E - Induction Coil
- F - Vycor Tube (25 mm)
- G - Pure Manganese
- H - Small Alumina Crucible (1/2" I.D. x 7/8")
- I - Molybdenum Susceptor
- J - Large Alumina Crucible (1" I.D. x 1.5")
- K - Alumina Sheet
- L - Argon Gas Inlet

FIG. 8 ELECTRODE MELTING APPARATUS

metal was kept molten for 10 minutes to insure good wetting of the tungsten lead. The melt was then slowly cooled in order to achieve the least strained structure possible. It was found that if cooled too quickly, the manganese casting would develop hairline cracks. Cooling took place under an argon atmosphere as did the heating cycle. Good buttons were obtained after slow cooling of the castings was employed. These castings were used in the cell as the standard manganese electrodes.

Thirty hours before the cell was to be assembled, 200 grams of electrolyte was prepared and placed in a 45 millimeter Vycor tube. The electrolyte composition was 42 weight percent sodium chloride, 53 weight percent potassium chloride, and 5 weight percent manganese chloride. The tube of electrolyte was sealed with a water-cooled brass head and put into an auxiliary resistance furnace at 700°C. The electrolyte was fused under vacuum and held that way until the cell was ready to be assembled.

The electrodes were then prepared. The alloys were weighed out to one ten-thousandth of a gram on an Ainsworth Analytical balance and placed in the alumina crucibles. The four alloy crucibles were then arranged in the bottom of the large alumina crucible. The brass head was placed on a ring stand above the crucibles and the prepared tungsten leads in the alumina sheathing were drawn through the holes of the porcelain positioning crucible and then through the port holes

of the head. The leads were then placed in contact with the alloys. The pure β - manganese standard electrodes were suspended above the small alumina crucibles. The thermocouple protection tube was then placed through the brass head, through the positioning crucible and into the space between the four alloy crucibles.

As soon as the entire crucible assembly was completed, the molten electrolyte was transferred from the Vycor tube to the cell crucible by means of the suction apparatus shown in Figure 9. Before being placed into the molten salt the Vycor transfer tube was heated to white heat by torch so that the salt would not freeze on it. When the transfer tube was in the salt, suction was applied to the mouthpiece (D) and salt was drawn up into the tube. This salt was then poured into the cell crucible. The salt quickly froze around the cell leads and crucibles. The entire assembly was then placed into the large Vycor furnace tube. The vacuum lines were then attached and the cell was evacuated to 10 millimeters of mercury for 20 minutes. After this period, a positive gage pressure of 30 millimeters of mercury was obtained with an argon atmosphere.

The cell was then transferred to the resistance furnace and brought up to the lowest temperature to be investigated. As soon as the cell attained a temperature of 700°C, the pinch clamps on the rubber tube seals were loosened and the tungsten leads were pushed into the liquid electrodes. The copper lead wires were then attached to the tungsten cell leads, the pinch

clamps tightened, and the cold junction filled with ice. The cell was allowed to equilibrate over night. In the morning the first readings were taken. Readings of temperature and potential were taken over an hour period or longer. Constant potentials were generally acquired after two hours from the time the temperature was changed. The temperature was increased and decreased so that a plot of potential versus temperature could be acquired. The potential difference between standard electrodes was about 0.15 millivolts in the lower range of temperatures and about 0.05 millivolts in the higher range of temperatures. Moving the leads in the crucibles gave no change in the potential readings. The runs usually lasted two or three days.

In some cells the leads were removed and the alloys weighed to one ten-thousandth of a gram. It was found that no measurable weight change was obtained. This meant that no measurable metal transfer was going on in the cell. The steady potentials also seemed to show the cell was reversible.

B. Manganese-Iron Study

1. Alloy Production

The manganese-iron alloys were melted in the apparatus shown in Figure 7. The recrystallized alumina crucible was filled with 454 grams of iron and manganese particles, weighed to the alloy composition desired. The entire crucible assembly was then placed into the furnace tube and the water-cooled brass

head was set in place. The system was then evacuated over night. In the morning, the induction coil was activated and melting was started. The melting initially took place under a hydrogen atmosphere. The hydrogen was first passed through a "deoxo" unit of palladized alundum pellets which removed the oxygen and then through a series of drying towers and bubblers.

The metal was allowed to remain molten for one-half hour before the system was purged with dry, pure argon. After one-half hour a Vycor tube, (16 mm), connected by a rubber tube to a glass bulb which contained the iron-manganese charge, was placed through the rubber gasket seals in the sampling port. The top section of the sampling port was then evacuated. After a few minutes, the top section of the sampling port was repressurized with argon. The valve of the sampling port was then opened and the Vycor charging tube was pushed down through the hole in the K-30 brick cover. When the charging tube was about one inch above the melt surface, the balance of the charge was added. This was accomplished by slowly raising the glass bulb into a vertical position. The charge was added slowly so as not to crack the alumina crucible. It took approximately two hours to charge 454 grams of metal. As soon as the charging of metal was completed the Vycor charging tube was removed, the sampling port valve was closed and hydrogen was again passed over the melt. Temperature measurements were then made with an optical pyrometer to insure that the temperature was not more than 200°C above the liquidus temperature.

After one hour the hydrogen atmosphere was again replaced by argon. Argon was allowed to purge the system for fifteen minutes. A Vycor tube, (9-mm), with an aspirator bulb attached to one end was then placed through the rubber seals in the sampling port. The top section of the sampling port was then evacuated. After a few minutes the top section was repressurized with argon. The valve of the sampling port was then opened and the Vycor sampling tube was pushed down into the melt. An eight inch sample of metal was then pulled up into the Vycor tube with the help of the aspirator bulb. The Vycor tube was then slowly raised out of the hot zone and allowed to cool in the furnace before being brought through the rubber gaskets in the sampling port.

After the rod cooled, its surface was ground down to remove all the glass that had adhered to it. The rods in the composition range, $X_{Mn} = 0$ to $X_{Mn} = 0.60$, were then pickled in concentrated sulfuric acid and an organic inhibitor. After removal of the piped section, the rods were hot rolled to 0.035" in one pass. This was accomplished by placing the rod in a furnace for five minutes at 1000°C and then quickly placing the rod under an almost tight-closed rolling mill. The 0.035" thick sheets were pickled again in concentrated sulfuric acid and an organic inhibitor to remove the oxide crust formed on hot rolling. The sheets were then cleaned in distilled water and acetone. The remaining oxide film was removed with a clean wire brush. The

clean alloy sheets were then cold rolled in three passes to 0.015". These thin alloy sheets were cleaned as before. Before winding into a coil the sheets were indented over their entire surface with a centerpunch so as to facilitate the coiling operation and to insure the coil surfaces against sticking together. After winding into coils, the manganese-iron alloys were hydrogen annealed for 3 hours at 950°C. The coils were then cleaned in the same manner as was previously stated. The coils were stored in a vacuum desiccator.

The 80 atomic percent manganese alloy was too brittle to roll successfully. Therefore, the alloy rod was crushed and used as a coarse powder.

2. Cell Assembly

Before the run, all Vycor tubes, alumina, and other cell materials which would be in contact with the manganese-iron alloy or the electrolyte were cleaned in nitric acid, distilled water and acetone. They were then placed into a drying oven at 140°C overnight. The next morning the lead-manganese alloy was weighed out. The calculation of the composition and amount of alloy is outlined in Appendix III. The manganese-iron coil which had been analyzed and weighed beforehand was then lowered into the bottom of the large alumina crucible shown in Figure 5. Above the coil, an alumina sheet was placed to keep the coil from floating to the surface of the lead-manganese melt. On top of the alumina sheet, a small alumina crucible was placed. The brass head was then placed on a ring stand

above the crucibles. The Vycor thermocouple protection tube was then placed through the center port of the brass head, through the center hole of the positioning crucible and into the small alumina crucible. The lead-manganese alloy was then placed in the large alumina crucible. This assembly was then lowered into the same large Vycor furnace tube used in the manganese-lead study. A long wire with a hook on one end was used to lower this assembly into the furnace tube. By twisting the wire gently, the wire could be removed from underneath the crucible assembly and therefore could be pulled up the side and out of the furnace tube. All the pinch clamps were then fastened, and the vacuum lines were attached. The assembly was then evacuated to 10 millimeters of mercury for 20 minutes. After this period a positive gage pressure of 30 millimeters of mercury was obtained with an argon atmosphere.

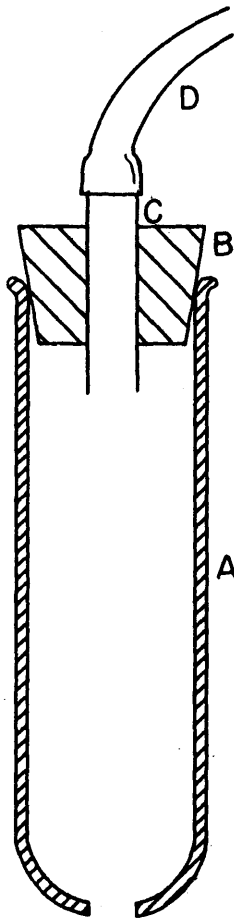
The assembly was then transferred to the resistance furnace and brought to 600°C. While the manganese-lead alloy was becoming molten, the electrolyte was being prepared as described before. After five hours the furnace was shut down and the melt was allowed to cool down and solidify around the small alumina crucible.

The next day, the crucible assembly was removed from the Vycor furnace tube. Then the brass head, with the thermocouple protection tube in it, was placed on a ring stand above the crucible which contained the lead-manganese alloy. The prepared tungsten leads, in the alumina sheathing, were drawn

through the holes of the porcelain positioning crucible and then through the portholes of the brass head. The one bare lead was placed in contact with the manganese-lead alloy and the two β - manganese standard electrodes were suspended above the melt. The electrolyte transfer was accomplished in the same manner as before. The cell with the electrolyte frozen around the leads was then placed into the Vycor furnace tube. This was then placed under vacuum and then repressurized with argon as before. The assembly was then placed in the resistance furnace and brought up to 750°C. After two hours, the one bare tungsten lead was pushed down into the manganese-lead bath. The copper lead wires were then attached to the tungsten cell leads and the reference junction bottle was filled with ice.

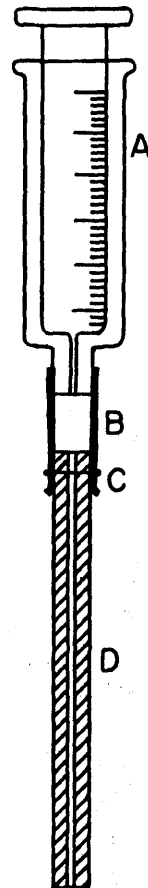
For the composition range in which the iron-manganese alloy was in powder form, the procedure was the same as described except for the substitution of the set-up in Figure 6(d) for the coil.

Readings of potential were taken at a particular temperature until the diffusion of manganese out of the manganese-iron alloy had ceased. This was indicated by a constant potential reading. A typical diffusion curve, (emf vs. time), is shown in Figure 25. When a constant potential was attained, sometimes taking as much as 90 hours, one of the pinch clamps was opened and the quartz sampling tube, Figure 10, was placed down into the manganese-lead bath and a 4 gram sample was taken.



- A - Vycor Tube (25mm) with 3mm hole
- B - Rubber Stopper
- C - Glass Tube
- D - Rubber Tube

FIG.9 ELECTROLYTE TRANSFER TUBE



- A - Tuberculin Syringe 1 C.C.
- B - Rubber Tubing
- C - Copper Wire Clamp
- D - Quartz Quill (1MM I.D. x 3 MM O.D.) 22" Long

FIG.10 SAMPLING APPARATUS

This was chemically analyzed for use in the calculation of the solid alloy composition in equilibrium with the lead-manganese bath. This calculation is outlined in Appendix IV.

The chemical analysis to determine manganese in the manganese-lead bath consisted of dissolving the manganese in HNO_3 , oxidizing with sodium bismuthate and precipitating the permanganate. This was checked with a standard potassium permanganate. The iron was determined by first separating it from lead by evaporation in sulphuric acid and then analyzed calorimetrically.

Chemical analyses of the lead-manganese baths in the cells containing the 56.9 wt.% Mn-33.1 wt.% Fe alloy and the 79.1 wt.% Mn-20.9 wt.% Fe alloy were inconsistent. The composition of these manganese-lead baths were assumed to be the same as those in the manganese-lead study, which gave the same potential value.

VI. RESULTS

A. Sources of Error

1. Reversibility Discussion

The primary assumption made in applying electrode potential measurements to the calculation of thermodynamic properties is that the cell operates in a reversible manner.

The transference of the manganese ions in these studies must have taken place without secondary reactions. The manganese ion must have been present in one valency state only and the manganese ion must also have been the least electronegative ion in the electrolyte. To insure this, the electrolyte used in the study was vacuum treated for at least 24 hours in a manner described in a previous section. The electrolyte varied in color from green to brown. It was clear at all times, precipitated particles never being present. It was quite satisfactory.

Wagner⁽¹²⁾ has estimated the error due to the displacement reaction in galvanic cells. Using his argument, it is estimated that a free energy difference of nearly 7 kilocalories/equivalent was required for the manganese-lead valence type to give an error of 1 percent in activity, when the mole fraction of lead is 0.01. Free energy data of the chlorides of these metals tabulated by Kubaschewski and Evans⁽⁴⁾ showed that there was over a 27 kilocalorie/equivalent difference at 1000°K. This is approximately 4 times the

theoretical requirement.

The difference between the free energy of formation/equivalent of manganese chloride and iron chloride is approximately 8 kilocalories at 1000°K. This is above the theoretical requirement, but is not as favorable as the free energy difference for the chlorides of manganese and lead. The iron-manganese alloy, however, was separated from the electrolyte by a lead-manganese bath. This bath acted as a kinetic barrier to the flow of iron from the solid iron-manganese alloy to the electrolyte. It should be emphasized that the activity of iron was the same in the solid alloy and the liquid bath at equilibrium. The concentration of iron was very low in the lead-manganese bath. Therefore, the displacement reaction between iron and the manganese chloride in the electrolyte was almost completely eliminated. An analysis of the electrolyte after completion of a run showed that only 0.005 weight percent iron was present. This probably is an insignificant amount.

Reversibility can be inferred from the behavior of the cell. In the manganese-lead study, the same potential was attained regardless of whether it was approached from the high or low side. In the manganese-iron study this could not be checked because the diffusion of manganese from the lead-manganese bath back into the iron-manganese coil was extremely slow. The potentials obtained in both studies were in agreement for lead-manganese alloys of similar mole fraction. Potentials were constant with time, thus indicating no metal

transfer. Also, reweighing of the electrodes in the manganese-lead study showed that metal transfer had been slight. One of the best methods for inferring reversibility is the comparison of results obtained by cell measurements with other activity studies. However, a literature survey indicated that no other activity work had previously been done on the manganese-lead system. Since the manganese-lead alloy also constitutes the electrode in the manganese-iron study, the reversibility of neither cell could be checked by a comparison with other work.

2. General

The standard manganese electrodes showed potential differences of 0.15 millivolts in the low temperature range and 0.05 millivolts in the high temperature range. Knowing the direction of the potential relative to the known composition made it possible to say which was the purer standard electrode. The potential difference between the purer standard electrode and the alloy was taken as the correct potential. The difference in potential between the two standards amounted to only a few calories and were not significant in comparison with the actual thermodynamic properties. The experimental potential values used in the manganese-lead system all fell on the straight lines shown in Figures 11 and 12.

Thermo - e.m.f.'s caused by temperature gradients in the cell were reduced greatly by the positioning crucible above the electrolyte crucible. The positioning crucible acted as a thermal shield. No temperature gradient was observed when the

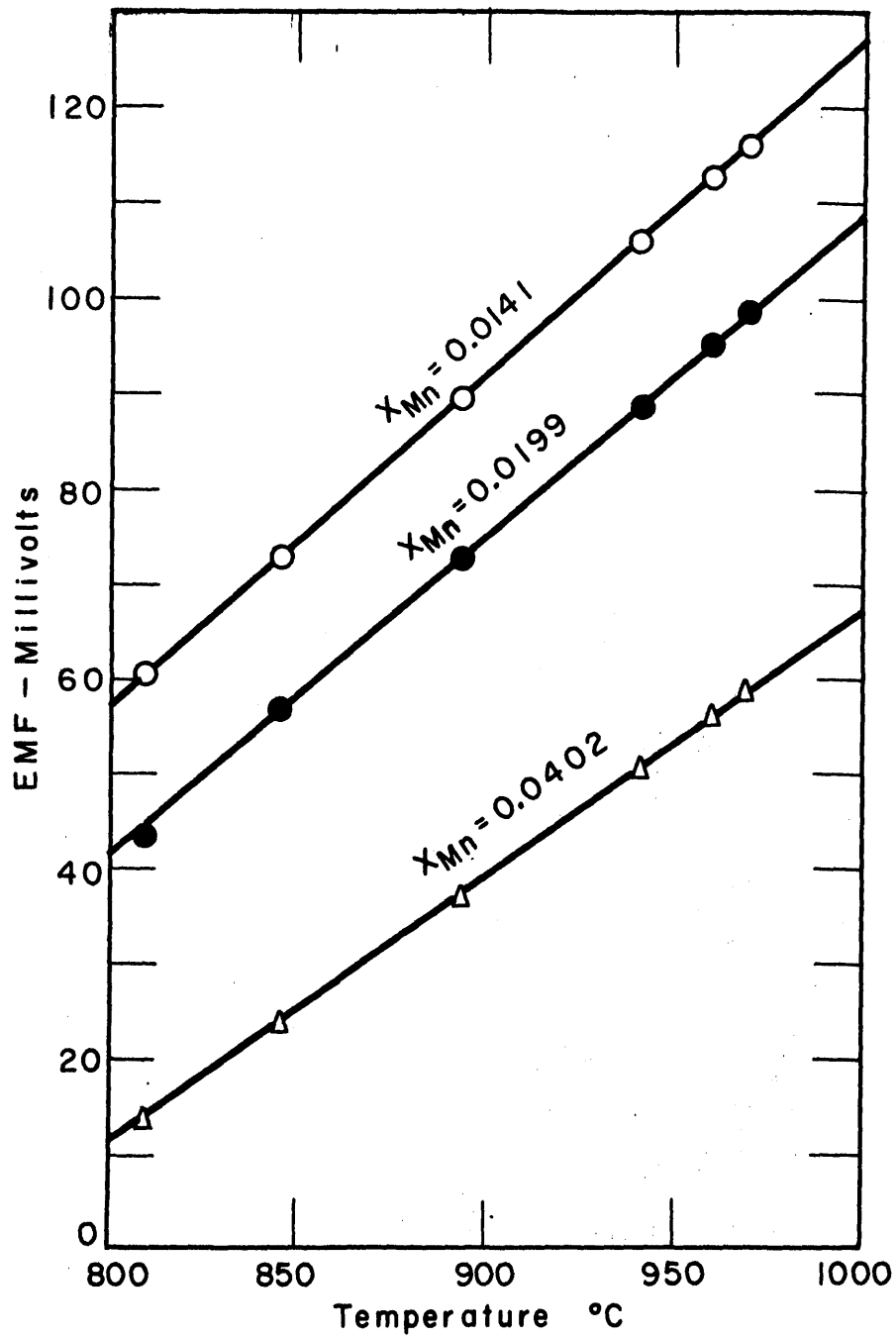


FIG. II THE POTENTIAL VS. TEMPERATURE PLOT FOR THE MANGANESE - LEAD SYSTEM

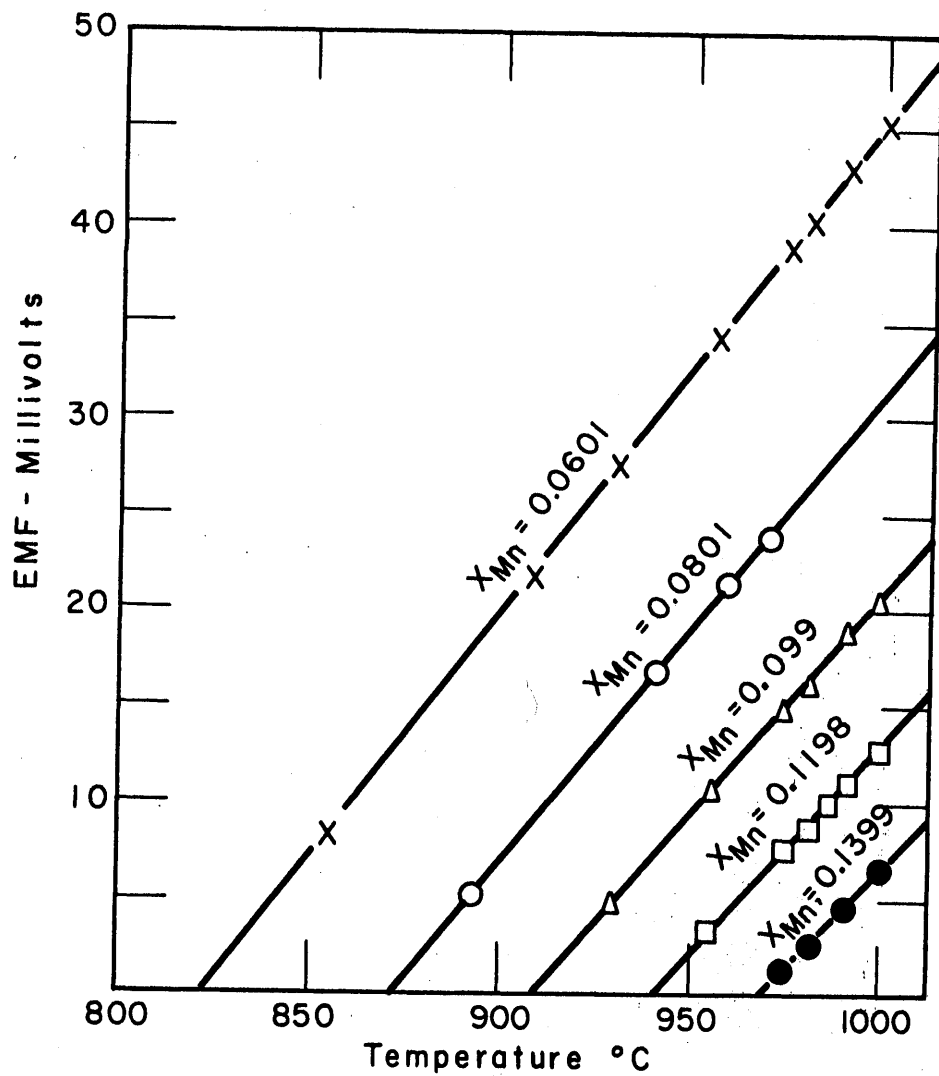


FIG. 12 THE POTENTIAL VS. TEMPERATURE PLOT FOR THE MANGANESE - LEAD SYSTEM

thermocouple was raised and lowered slowly in the electrolyte.

The temperature was probably given within $\pm 0.5^\circ\text{C}$.

B. The Thermodynamic Properties of the Manganese-Lead System

1. Plots and Calculations

In Figure 11 and Figure 12, plots of potential versus temperature are given. The data used is given in Appendix I. This data was actually plotted on 18 by 24 inch graph paper. These large plots were used to obtain the data for subsequent calculations.

From the slopes of the straight line potential versus temperature plots, the temperature coefficient of potential for each composition was obtained. This property at 980°C is plotted in Figure 13. The other thermodynamic properties of the manganese-lead system were also calculated for a temperature of 980°C . All the data for the plots are given in Appendix II.

Using the potential data and equation 5, the activity of manganese, (a_{Mn}), was calculated. The activity coefficient of manganese, γ_{Mn} , was calculated with the aid of equation 7:

$$\gamma_{\text{Mn}} = \frac{a_{\text{Mn}}}{X_{\text{Mn}}} \quad (7)$$

where X_{Mn} is the mole fraction of manganese. From these data the plot given in Figure 14 was made. A smooth curve was drawn through the points and all subsequent activity and free energy data were taken from this curve.

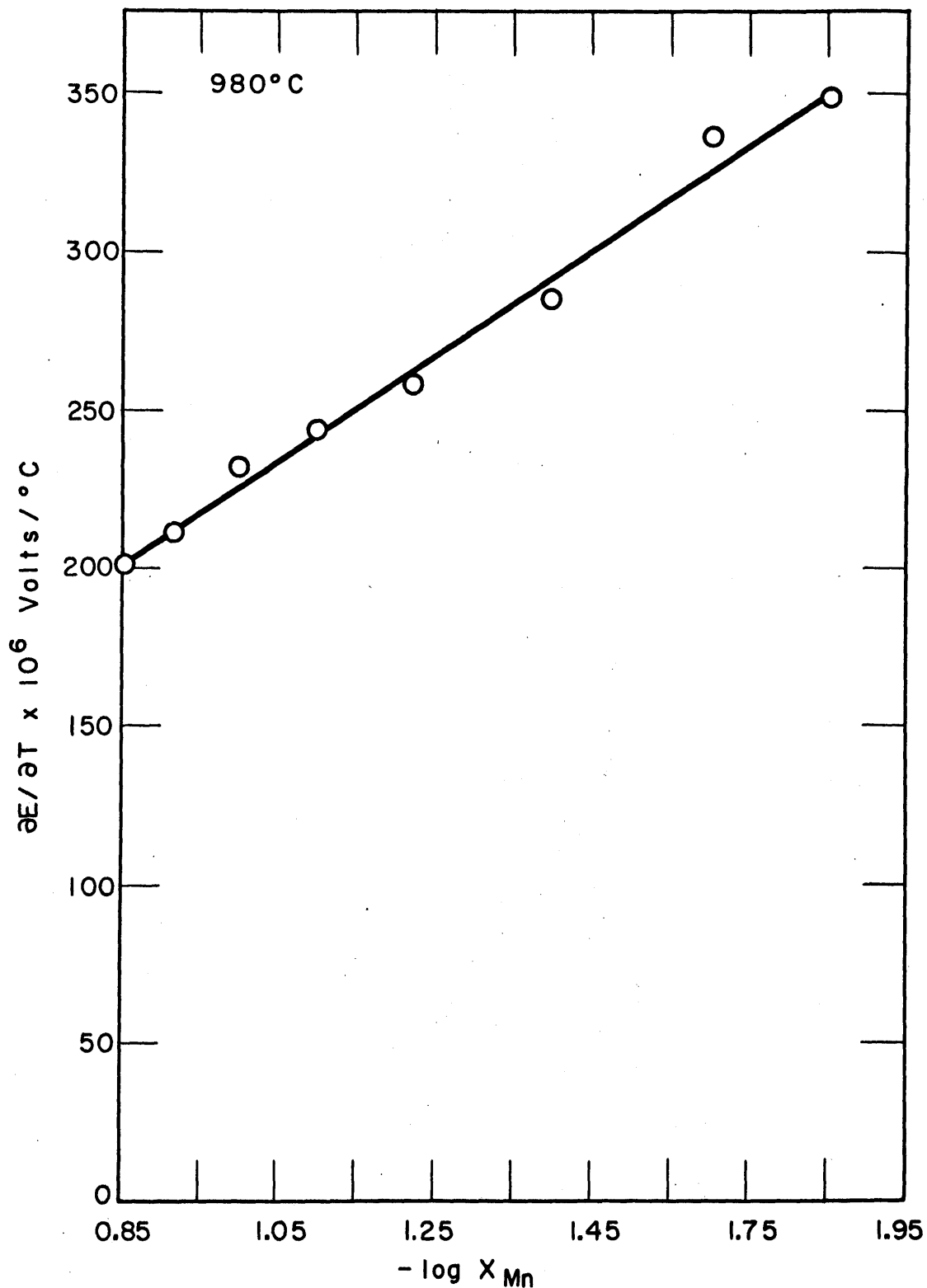


FIG. 13 THE TEMPERATURE COEFFICIENT OF ELECTROMOTIVE FORCE FOR THE MANGANESE-LEAD SYSTEM AT 980°C

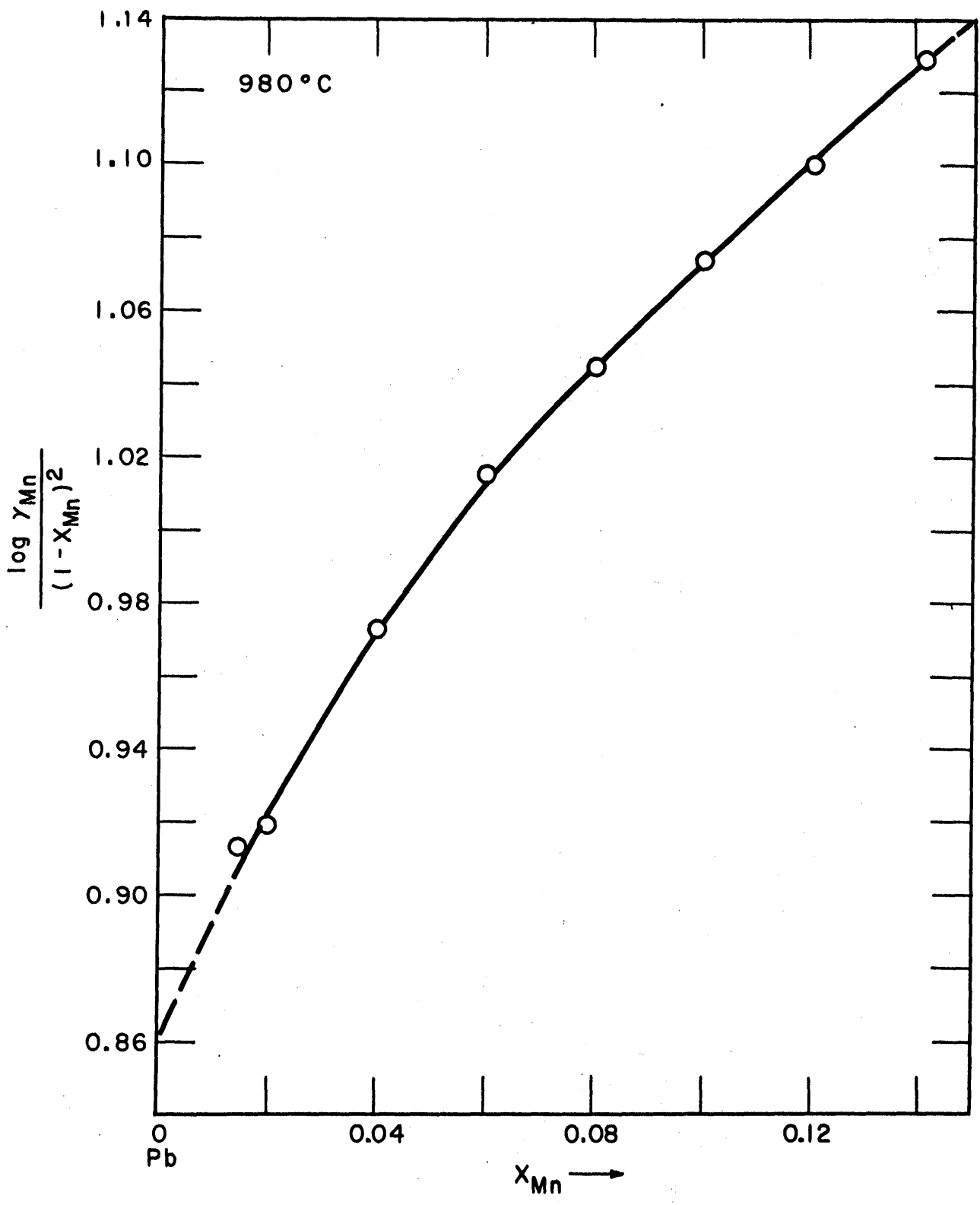


FIG. 14 THE ACTIVITY COEFFICIENT FUNCTION OF MANGANESE IN THE MANGANESE -LEAD SYSTEM AT 980°C

Using the activity coefficient of manganese from Figure 14, the excess partial molar free energy of mixing of manganese, (F_{Mn}^E), was calculated with the aid of equation 8:

$$F_{Mn}^E = F_{Mn}^M - F_{Mn}^M(\text{ideal}) = RT \ln \gamma_{Mn} \quad (8)$$

F_{Mn}^E is equal to the partial molar free energy of mixing of manganese in the system studied minus the partial molar free energy of mixing of manganese if the system studied were ideal. F_{Mn}^E was plotted versus the mole fraction of manganese in Figure 16. The activity of manganese was calculated from the activity coefficient of manganese taken from Figure 14, with the aid of equation 7. The activity of manganese was plotted versus the mole fraction of manganese in Figure 22. The partial molar free energy of mixing of manganese, (F_{Mn}^M), was then calculated with the aid of equation 5.

To obtain the thermodynamic properties of lead, the Gibbs-Duhem equation, integrated by parts, (equation 9), according to a method suggested by Wagner⁽¹³⁾ was used.

$$\log \gamma_{Pb} = - \frac{\log \gamma_{Mn}}{(1-X_{Mn})^2} X_{Mn} X_{Pb} + \int_{X_{Mn}=0}^{X_{Mn}} \frac{\log \gamma_{Mn}}{(1-X_{Mn})^2} dX_{Mn} \quad (9)$$

The second term on the right side of equation 9 was integrated by obtaining the area under the plot of $\log \gamma_{Mn} / (1-X_{Mn})^2$ versus the mole fraction of manganese. It was for the purpose of obtaining the second term of equation 9 that Figure 14,

Figure 15 and Figure 18 were plotted. By substituting F_{Mn}^E , the excess partial molar free energy of mixing, and H_{Mn}^E , the excess partial molar heat of mixing, in equation 9, an analogous equation was obtained for Figure 15 and Figure 18 respectively. The excess functions were used since they approach finite limits as the mole fraction of manganese approaches zero, instead of becoming infinite as the partial molar properties do. This finite limit made possible the required integration. The excess partial molar free energy of lead, F_{Pb}^E , was plotted in Figure 16 and the partial molar free energy of mixing of lead, F_{Pb}^H , was plotted in Figure 17. The activity of lead was plotted in Figure 22.

The excess partial molar heat of mixing of manganese was calculated directly from the potential data with the aid of equation 6. The function $H_{Mn}^E/(1-X_{Mn})^2$ was then plotted versus the mole fraction of manganese in Figure 18. A straight line was drawn through the calculated points. The excess partial molar heats of mixing of manganese were taken off this straight line. The excess partial molar heat of mixing of lead was calculated with the aid of equation 10 and Figure 18.

$$H_{Pb}^E = - \frac{H_{Mn}^E}{(1-X_{Mn})^2} X_{Pb} X_{Mn} + \int_{X_{Mn}=0}^{X_{Mn}} \frac{H_{Mn}^E}{(1-X_{Mn})^2} dX_{Mn} \quad (10)$$

The excess partial molar heat of mixing of manganese and lead are plotted in Figure 19.

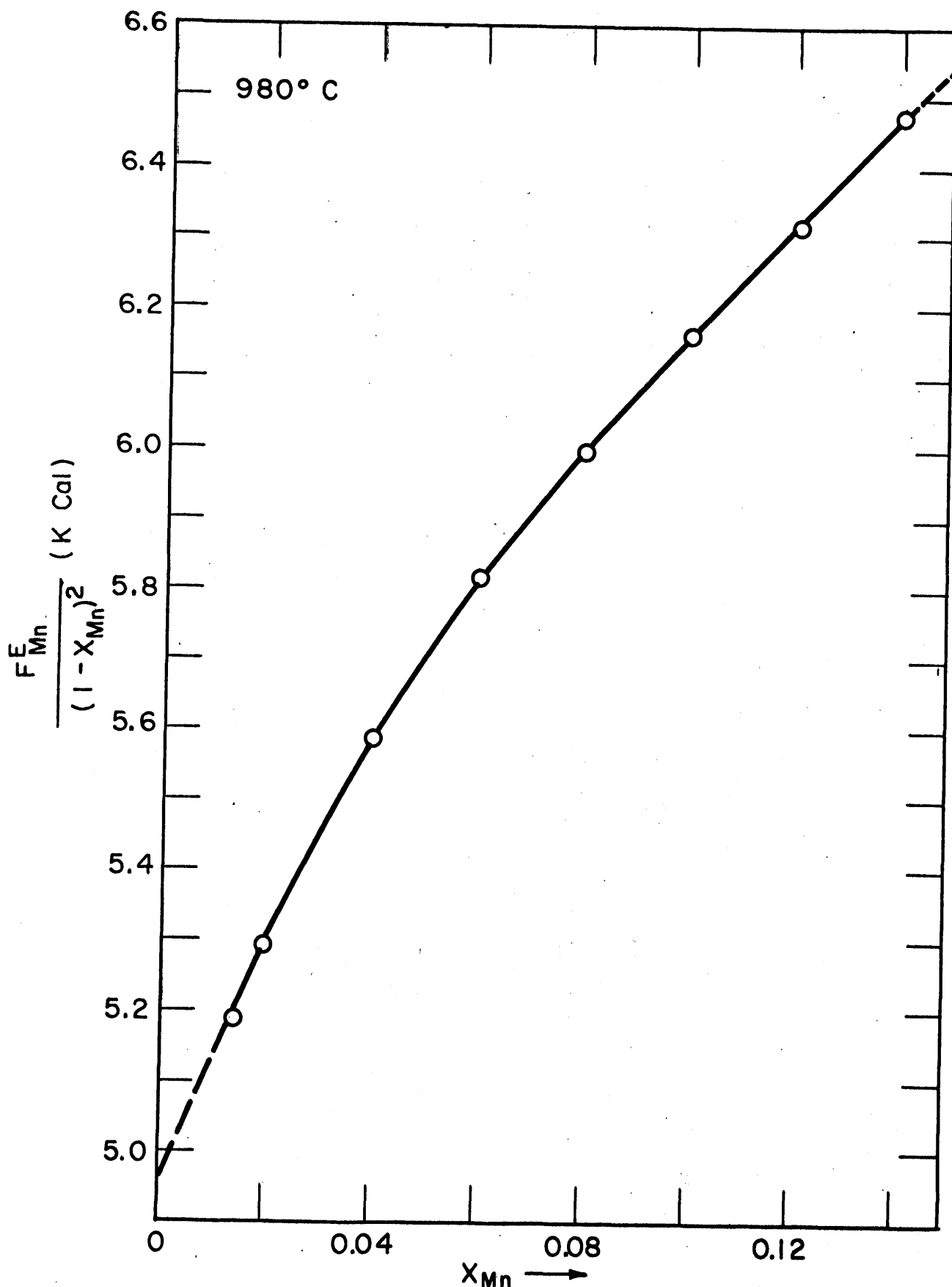


FIG. 15 THE FREE ENERGY FUNCTION OF MANGANESE IN THE MANGANESE LEAD SYSTEM AT 980° C

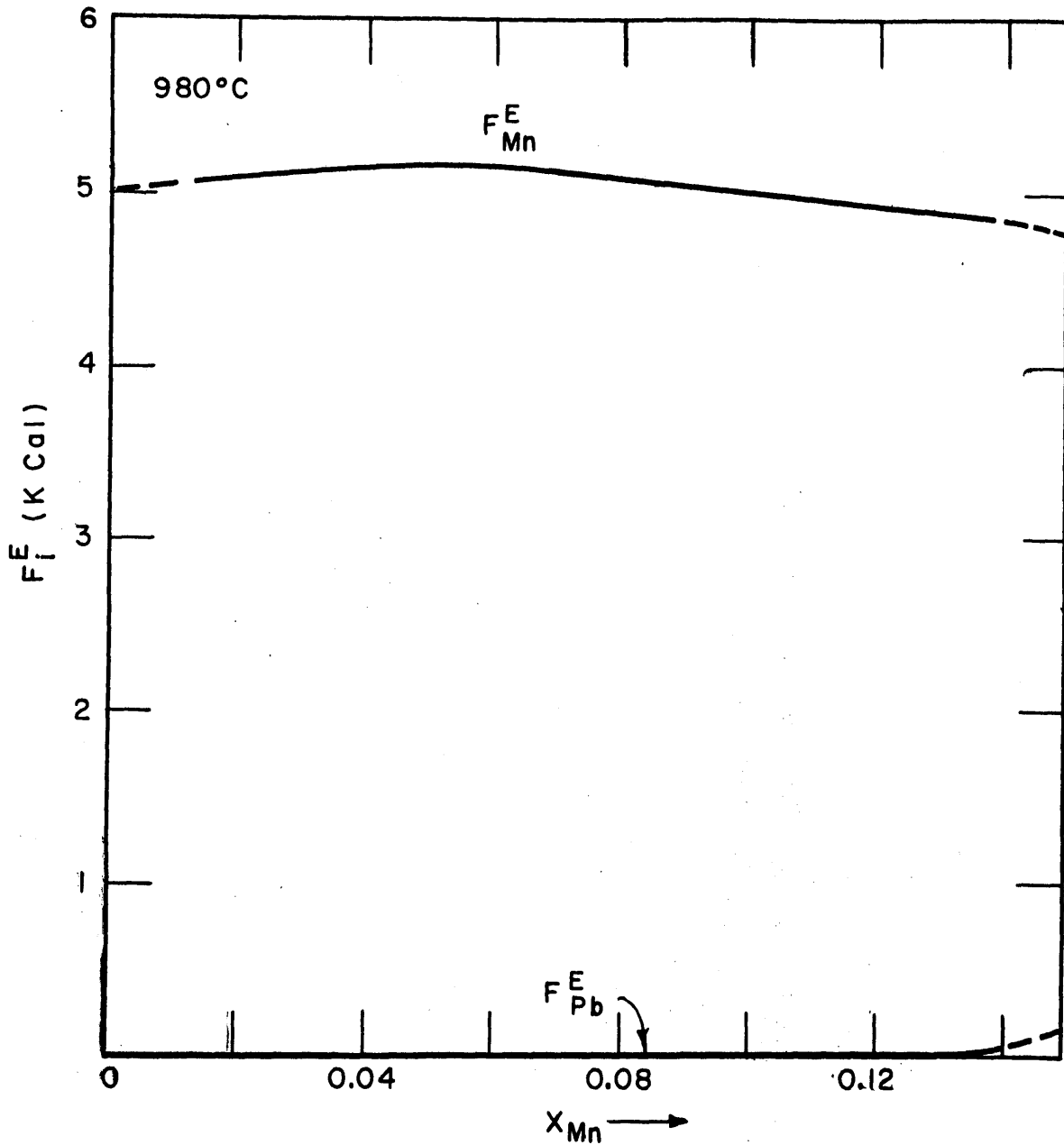


FIG. 16 THE EXCESS PARTIAL MOLAR FREE ENERGY OF MIXING FOR MANGANESE AND LEAD IN THE MANGANESE - LEAD SYSTEM AT 980°C

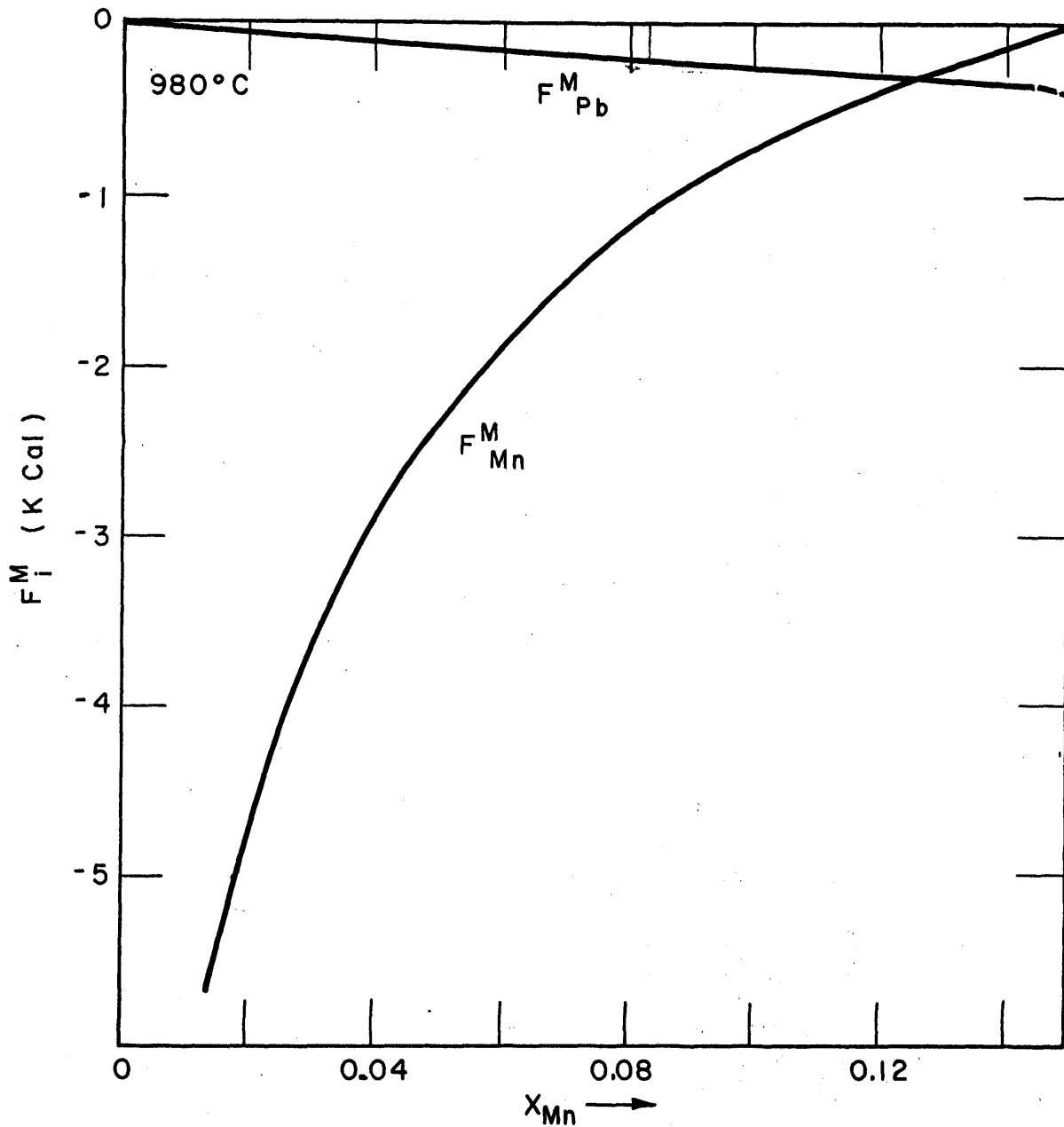


FIG. 17 THE PARTIAL MOLAR FREE ENERGY OF MIXING OF MANGANESE AND LEAD IN THE MANGANESE-LEAD SYSTEM AT 980°C

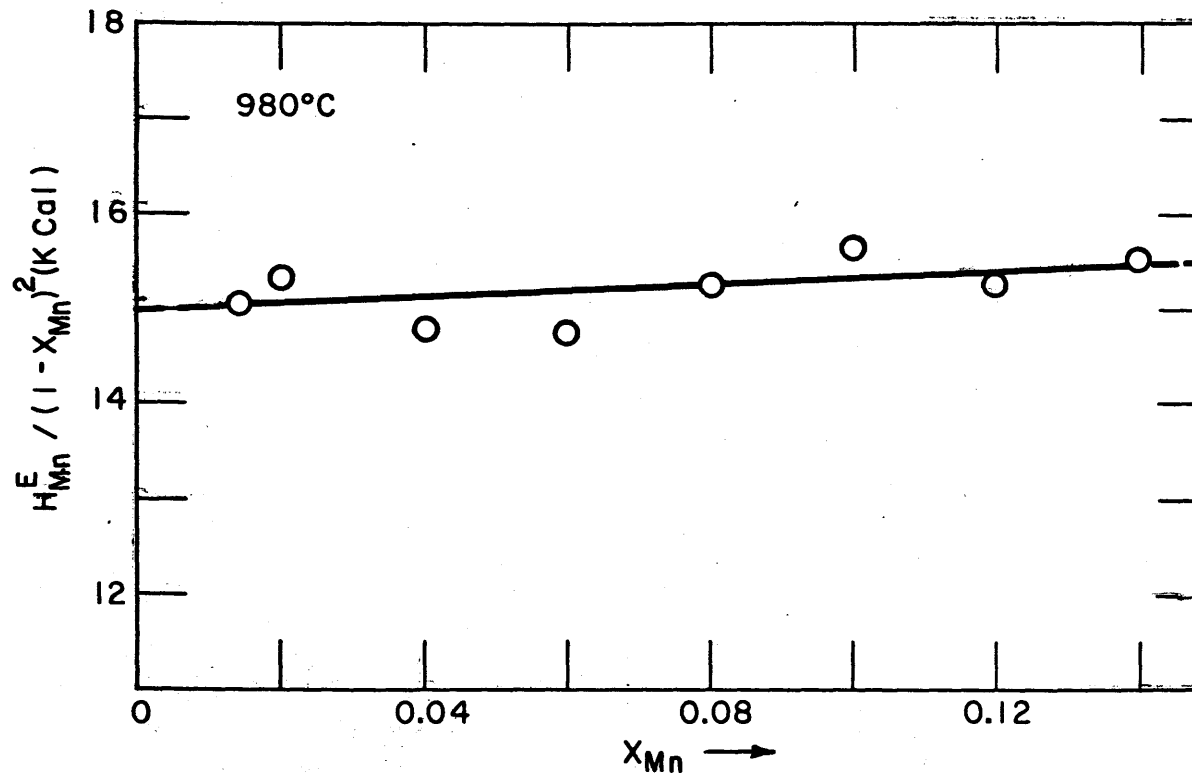


FIG. 18 THE HEAT OF MIXING FUNCTION OF MANGANESE IN THE MANGANESE - LEAD SYSTEM AT 980°C

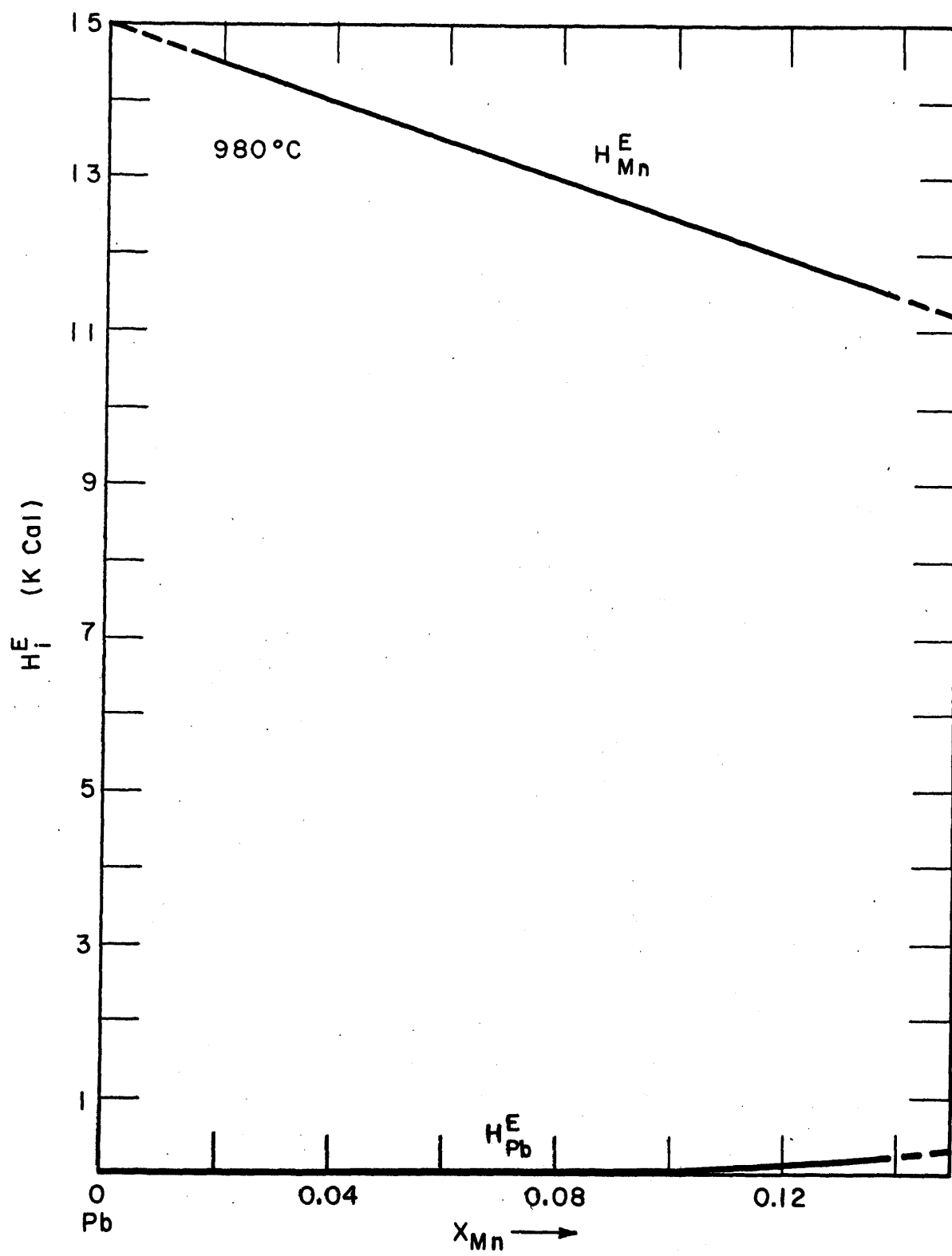


FIG. 19 THE PARTIAL MOLAR HEAT OF MIXING FOR MANGANESE AND LEAD IN THE MANGANESE-LEAD SYSTEM AT 980°C

In Figure 20 the excess molar quantities are reported. The excess molar free energy, F^E , was obtained with the aid of equation 11.

$$F^E = X_{Pb} \int_{X_{Mn} = 0}^{X_{Mn}} \frac{F_{Mn}^E}{(1-X_{Mn})^2} dX_{Mn} \quad (11)$$

The excess molar heat of mixing was calculated by equation 12.

$$H^E = X_{Pb} \int_{X_{Mn} = 0}^{X_{Mn}} \frac{H_{Mn}^E}{(1-X_{Mn})^2} dX_{Mn} \quad (12)$$

The entropy term was obtained using equation 13.

$$F^E = H^E - TS^E \quad (13)$$

In Figure 21 the molar quantities are reported. The molar free energy was obtained by equation 14.

$$F^M = \sum_1^i X_i F_i^M \quad (14)$$

The molar heat of mixing is identical to the excess molar heat of mixing. Equation 13 also holds for molar quantities. Therefore, the molar entropy term may be calculated.

An estimation of the liquidus line of the manganese-lead

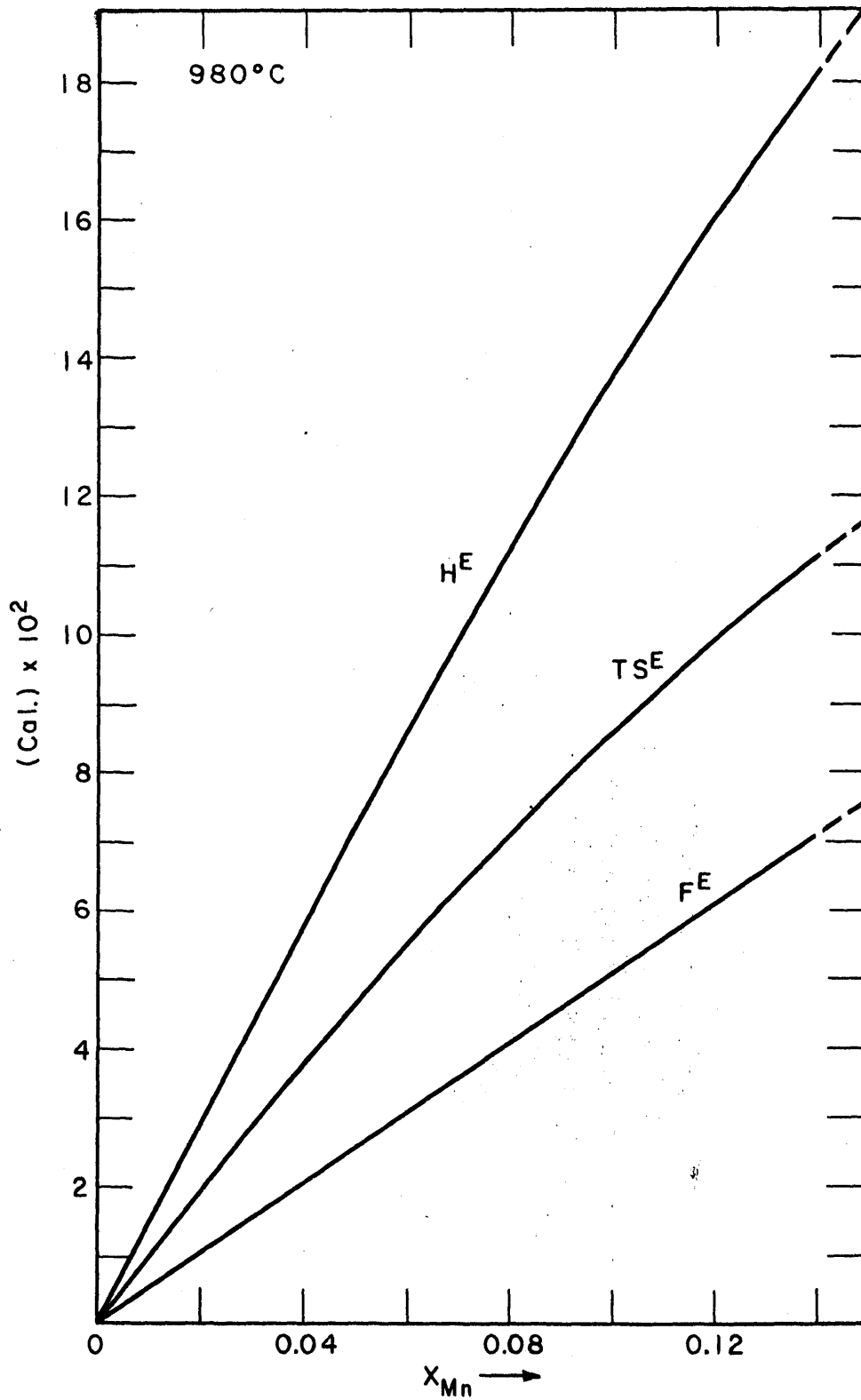


FIG. 20 THE EXCESS MOLAR PROPERTIES OF THE MANGANESE - LEAD SYSTEM AT 980°C

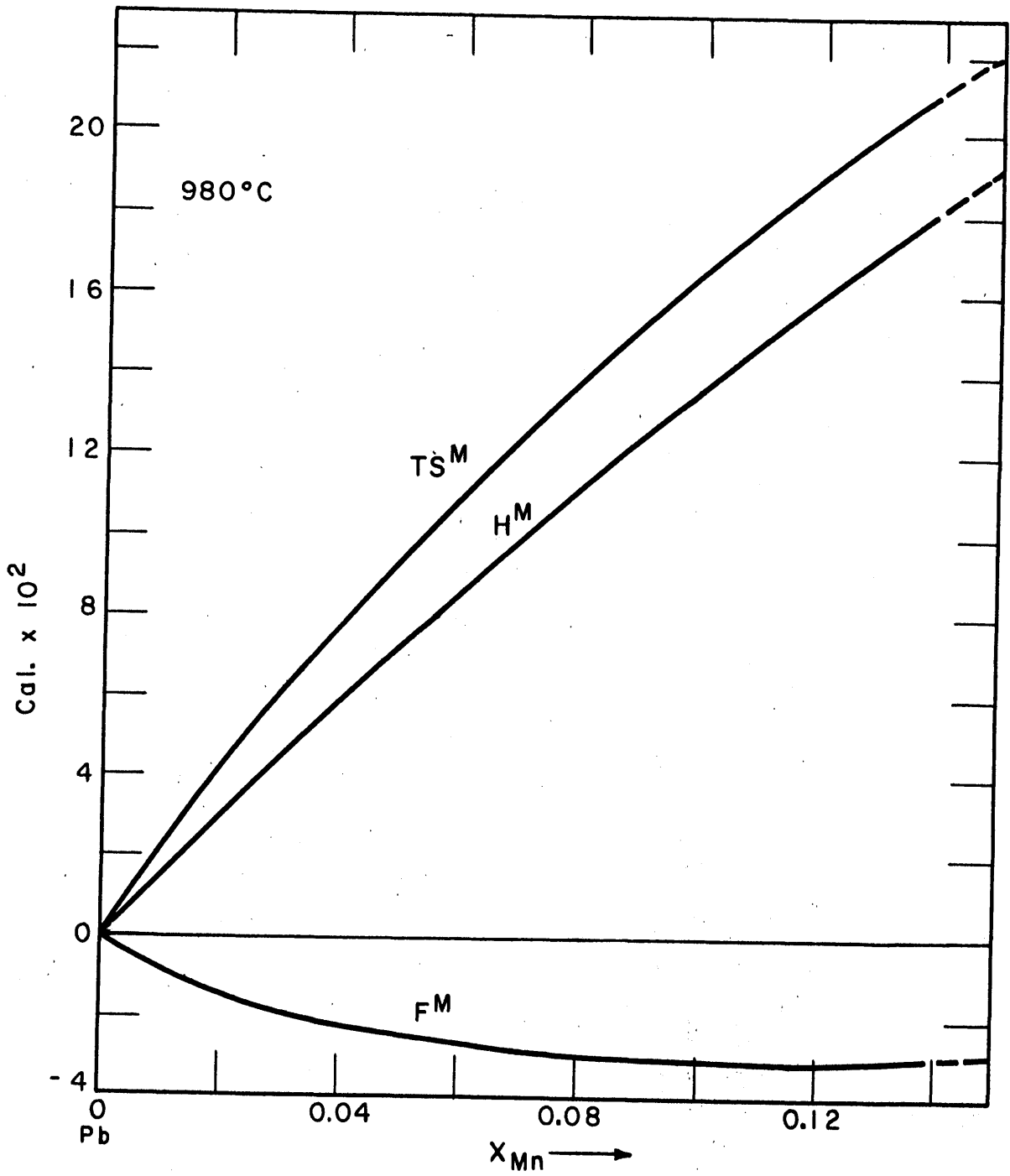


FIG. 21 THE MOLAR PROPERTIES OF THE MANGANESE-LEAD SYSTEM AT 980°C

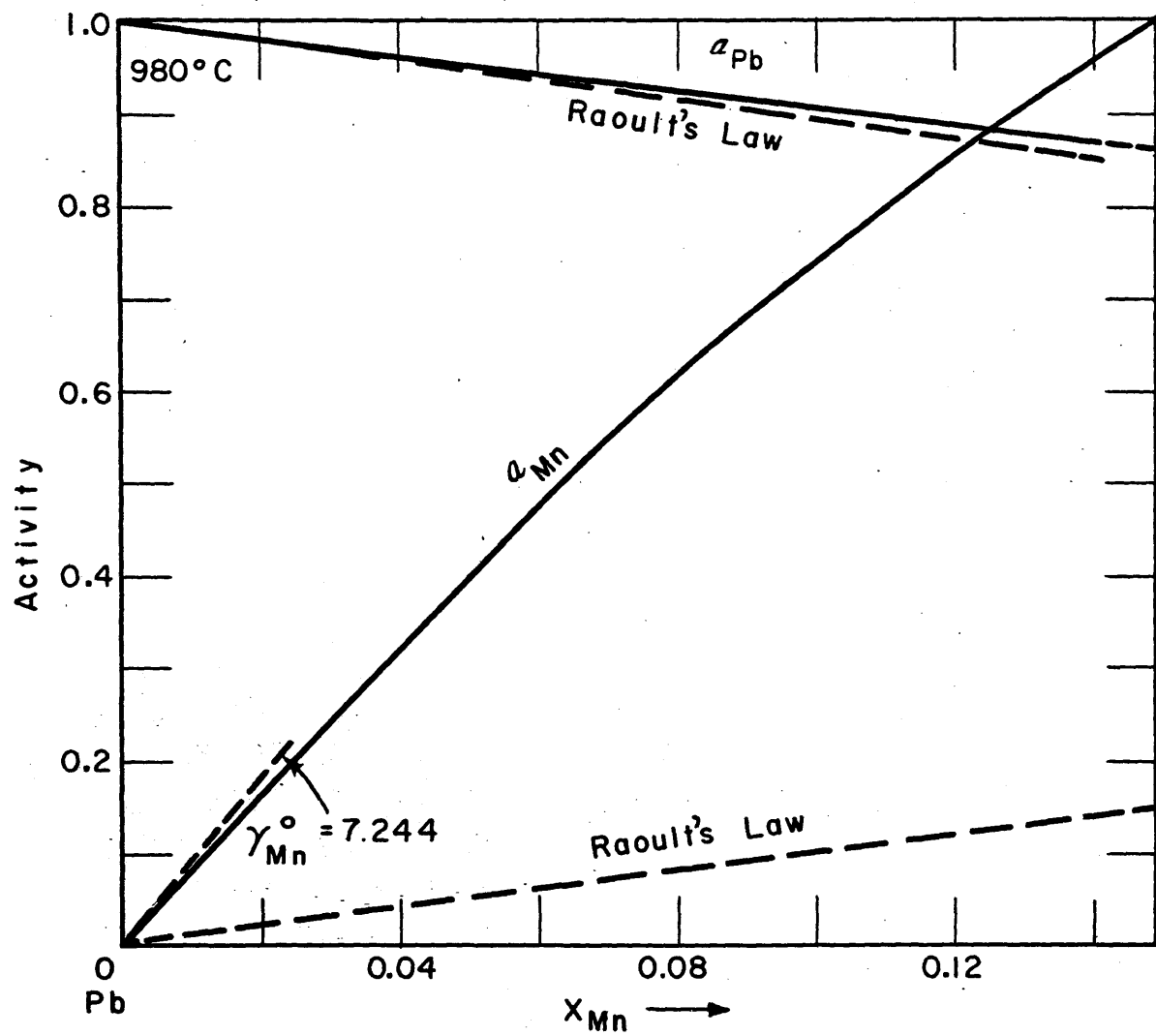


FIG. 22 THE ACTIVITY OF MANGANESE AND LEAD IN THE MANGANESE -LEAD SYSTEM AT 980°C

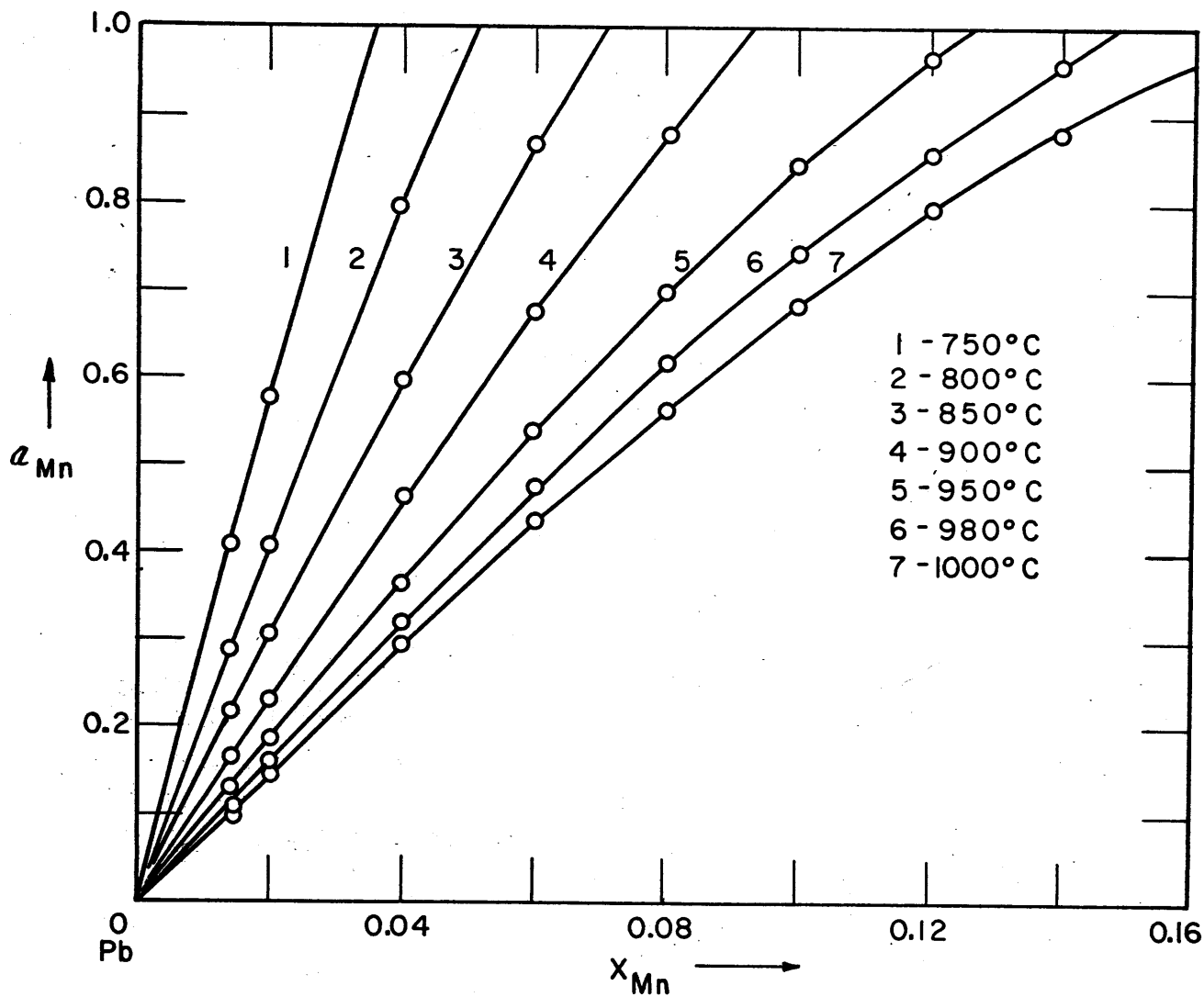


FIG. 23 THE ACTIVITY OF MANGANESE VS. X_{Mn} FROM 750°C TO 1000°C

phase diagram Figure 24, assuming pure manganese precipitates out as the solid phase, is given in Figure 24. The points at which the constant mole fraction-potential versus temperature straight lines intersect the zero potential axis determines the liquidus line. At these intersection points, the activity of manganese is equal to one. The melt is therefore saturated with manganese at the intersected temperature.

2. Discussion of the Manganese-Lead System

In Figure 20, the partial molar entropy of mixing for manganese is shown to be much greater than ideal. The entropy term is extremely large across the entire liquid system studied. Most systems show a greater than ideal entropy independent of the type of activity deviation from ideality. Elliott and Chipman⁽²⁾ gave some examples of this tendency for liquid metal alloys.

The activity curves in Figure 22 show a positive deviation from ideality. The partial molar free energy of mixing curve for manganese goes to zero at the solubility limit as it should. Lead is shown to act almost ideally in the composition range studied. The excess partial molar free energy curve for manganese shows a convergence towards a zero value at $X_{Mn} = 1$ and the excess partial molar free energy curve for lead shows a zero value at $X_{Pb} = 1$. The partial molar heat of mixing of manganese is decreased by increasing amounts of manganese. The heat of mixing in this system is shown to be large.

The shape of the liquidus curve, Figure 24, is in general agreement with the positive deviation from ideality in this

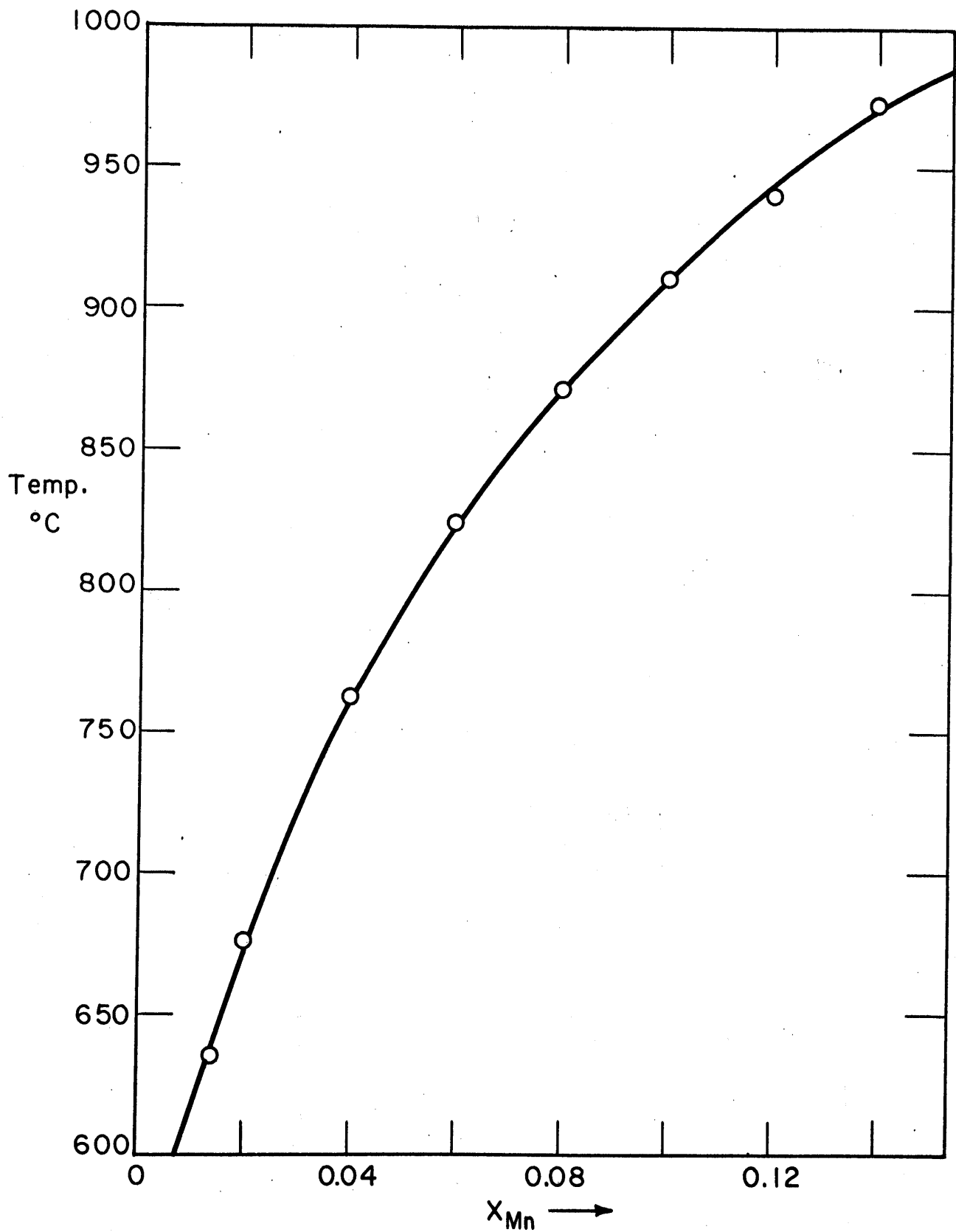


FIG. 24 ESTIMATION OF PORTION OF LIQUIDUS CURVE FOR THE MANGANESE - LEAD SYSTEM

system. No previous experimental work was done on this liquidus line. In 1907 Williams⁽¹⁴⁾ estimated the liquidus line to have greater solubility than was found in this study. He stated no direct evidence for his estimate. The two lines are parallel and differ by 5 atomic percent at 850°C. In this study manganese was assumed to be the solid in the two phase region. On crossing the liquidus temperature an extremely small negative e.m.f. was observed. This e.m.f. was well within experimental error. It was probably due to a small amount of supercooling. The negative e.m.f. seemed to remain fairly constant with time.

The activity coefficient of manganese at infinite dilution was found to be 7.244 ($\gamma_{\text{Mn}}^{\circ} = 7.244$).

C. Thermodynamic Properties of the Manganese-Iron System

1. Plots and Calculations

The activity coefficient functions of manganese in the Fe-Mn system are shown in Figure 26 for the temperature range 750° - 850°C. It can be seen that the effect of temperature on the activity coefficient function within the temperature range studied is negligible. The activity therefore was assumed constant with temperature. The activities obtained from potential data in the 800°C range were therefore assumed to be the activities at 800°C. All experimental data used in the thermodynamic calculations are compiled in Appendix IV, and the thermodynamic properties calculated at 800 C are given in Appendix V.

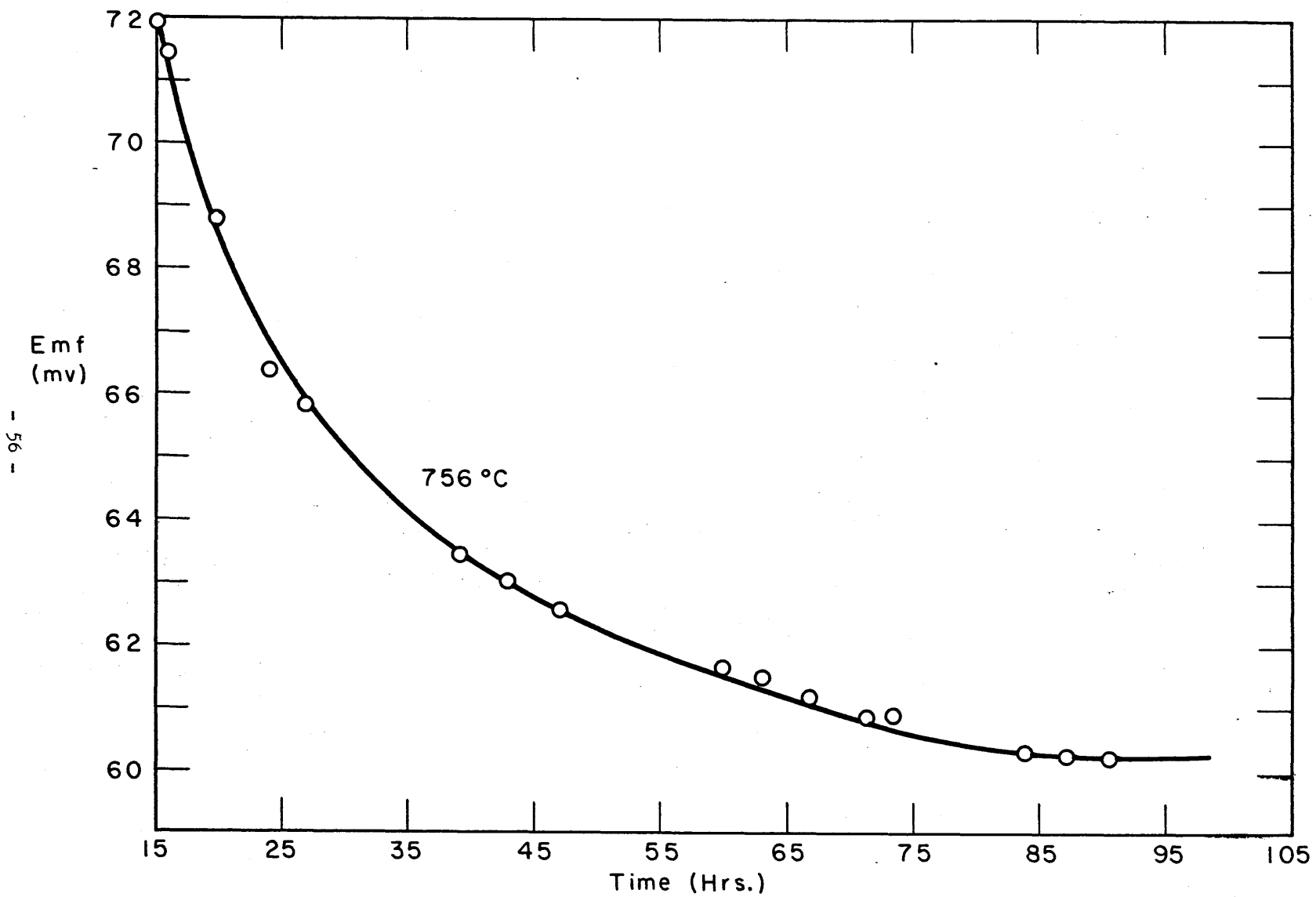


FIG. 25 DIFFUSION CURVE (Emf vs Time) FROM Mn - Fe STUDY ; $X_{Mn} \approx 0.365$

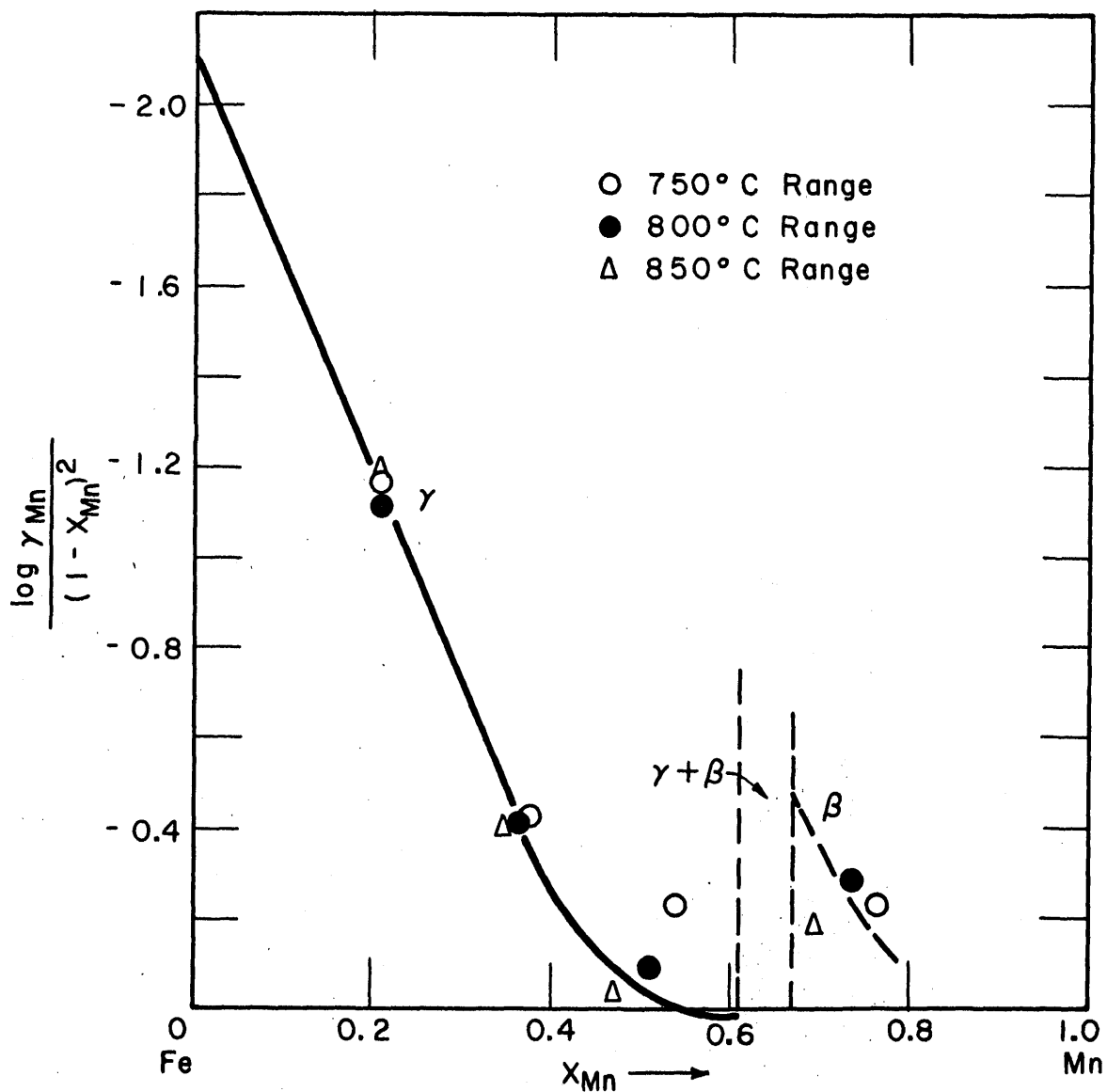


FIG. 26 THE ACTIVITY COEFFICIENT FUNCTION OF MANGANESE IN THE MANGANESE-IRON SYSTEM IN THE TEMPERATURE RANGE 750° C -850° C

The problem of determining the plot of the activity coefficient function of manganese was first attacked. From the phase diagram of the manganese-iron system compiled by Hanson⁽¹⁵⁾ two two-phase regions were seen to be present at 800°C. The first two-phase region, containing the phases α and γ , is present from 2 atomic percent manganese to 5 atomic percent manganese. The second two-phase region, containing the phases γ and β , is present from 61 atomic percent manganese to 67 atomic percent manganese. Since pure β - manganese was the standard electrode, pure β - manganese was used as the standard state and the activity of β - manganese was made unity.

In the first set of calculations the γ phase was assumed stable across the composition range of 0 atomic percent manganese to 61 atomic percent manganese. Using this assumption, and integrating the Gibbs-Duhem equation by parts, the thermodynamic properties of iron were obtained relative to a standard state of pure γ -iron ($a_{\gamma\text{Fe}} = 1$). From the experimental data the activity coefficient function was calculated for $X_{\text{Mn}} = 0.2074$, $X_{\text{Mn}} = 0.3659$, $X_{\text{Mn}} = 0.5079$ and $X_{\text{Mn}} = 0.7350$. To obtain the value of this function at $X_{\text{Mn}} = 0.61$, (the boundary of the two-phase region), the activity coefficient of manganese was plotted versus the mole fraction, (Figure 27). From this plot, the activity coefficient of manganese at $X_{\text{Mn}} = 0.61$ was found to be equal to 1.002. Using equation 7 the activity at $X_{\text{Mn}} = 0.61$ was calculated. The activity must remain constant in the two-

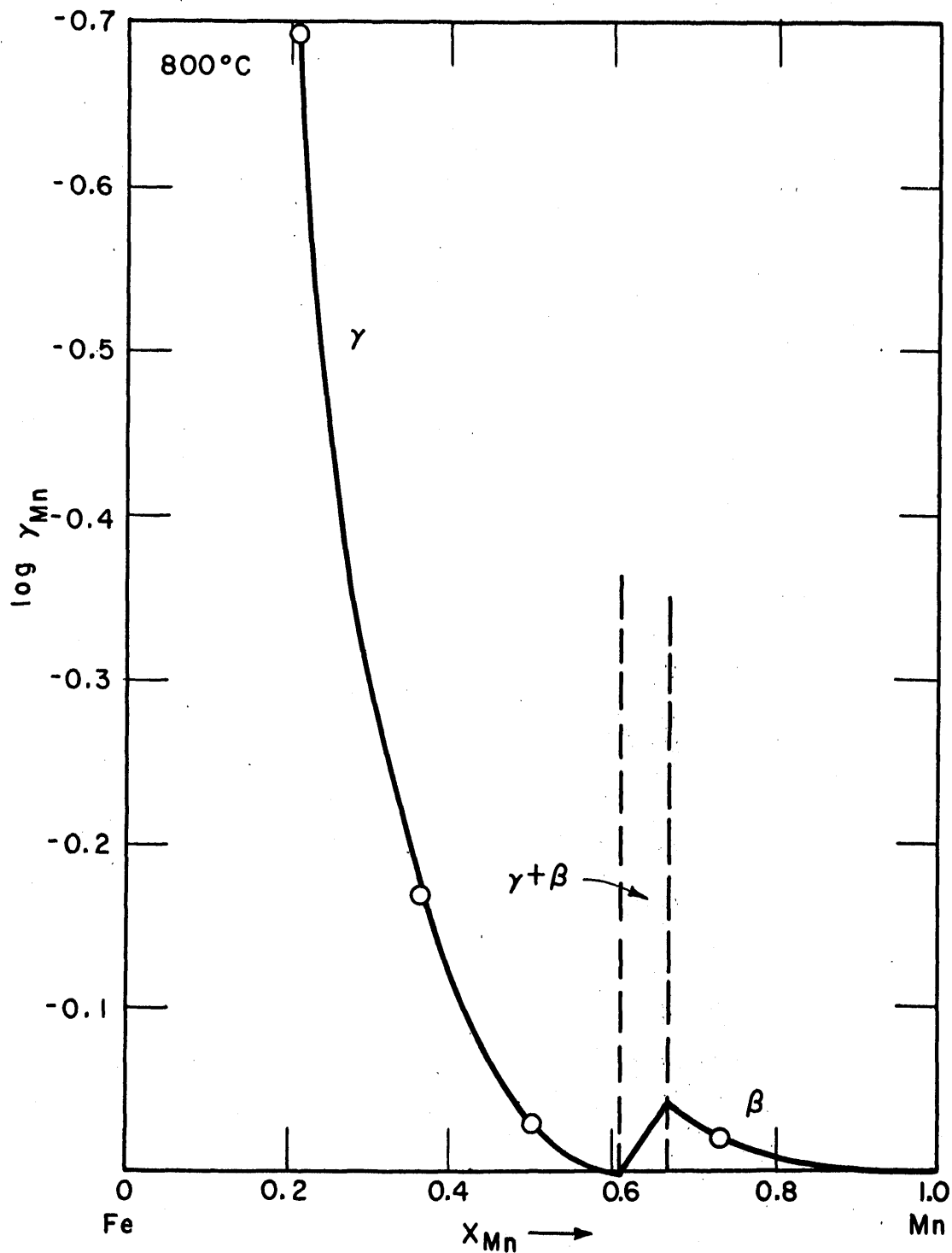


FIG. 27 THE ACTIVITY COEFFICIENT OF MANGANESE IN THE MANGANESE-IRON SYSTEM VERSUS X_{Mn} AT 800°C (STANDARD STATE $a_{\beta_{Mn}} = 1, a_{\gamma_{Fe}} = 1$)

phase region, therefore, the activity coefficient function was calculated for alloys in the range of $X_{\text{Mn}} = 0.61$ to $X_{\text{Mn}} = 0.67$. Knowing the activity of manganese at $X_{\text{Mn}} = 0.67$, $X_{\text{Mn}} = 0.735$, and $X_{\text{Mn}} = 1$, the activity curve for manganese in the β - manganese-iron alloy region was drawn. Using activities from this plot, the activity coefficient function was calculated for $X_{\text{Mn}} = 0.7$, $X_{\text{Mn}} = 0.8$, and $X_{\text{Mn}} = 0.9$. The entire activity coefficient function of manganese for a standard state given by the $a_{\beta - \text{Mn}} = 1$ and the $a_{\gamma - \text{Fe}} = 1$ is shown in Figure 28.

For the second set of calculations, the small two-phase region containing the α and γ phases was considered. Using the value of the activity coefficient function of manganese at $X_{\text{Mn}} = 0.05$, taken from Figure 28, the activity of manganese for the range $X_{\text{Mn}} = 0.02$ to $X_{\text{Mn}} = 0.05$ was calculated. The activity coefficient functions for these compositions were then calculated. Assuming Henry's Law to hold in the extremely dilute section of this system, a straight line was drawn for the activity coefficient function from $X_{\text{Mn}} = 0.02$ to $X_{\text{Mn}} = 0$. The remaining part of the activity coefficient function plot for the standard state considered in this case, ($a_{\beta - \text{Mn}} = 1$, $a_{\alpha - \text{Fe}} = 1$), was identical with that in Figure 28. The entire activity coefficient function of manganese for the standard state given by the $a_{\beta - \text{Mn}} = 1$ and the $a_{\alpha - \text{Fe}} = 1$ is given in Figure 29.

The excess free energies of mixing for manganese (F_{Mn}^E) were calculated for each of the two standard states with the aid of equations 9 and 10 and Figures 28 and 29. The remaining

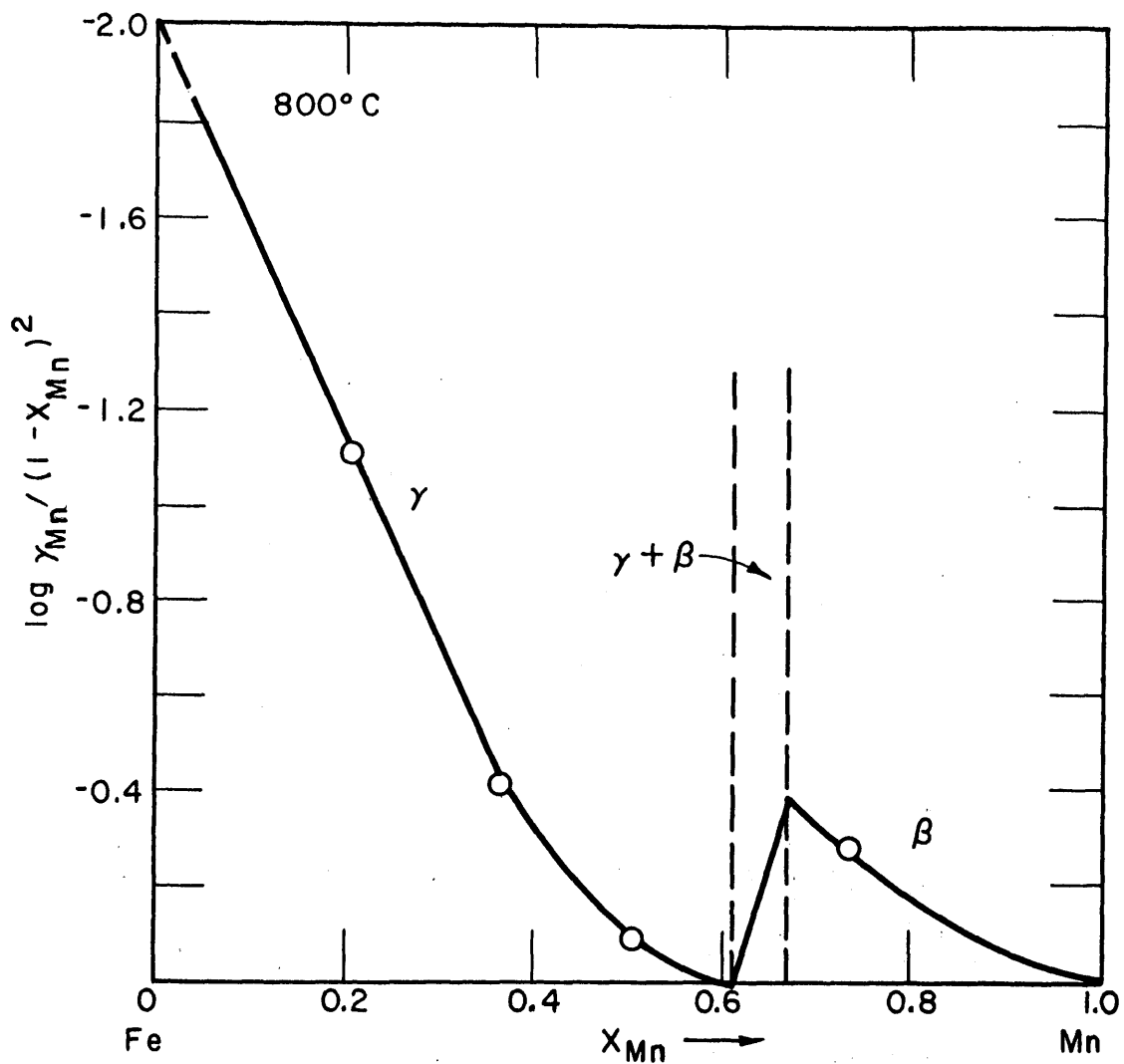


FIG. 28 THE ACTIVITY COEFFICIENT FUNCTION OF MANGANESE IN THE MANGANESE - IRON SYSTEM AT 800°C
(STANDARD STATE: $a_{\beta_{Mn}} = 1$; $a_{\gamma_{Fe}} = 1$)

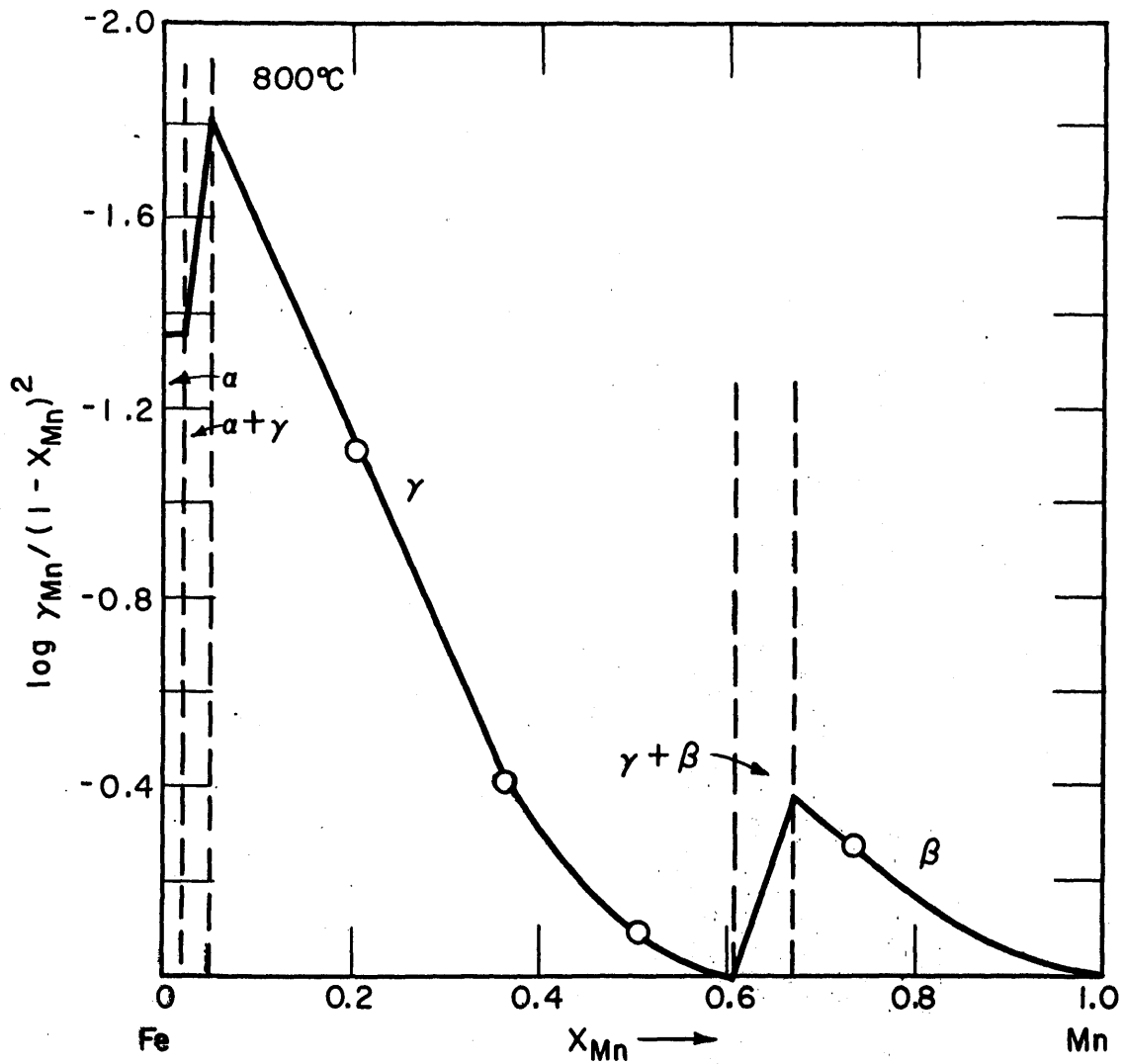


FIG. 29 THE ACTIVITY COEFFICIENT FUNCTION OF MANGANESE IN THE MANGANESE-IRON SYSTEM AT 800°C
 STANDARD STATE: $a_{\beta \text{Mn}} = 1$; $a_{\alpha \text{Fe}} = 1$

thermodynamic properties were calculated in a manner similar to that described for the manganese-lead system calculations.

The excess partial molar free energies of mixing for manganese and iron using the two different standard states are shown in Figures 30 and 31. The partial molar free energies of mixing for the different standard states are shown in Figures 32 and 33. The excess molar free energy of mixing and the molar free energy of mixing for the two standard states are shown in Figures 34 and 35.

The activities of manganese and iron calculated for the different standard states are shown in Figures 36 and 37. The dashed activity lines in Figures 36 and 37 give the activity of manganese, assuming the γ phase was stable over the entire β phase region, (no β was present). The activity of pure γ - manganese relative to a standard state of pure β - manganese was calculated to be equal to 1.087. This was obtained with the aid of the free energy data of Weiss and Tauer.⁽¹⁶⁾ The free energy of transformation from γ - manganese to β - manganese was given as 180 calories/mole at 800°C.

2. Discussion of the Manganese-Iron System

The activity curves in Figures 36 and 37 show negative deviation from ideality. The deviation was quite significant in the high iron side of the diagram. The activity curve for manganese shows almost ideal behavior from $X_{\text{Mn}} = 0.5$ to $X_{\text{Mn}} = 1$. The activity curve for iron shows strong negative deviation over the entire composition range.

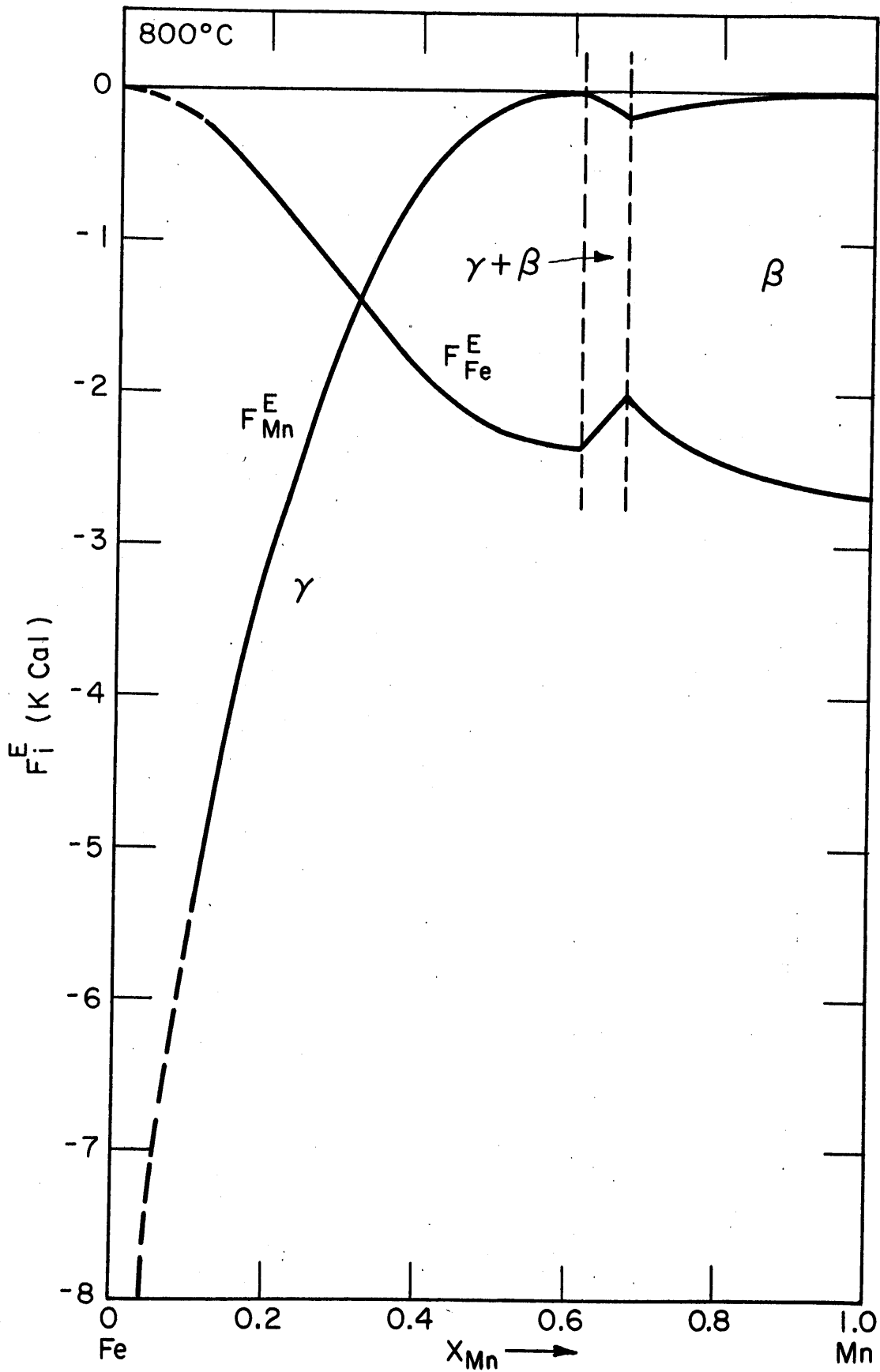


FIG. 30 THE EXCESS PARTIAL MOLAR FREE ENERGY OF MIXING OF MANGANESE AND IRON IN THE MANGANESE - IRON SYSTEM AT 800°C (STANDARD STATE: $a_{\beta_{Mn}} = 1$; $a_{\gamma_{Fe}} = 1$)

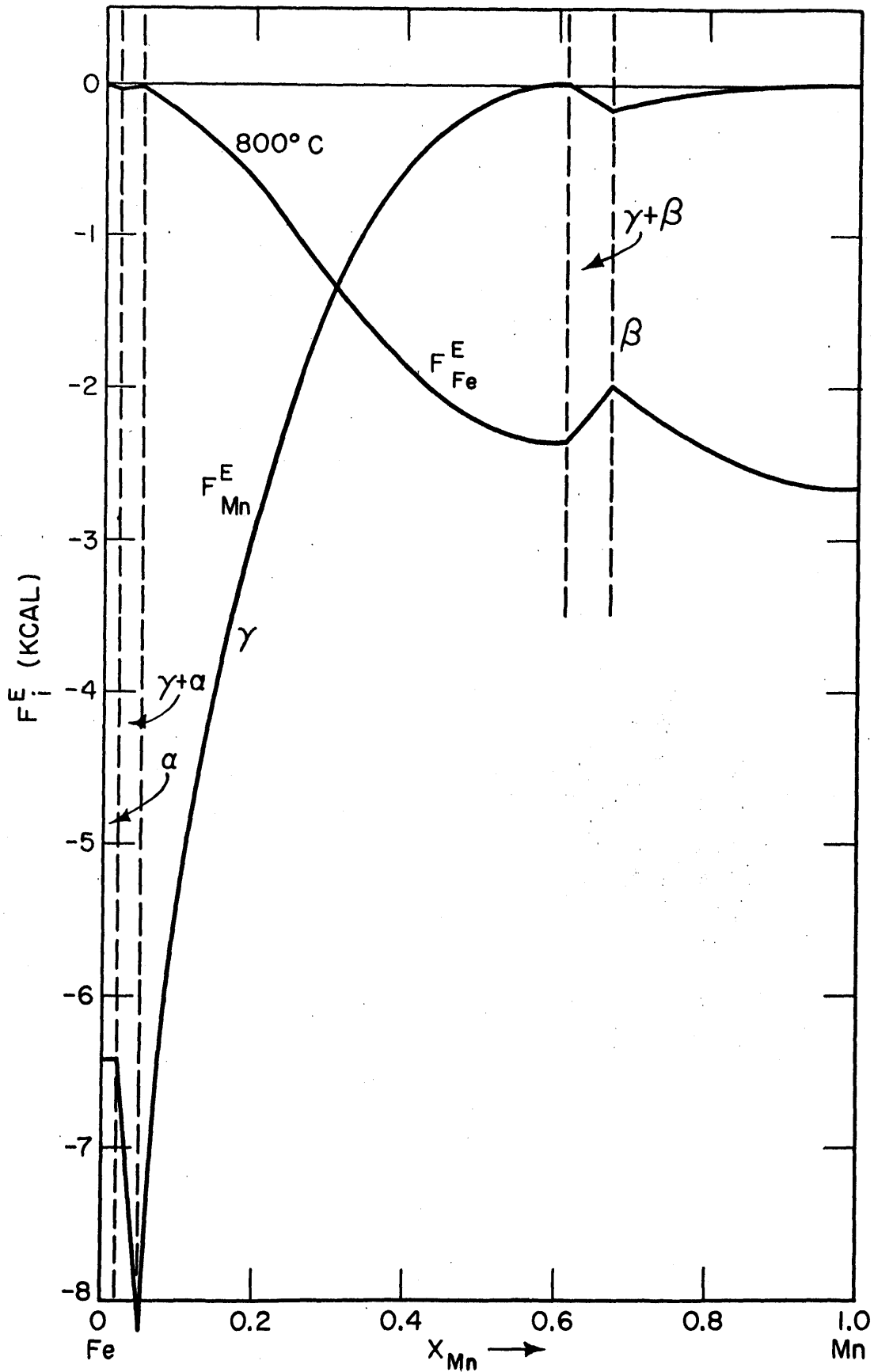


FIG. 31 THE EXCESS PARTIAL MOLAR FREE ENERGY OF MIXING OF MANGANESE AND IRON IN THE MANGANESE - IRON SYSTEM AT $800^\circ C$. (STANDARD STATE $a_{\beta_{Mn}} = 1$; $a_{\alpha_{Fe}} = 1$.)

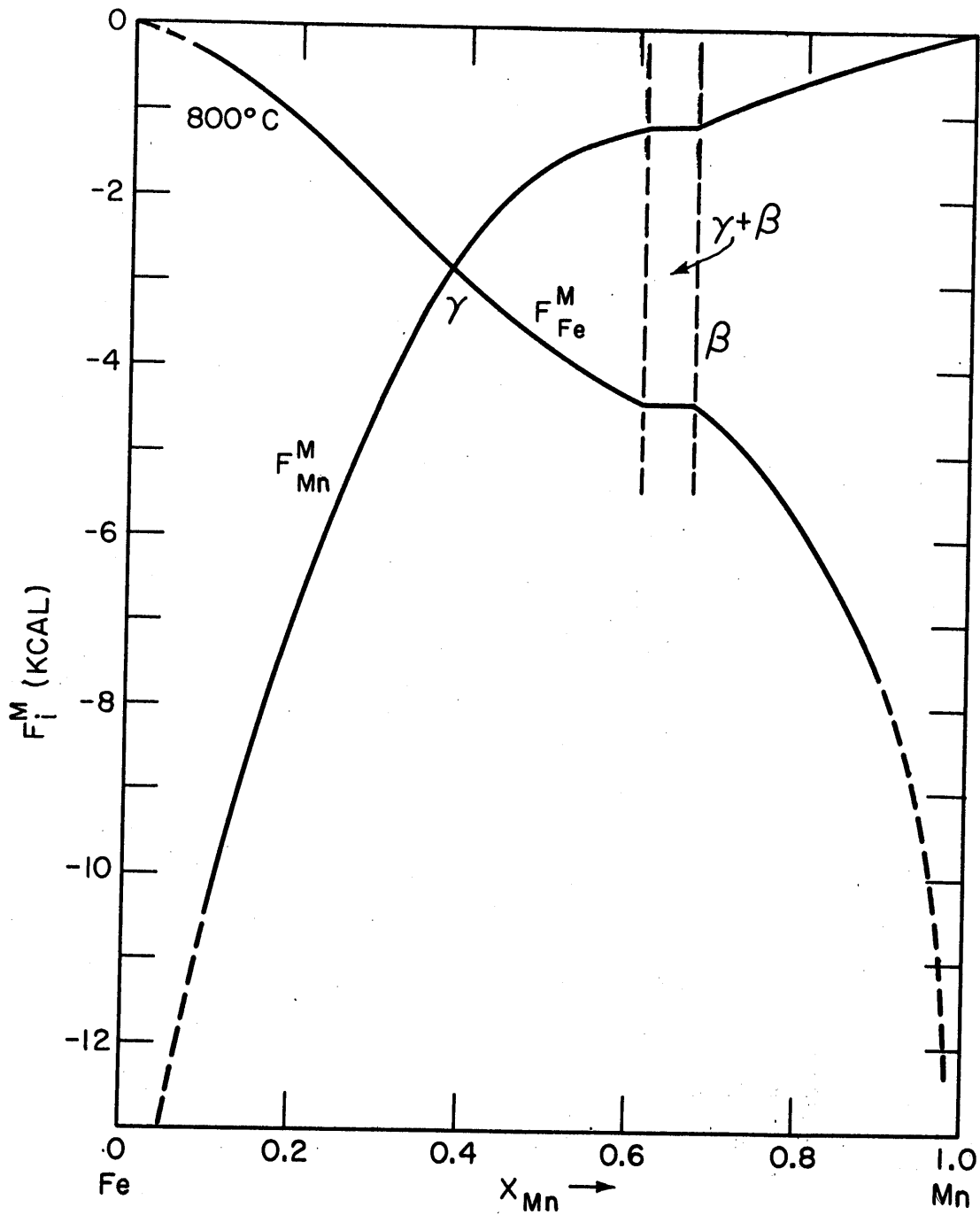


FIG. 32 THE PARTIAL MOLAR FREE ENERGIES OF MIXING OF MANGANESE AND IRON IN THE MANGANESE-IRON SYSTEM AT 800°C. (STANDARD STATE $\alpha_{\beta_{Mn}} = 1$; $\alpha_{\gamma_{Fe}} = 1$.)

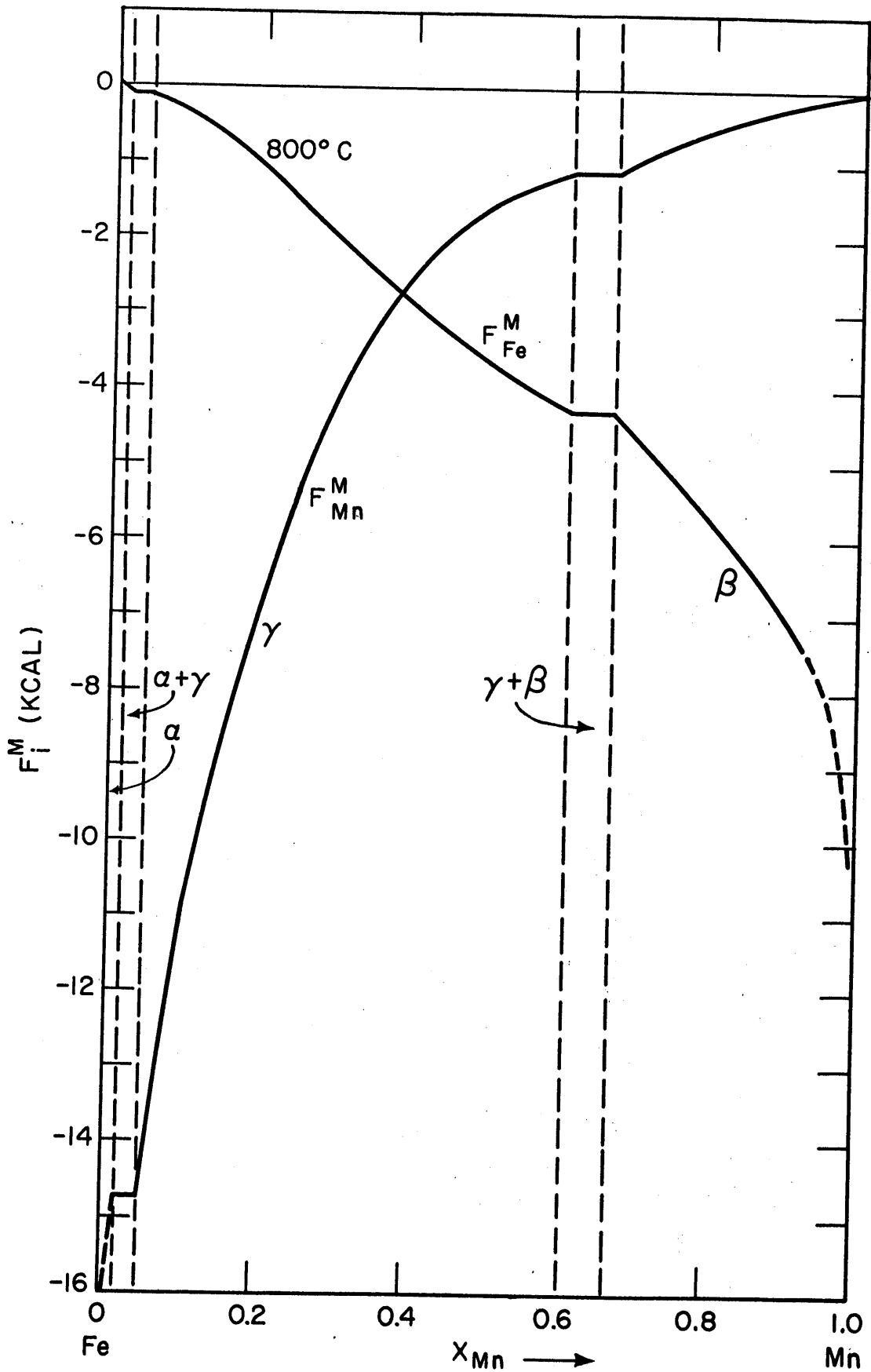


FIG. 33 THE PARTIAL MOLAR FREE ENERGY OF MIXING OF MANGANESE AND IRON IN THE MANGANESE-IRON SYSTEM AT 800°C. (STANDARD STATE: $a_{\beta_{Mn}} = 1$; $a_{\alpha_{Fe}} = 1$.)

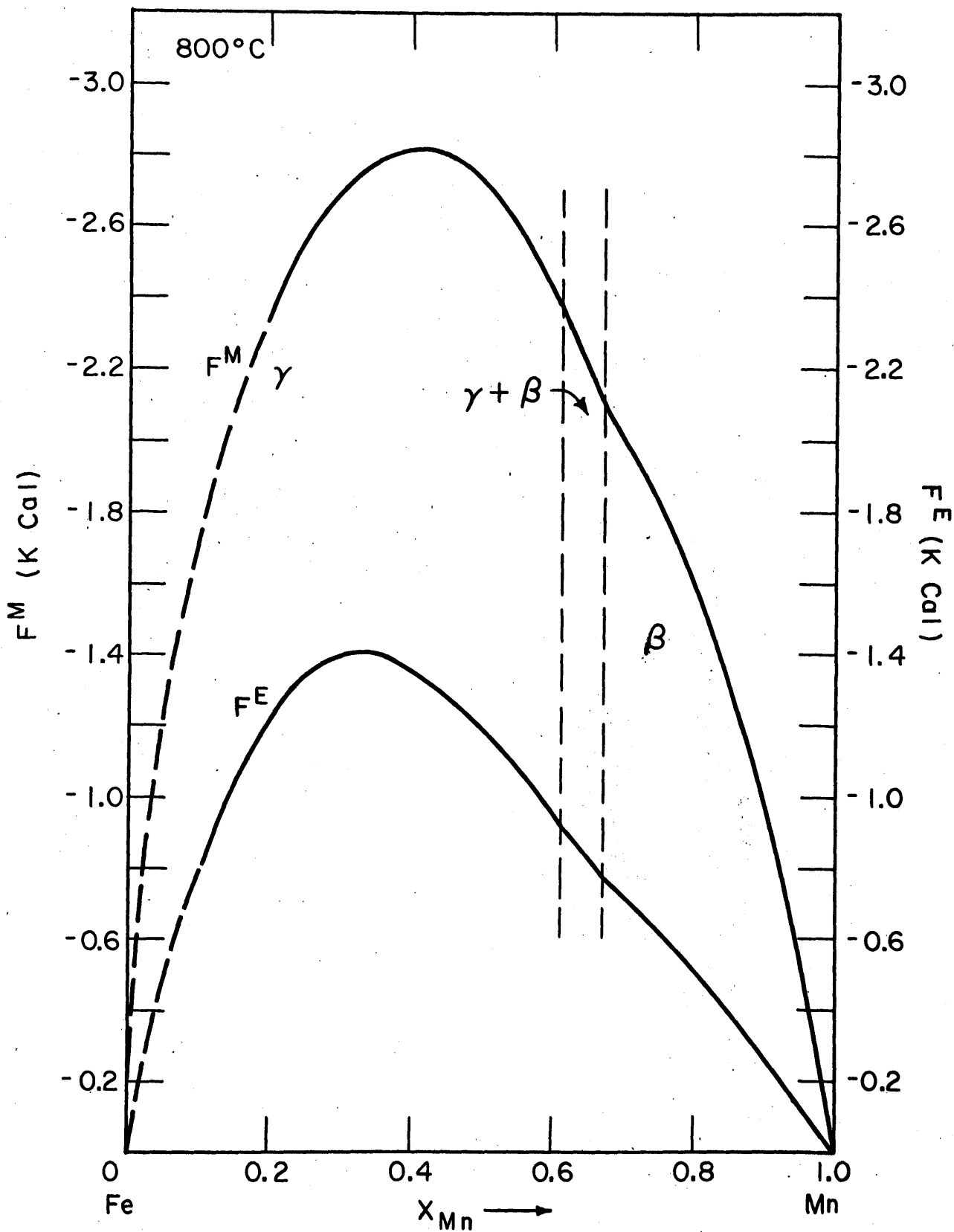


FIG. 34 THE EXCESS MOLAR FREE ENERGY OF MIXING AND THE MOLAR FREE ENERGY OF MIXING OF THE MANGANESE-IRON SYSTEM AT 800°C (STANDARD STATE: $a_{\beta Mn} = 1$, $a_{\gamma Fe} = 1$)

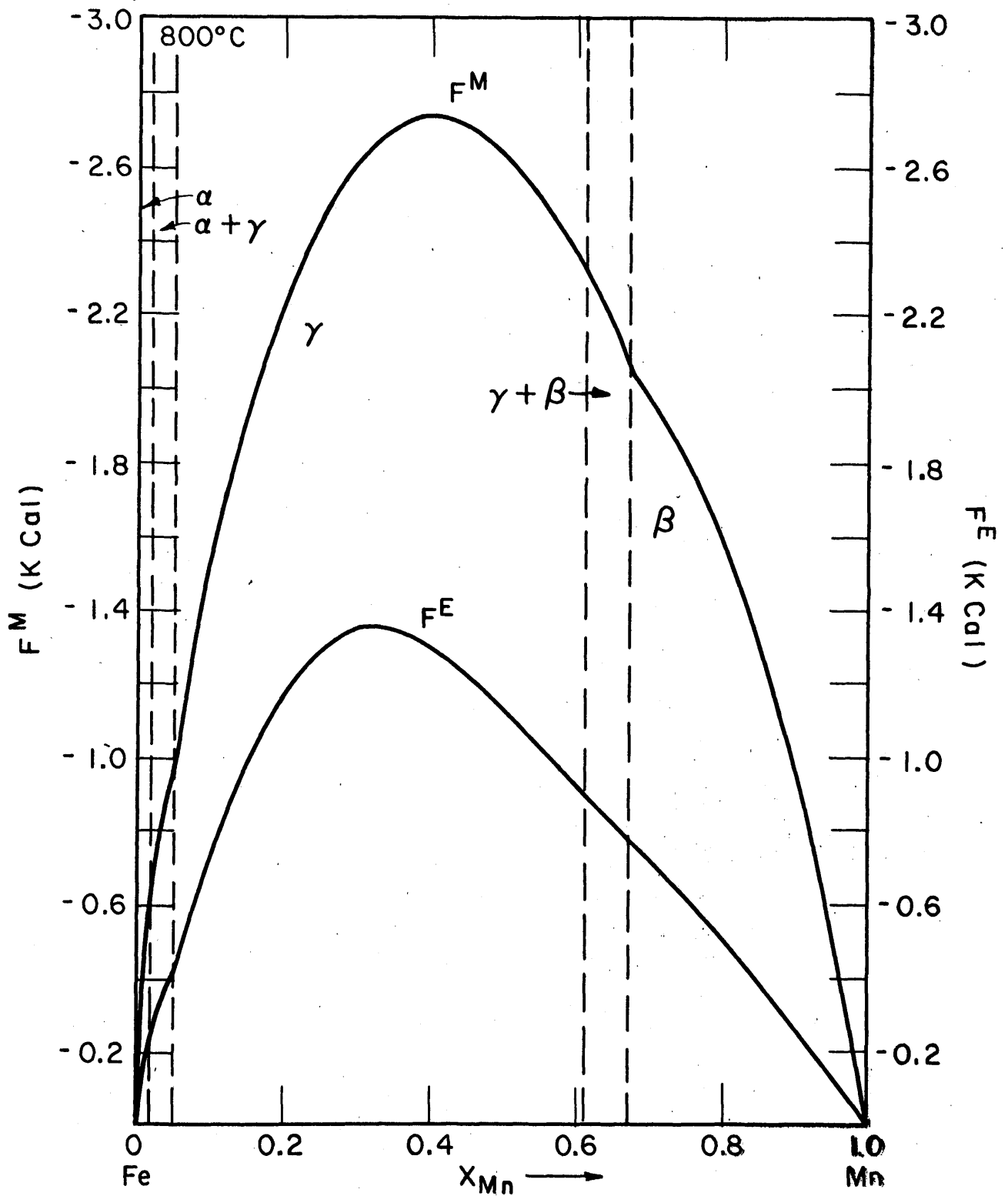


FIG. 35 THE EXCESS MOLAR FREE ENERGY OF MIXING AND THE MOLAR FREE ENERGY OF MIXING OF THE MANGANESE - IRON SYSTEM AT 800°C (STANDARD STATE: $a_{\beta_{Mn}} = 1, a_{\alpha_{Fe}} = 1$)

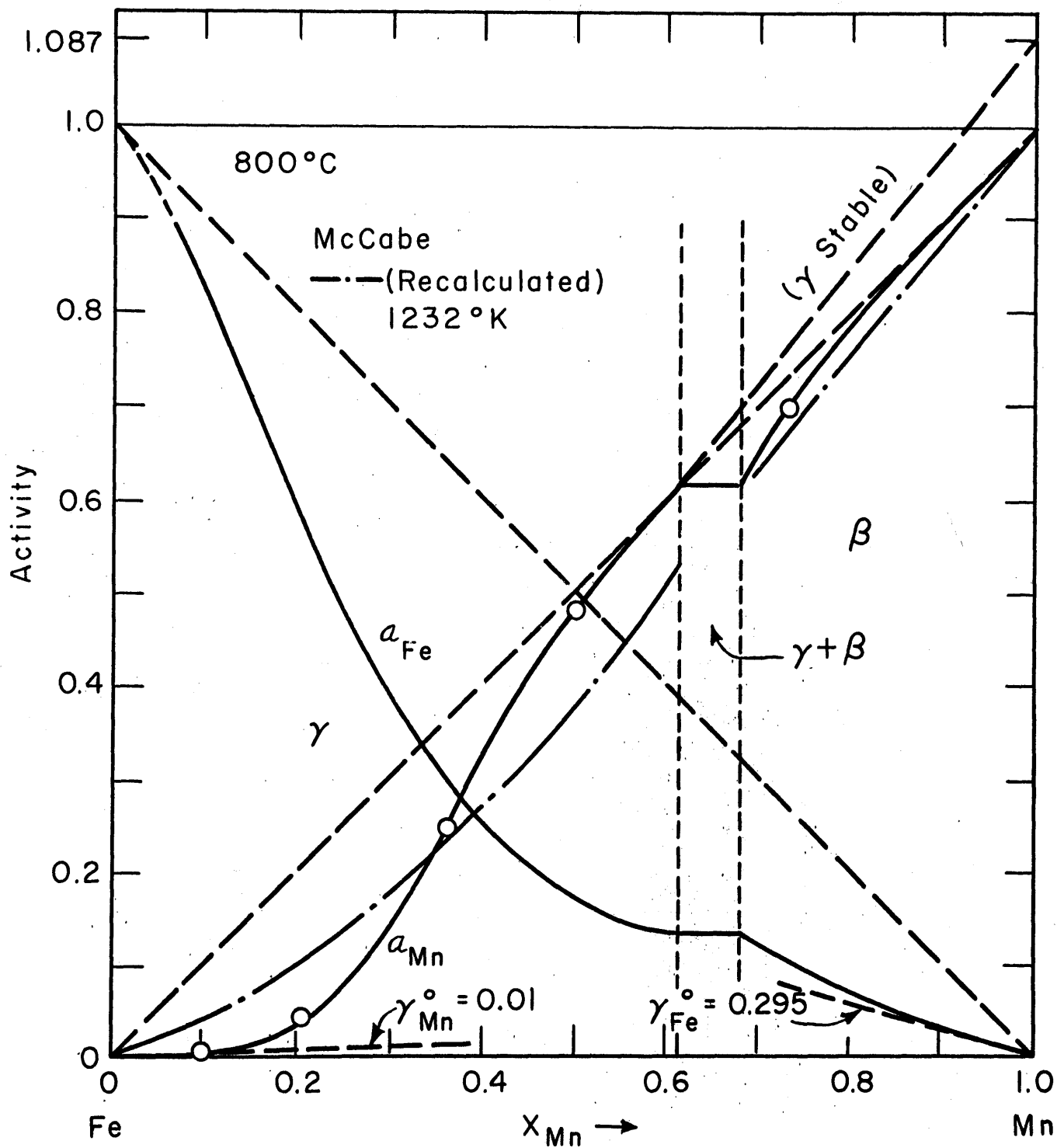


FIG. 36 THE ACTIVITY OF MANGANESE AND IRON IN THE MANGANESE-IRON SYSTEM AT 800°C. (STANDARD STATE: $a_{\beta_{Mn}} = 1$; $a_{\gamma_{Fe}} = 1$)

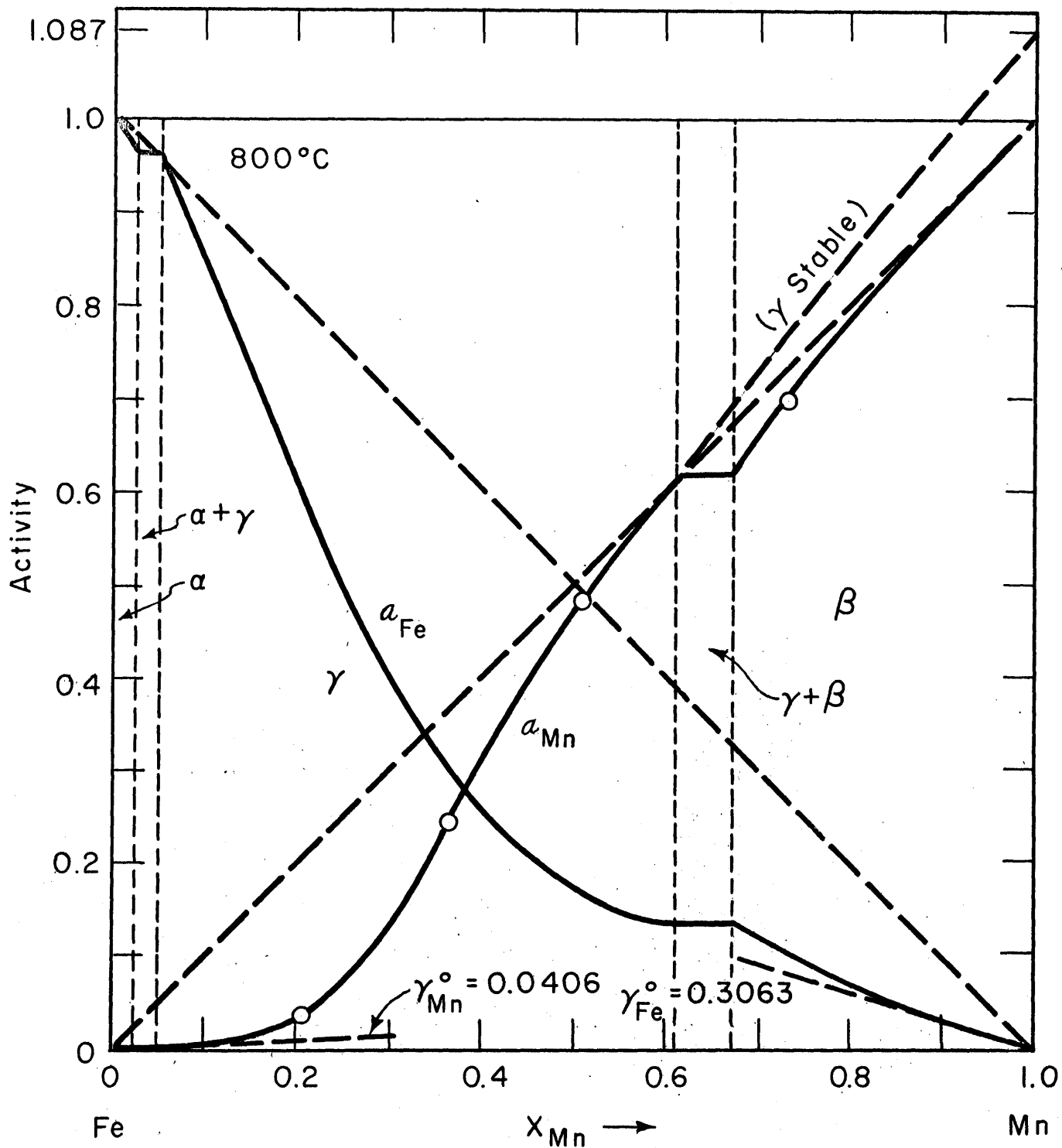


FIG. 37 THE ACTIVITY OF MANGANESE AND IRON IN MANGANESE-IRON SYSTEM AT 800°C (STANDARD STATE: $a_{\beta_{Mn}} = 1$; $a_{\alpha_{Fe}} = 1$)

The results of McCabe⁽⁷⁾ at 1232°K are shown in Figure 36. He obtained these results by a partial pressure measurement. In this determination, the vapor pressure of manganese over the solid iron-manganese alloy was measured. The Knudsen effusion method was used to measure the vapor pressure of manganese. This method has an error of approximately 5% or greater.⁽²⁾ McCabe used a standard state of γ - manganese in the region where the γ - iron manganese alloy is stable. β - manganese was used as the standard state in the region where the β iron - manganese alloy is stable. He then assumed the system followed regular solution behavior. An activity coefficient function equal to -0.95 was used to calculate the activities in the β - iron-manganese alloy region. The present study agreed very well with values in the β region. McCabe's data in the γ - iron-manganese alloy region were recalculated using the activity coefficient function of the β - region in order to obtain the activities relative to a standard state of β - manganese (as used in this study). In the γ -alloy region the comparison between the two studies was poor.

All the free energy plots showed changes of slope at the two-phase region boundaries.

Figure 26 showed that the activity of manganese was not effected to any great extent by temperature. A cell which contained solid manganese-iron electrodes welded to tungsten leads, also gave a similar result. Data from this cell are given in Appendix VII.

The activity coefficient of manganese at infinite dilution was found to be equal to 0.010 ($\gamma_{\text{Mn}}^{\circ} = 0.010$) relative to the standard state $a_{\beta_{\text{Mn}}} = 1$; $a_{\gamma_{\text{Fe}}} = 1$ and equal to 0.0406 relative to the standard state $a_{\beta_{\text{Mn}}} = 1$, $a_{\alpha_{\text{Fe}}} = 1$. The activity coefficient of iron at infinite dilution was found to be equal to 0.295 relative to the standard state $a_{\beta_{\text{Mn}}} = 1$; $a_{\gamma_{\text{Fe}}} = 1$ and equal to 0.3063 relative to the standard state $a_{\beta_{\text{Mn}}} = 1$; $a_{\alpha_{\text{Fe}}} = 1$.

VII. GENERAL DISCUSSION

The partial molar entropy of mixing for manganese in the liquid manganese-lead system was shown to be greater than ideal. This is typical of liquid metal alloys.

In the solid manganese-iron system the activity remained fairly constant with temperature. This is true in general for solid metallic systems. The liquid manganese-lead system showed a larger change in activity with temperature. This is typical behavior for liquid metal solutions.

In the manganese-iron study, the small activity coefficient of manganese at infinite dilution and the corresponding negative deviation from ideality, seem unreasonable when the chemical similarity between manganese and iron is considered. The qualitative assumption that due to their similarity, manganese and iron act ideally when in solution together, is not valid. Solutions do not always act in a simple manner as can be seen by the behavior of the iron-nickel system.

The combination electrode potential measurement and distribution measurement used in the manganese-iron study seem quite successful. This cell was shown to be reversible by the experimental criteria mentioned in the previous section on reversibility. Only 0.005 weight percent iron was found in the electrolyte after a run. This infers that the manganese-lead bath acted as an extremely effective kinetic barrier to the flow of iron from the alloy to the electrolyte. The potentials obtained in both studies were in

agreement for lead-manganese alloys of similar mole fractions. The success of this technique should enable electrode potential studies to be made on systems which do not have the extremely favorable free energies necessary for the normal electrode potential measurement. The manganese-lead bath is merely a kinetic barrier ($a_{\text{Fe[in Pb-Mn]}} \neq a_{\text{Fe[in Fe-Mn]}}$). Therefore, if the free energies of the system are very unfavorable for electrode potential measurements this technique will not work. An advantage of this technique over one which includes separate measurements of potentials and distribution ratios, is that the chemical analysis and sampling procedure are not of extreme importance.

The diffusion coefficient of a constituent in a liquid solution is much greater than that in a solid phase. In the experiment which used a solid iron-manganese alloy spot welded to a tungsten lead, the electrode potential readings were difficult to obtain with any reasonable consistency. This was due to a small amount of current flow occurring when the potentiometer was being balanced, thus causing a certain amount of metal transfer and an associated slight depletion of manganese from the surface. The flow of manganese back into the solid alloy was slow, hence the inconsistent readings. Steady potentials were obtained with the liquid manganese-lead bath acting as the electrode.

Diffusion of manganese out of the solid coil into the liquid melt was found to be much faster than diffusion of manganese out of the liquid melt back into the solid coil. This type of behavior was also observed by Fleischer. (17)

VIII. CONCLUSIONS

1. The liquid manganese-lead system showed positive deviation from ideality.
2. The solid manganese-iron system shows negative deviation from ideality.
3. The combination electrode potential measurement and distribution measurement used in the manganese-iron study was quite successful.
4. The cells used in both studies were shown to be reversible.

IX. SUGGESTIONS FOR FURTHER STUDY

The rate of solution of a constituent in a solid into a liquid metal may be followed by a technique similar to that used in the manganese-iron study.

The mechanism by which a constituent diffuses from a liquid into a solid should be investigated.

Electrode potential measurements should be attempted at higher temperatures and with more complex systems using the technique employed in the manganese-iron study.

The experimental set-up used in the manganese-iron study should be revised so that more than one alloy composition can be studied during each run.

Activities in solids should be investigated further to increase the understanding of processes such as nucleation, volume diffusion, oxidation, and the martensite transformation.

More work should be done on the solid manganese-iron system so that the validity of the negative deviation from ideality found in the present study may be assessed.

X. BIBLIOGRAPHY

1. N. W. Taylor, "The Activities of Zinc, Cadmium, Tin, Lead and Bismuth in Their Binary Liquid Mixtures," Journal Am. Chem. Soc., 45, 2865 (1923).
2. J. Chipman and J. F. Elliott, "The Thermodynamics of Liquid Metallic Solutions," Thermodynamics in Physical Metallurgy, American Society of Metals (1952).
3. C. Wagner, Thermodynamics of Alloys, Addison-Wesley Press, Inc. (1952).
4. O. Kubaschewski and E. LL. Evans, Metallurgical Thermochemistry, Pergamon Press, Ltd. (1956).
5. H. L. Harman, "The Thermodynamic Properties of the Liquid Manganese-Bismuth and Manganese-Lead Solutions," M. S. Thesis, M. I. T. (1957).
6. K. Sanbongi and M. Ohtani, "Activities of Coexisting Elements in Molten Iron-III. Activity of Manganese in Molten Iron-Manganese Alloys," Science Repts., Research Insts., Tohoku University series A, 7 204 - 9 (1955).
7. C. L. McCabe, Progress Report No. 2, "Thermodynamics of Slag and Carbide Systems," submitted to A. I. S. I. April 30, 1958.
8. L. S. Darken, "Diffusion Mobility and Their Interrelation Through Free Energy in Binary Metallic Systems," Trans. A.I.M.E., 175, 184 (1948).
9. C. Wagner, "Diffusion and High Temperature Oxidation of Metals," Atom Movements, American Society of Metals (1951).

10. J. H. Hollomon and D. Turnbull, "Nucleation," Progress in Metal Physics, 4, Pergamon Press, Ltd. (1953).
11. L. Kaufman and M. Cohen, "Martensite Transformation in the Iron-Nickel System," Trans. A.I.M.E., 206, 153 (1956).
12. C. Wagner, "The Role of Displacement Reactions in the Determination of Activities in Alloys with the Aid of Galvanic Cells," unpublished (1956).
13. C. Wagner, in Masing's Handbuch der Metallphysik, Vol. III, Part III, Leipzig (1940).
14. R. S. Williams, "Metallographische Mitteilungen des Mangans mit Zin und Blei," Z. Anorg. Chem., 55, 31 (1907).
15. M. Hanson and K. Anderko, Constitution of Binary Alloys, McGraw-Hill Publishing Company, Inc. (1958).
16. R. J. Weiss and K. J. Tauer, "Thermodynamics and Magnetic Structures of the Allotropic Modifications of Manganese," J. Phys. Chem. Solids, 4, 135 (1958).
17. B. Fleischer, "The Solubility of Iron, Nickel and Iron-Nickel Alloys in Liquid Lead (700 - 1100°C)," M. S. Thesis, M. I. T. (1956).

APPENDIX I

EXPERIMENTAL DATA OF THE MANGANESE-LEAD SYSTEM(POTENTIAL DATA)

<u>Temp. °C</u>	<u>Mole Fraction Manganese</u>							
	<u>.0141</u>	<u>.0199</u>	<u>.0402</u>	<u>.0601</u>	<u>.0801</u>	<u>.0999</u>	<u>.1198</u>	<u>.1399</u>
809.75	60.54*	43.68*	13.50*					
845.50	72.80	56.60	23.93					
855				8.150*				
893	89.93	72.40	36.95		5.080*			
908				21.75				
929.5				27.35		4.760*		
940.75	106.15	88.86	50.65		16.78			
956.25				33.90		10.490	3.270*	
959	112.60	95.25	55.70		21.30			
968.5	116.00	98.50	59.00		23.80			
975				38.84		14.96	7.25	1.45*
981.25				40.34		16.30	8.690	2.555
991				43.05		18.60	10.625	4.455
999.75				45.25		20.55	12.55	6.150

* Potentials in millivolts.

APPENDIX II

CALCULATED THERMODYNAMIC PROPERTIES OF THE MANGANESE-LEAD SYSTEM

(Figures significant to four places; extended for calculation purposes)

1. Activity of Manganese at Different Temperatures (using potential data directly)

a. a_{Mn} at 750°C (1023°K)

$$\log a_{\text{Mn}} = -9.855 \times 10^{-3} \times \xi_{\text{mv}}$$

<u>X_{Mn}</u>	<u>ξ_{mv}</u>	<u>$\log a_{\text{Mn}}$</u>	<u>a_{Mn}</u>
0.0141	40.10	-0.3952	0.4025
0.0199	24.50	-0.2415	0.5735

b. a_{Mn} at 800°C (1073°K)

$$\log a_{\text{Mn}} = -9.396 \times 10^{-3} \times \xi_{\text{mv}}$$

0.0141	57.45	-0.5398	0.2885
0.0199	41.40	-0.3889	0.4084
0.0402	10.70	-0.1005	0.7933

c. a_{Mn} at 850°C (1123°K)

0.0141	74.60	-0.6697	0.2139
0.0199	58.20	-0.5225	0.3004
0.0402	25.00	-0.2244	0.5964
0.0600	6.80	-0.0610	0.8689

d. a_{Mn} at 900°C (1173°K)

$$\log a_{\text{Mn}} = -8.595 \times 10^{-3} \times \mathcal{E}_{\text{mv}}$$

X_{Mn}	\mathcal{E}_{mv}	$\log a_{\text{Mn}}$	a_{Mn}
0.0141	91.90	-0.78989	0.1622
0.0199	75.00	-0.6446	0.2267
0.0402	39.10	-0.3361	0.4612
0.0600	19.70	-0.1693	0.6771
0.0801	6.80	-0.0584	0.8741

e. a_{Mn} at 950°C (1223°K)

$$\log a_{\text{Mn}} = -8.2437 \times 10^{-3} \mathcal{E}_{\text{mv}}$$

0.0141	109.25	-0.9006	0.1257
0.0199	91.75	-0.7564	0.1835
0.0402	53.25	-0.43898	0.3640
0.0600	32.58	-0.2686	0.5388
0.0800	19.05	-0.1570	0.6966
0.0999	9.05	-0.07461	0.8422
0.1198	2.10	-0.01731	0.9609

f. a_{Mn} at 980°C (1253°K)

$$\log a_{\text{Mn}} = -8.0462 \times 10^{-3} \times \mathcal{E}_{\text{mv}}$$

X_{Mn}	\mathcal{E}_{mv}	$\log a_{\text{Mn}}$	a_{Mn}
0.0141	119.70	-0.96314	0.1088
0.0199	101.80	-0.81911	0.1517
0.0402	62.00	-0.4989	0.3170
0.0600	40.25	-0.3239	0.4744
0.0800	26.38	-0.2123	0.6134
0.0999	16.10	-0.12954	0.7421
0.1198	8.40	-0.0676	0.8559
0.1399	2.35	-0.0189	0.9574

g. a_{Mn} at 1000°C (1273°K)

$$\log a_{\text{Mn}} = -7.9198 \times 10^{-3} \times \mathcal{E}_{\text{mv}}$$

0.0141	126.65	-0.1003	0.0993
0.0199	106.25	-0.8415	0.1441
0.0402	67.70	-0.5362	0.2910
0.0600	45.40	-0.3596	0.4370
0.0800	31.20	-0.2471	0.5661
0.0999	20.70	-0.1639	0.6849
0.1198	12.60	-0.0998	0.7946
0.1399	6.35	-0.0529	0.8853

2. Activity Coefficient Function Calculation (from potential data)
at 980°C

X_{Mn}	\mathcal{E}_{mv}	$\log a_{Mn}$	a_{Mn}	γ_{Mn}	$\log \gamma_{Mn}$	$(1-X_{Mn})^2$	$\frac{\log \gamma_{Mn}}{(1-X_{Mn})^2}$
0.0141	119.70	-0.9631	0.1088	7.716	0.8875	0.9720	0.91308
0.0199	101.80	-0.8191	0.1517	7.623	0.8821	0.9606	0.9103
0.0402	62.00	-0.4989	0.3170	7.886	0.8968	0.9212	0.9735
0.0600	40.25	-0.3239	0.4744	7.906	0.8980	0.8836	1.0163
0.0801	26.38	-0.2122	0.6134	7.668	0.8847	0.8464	1.0452
0.0999	16.10	-0.1295	0.7421	7.428	0.8709	0.8102	1.075
0.1198	8.40	-0.0676	0.8559	7.144	0.8540	0.7748	1.102
0.1399	2.35	-0.0189	0.9574	6.843	0.8353	0.7398	1.129

3. Temperature Coefficient of Potential (from emf vs. temp. plots)
at 980°C

X_{Mn}	$\frac{\partial \mathcal{E}}{\partial T} (\times 10^6 \text{ volts/}^\circ\text{C})$
0.0141	348
0.0199	336
0.0402	285.3
0.0600	257.5
0.0801	243.8
0.0999	232.6
0.1198	210.9
0.1399	200.9

4. Calculation of the Excess Partial Molar Free Energy of Mixing of Manganese (F_{Mn}^E) and the Free Energy Function of Manganese ($F_{Mn}^E/(1-X_{Mn})^2$) at 980°C

$$F_{Mn}^E = 4.576 T \log \gamma = 5.732 \times 10^3 \times \log \gamma$$

X_{Mn}	$\log \gamma_{Mn}/(1-X_{Mn})^2$ *	$F_{Mn}^E/(1-X_{Mn})^2$	F_{Mn}^E
0.000	0.860	4,929.5 cal/mole	4930 cal/mole
0.0141	0.905	5,187.9 "	5,043 "
0.0199	0.923	5,291.1 "	5,083 "
0.0402	0.974	5,583.4 "	5,143 "
0.0600	1.0138	5,811.6 "	5,135 "
0.0801	1.0460	5,996.2 "	5,075 "
0.0999	1.0749	6,162.2 "	4,992 "
0.1198	1.102	6,317.2 "	4,894 "
0.1399	1.129	6,471.9 "	4,787 "

* The value of this function is taken from the plot in Figure 14.

5. Calculation of γ_{Mn} , a_{Mn} , and the Partial Molar Free Energy of Mixing of Manganese at 980°C

X_{Mn}	$\log \gamma_{Mn}$	γ_{Mn}	a_{Mn}	$\log a_{Mn}$	$F_{Mn}^M = RT \ln a_{Mn}$
0.000	0.860	7.244	0.000	0.00	-
0.0141	0.8797	7.580	0.1069	-0.9711	-5,567 cal/mole
0.0199	0.8866	7.702	0.1533	-0.8145	-4,669 "
0.0402	0.8973	7.894	0.3173	-0.4985	-2,859 "
0.0600	0.8958	7.867	0.4720	-0.3261	-1,869 "
0.0801	0.8853	7.680	0.6152	-0.21098	-1,209 "
0.0999	0.8710	7.428	0.7421	-0.12954	- 742.6 "
0.1198	0.8538	7.141	0.8555	-0.06778	- 388.5 "
0.1399	0.8352	6.842	0.9572	-0.019	- 108.9 "

6. Calculation of the Excess Partial Molar Free Energy of Mixing of Manganese (H_{Mn}^E) (from potential data) at 980°C

$$H_{Mn}^E = - n f [\mathcal{E} - T \frac{\partial \mathcal{E}}{\partial T}]$$

X_{Mn}	$n f \mathcal{E}$	$n f T \frac{\partial \mathcal{E}}{\partial T}$	H_{Mn}^E	$H_{Mn}^E / (1-X_{Mn})^2$
0.0141	5,521	20,113	14,592 cal/mole	15,013 cal/mole
0.0199	4,696	19,419	14,723 "	15,327 "
0.0402	2,860	16,487	13,627 "	14,792 "
0.0600	1,857	14,883	13,026 "	14,742 "
0.0801	1,217	14,088	12,871 "	15,206 "
0.0999	743	13,442	12,699 "	15,674 "
0.1198	387	12,187	11,800 "	15,231 "
0.1399	108	11,614	11,506 "	15,553 "

7. Calculation of H_{Mn}^E , from the Function $H_{Mn}^E / (1-X_{Mn})^2$ vs. X_{Mn} which is Obtained from the Plot in Figure 18

X_{Mn}	$H_{Mn}^E / (1-X_{Mn})^2$	H_{Mn}^E
0.000	14,800 cal/mole	14,800 cal/mole
0.0141	15,000 "	14,579 "
0.0199	15,020 "	14,428 "
0.0402	15,100 "	13,910 "
0.0600	15,180 "	13,413 "
0.0801	15,260 "	12,916 "
0.0999	15,340 "	12,428 "
0.1198	15,420 "	11,947 "
0.1398	15,500 "	11,466 "

8. Calculation of the Excess Partial Molar Free Energy of Lead (F_{Pb}^E)

Using the Gibbs-Duhem Equation Integrated by Parts. (980°C)

$$\log \gamma_{Pb} = - \log \gamma_{Mn} / (1-X_{Mn})^2 \cdot X_{Mn} \cdot X_{Pb} + \int_{X_{Mn}=0}^{X_{Mn}} \frac{\log \gamma_{Mn}}{(1-X_{Mn})^2} dX_{Mn}$$

X_{Mn}	$\log \gamma_{Mn} / (1-X_{Mn})^2$	$X_{Mn} \cdot X_{Pb}$	(1)	(2)	$\log \gamma_{Pb}$	F_{Pb}^E
0.000	0.855	0.000	0.000	0.000	0.000	0.000
0.0141	0.905	0.0139	0.012579	0.012443	-0.000136	-0.7807 cal/mole
0.0199	0.923	0.0195	0.017999	0.017721	-0.000278	-1.591 "
0.0402	0.974	0.0386	0.037596	0.036971	-0.000625	-3.585 "
0.0600	1.014	0.0564	0.057178	0.056672	-0.000506	-2.902 "
0.0801	1.046	0.0737	0.077090	0.077385	-0.000295	1.6899 "
0.0999	1.075	0.0899	0.096638	0.098393	-0.001755	10.06 "
0.1198	1.102	0.1054	0.116151	0.120064	-0.003913	22.43 "
0.1398	1.129	0.1202	0.135706	0.144904	-0.009198	52.73 "

9. Calculation of γ_{Pb} , a_{Pb} , and the Partial Molar Free Energy of

Mixing of Lead (F_{Pb}^E) at 980°C

X_{Mn}	X_{Pb}	γ_{Pb}	a_{Pb}	$\log a_{Pb}$	$F_{Pb}^M = RT \ln a_{Pb}$
0.000	1.000	1.000	1.000	0.000	0.000
0.0141	0.9859	0.9997	0.9856	-0.0063	-36.34 cal/mole
0.0199	0.9801	0.9994	0.9742	-0.0113	-65.06 "
0.0402	0.9598	0.9986	0.9584	-0.0185	-105.76 "
0.0600	0.94	0.9988	0.9389	-0.0274	-156.96 "
0.0801	0.9199	1.0007	0.9205	-0.03598	-206.25 "
0.0999	0.9001	1.004	0.9036	-0.04398	-256.11 "
0.1198	0.8802	1.009	0.8882	-0.0515	-295.17 "
0.1399	0.8602	1.021	0.8786	-0.0562	-322.22 "

10. Calculation of the excess Partial Molar Heat of Mixing of Lead

(H_{Pb}^E) Using the Gibbs-Duhem Equation Integrated by Parts (980°C)

$$H_{Pb}^E = - \frac{H_{Mn}^E}{(1-X_{Mn})^2} X_{Mn} X_{Pb} + \int_{X_{Mn}=0}^{X_{Mn}} \frac{H_{Mn}^E}{(1-X_{Mn})^2} dX_{Mn}$$

X_{Mn}	$H_{Mn}^E / (1-X_{Mn})^2$	$X_{Mn} X_{Pb}$	(1)	(2)	H_{Pb}^E
0.000	14,800 cal/mole	0.000	0.0	0.0	0.000 cal/mole
0.0141	15,000 "	0.0139	208.5	211.1	2.5 "
0.0199	15,020 "	0.0195	292.9	298.2	5.3 "
0.0402	15,100 "	0.0386	582.9	603.9	31.0 "
0.0600	15,180 "	0.0564	856.2	903.7	47.5 "
0.0801	15,260 "	0.0737	1,124.7	1,223.1	98.4 "
0.0999	15,340 "	0.0899	1,379.1	1,512.6	133.5 "
0.1198	15,420 "	0.1054	1,625.3	1,818.8	193.5 "
0.1398	15,500 "	0.1202	1,863.1	2,128.0	264.9 "

11. Calculation of the Excess Molar Properties Using the Following Equations:

$$H^E = X_{Pb} \int_{X_{Mn=0}}^{X_{Mn}} \frac{H_{Mn}^E}{(1-X_{Mn})^2} dX_{Mn} ; \quad F^E = X_{Pb} \int_{X_{Mn=0}}^{X_{Mn}} \frac{RT \ln \gamma_{Mn}}{(1-X_{Mn})^2} dX_{Mn}$$

X_{Mn}	H^E	F^E	$TS^E = H^E - F^E$
0.000	0.0 cal/mole	0.0 cal/mole	0.0 cal/mole
0.0141	208.1 "	70.33 "	137.8 "
0.0199	292.3 "	99.56 "	192.7 "
0.0402	579.6 "	203.4 "	376.2 "
0.0600	849.5 "	305.4 "	544.1 "
0.0801	1,125.1 "	408.1 "	717.1 "
0.0999	1,361.5 "	507.7 "	853.8 "
0.1198	1,600.9 "	605.8 "	995.1 "
0.1399	1,830.5 "	714.5 "	1,116.0 "

12. Calculation of the Molar Properties Using the Relationships:

$$H^M = \sum_1^i X_i H_i^M ; \quad F^M = \sum_1^i X_i F_i^M ; \quad TS^M = H^M - F^M$$

X_{Mn}	H^M	F^M	TS^M
0.000	0.0 cal/mole	0.0 cal/mole	0.0 cal/mole
0.0141	208.1 "	-114.3 "	322.4 "
0.0199	292.3 "	-156.7 "	449.0 "
0.0402	579.6 "	-216.4 "	796.0 "
0.0600	849.5 "	-259.7 "	1,109.2 "
0.0801	1,125.0 "	-286.6 "	1,411.6 "
0.0999	1,361.5 "	-301.1 "	1,662.6 "
0.1198	1,600.9 "	-306.3 "	1,907.2 "
0.1399	1,830.5 "	-292.4 "	2,122.9 "

13. Estimation of Liquidus Line - Temperature and Composition Where
 $a_{Mn} = 1$; from Intersections of Potential vs. Temperature Plots
with Zero Potential Axis

<u>X_{Mn}</u>	<u>Temp. °C</u>
0.014	635
0.02	676.2
0.04	762.5
0.06	823.5
0.08	871.75
0.10	911
0.12	940
0.14	974.5

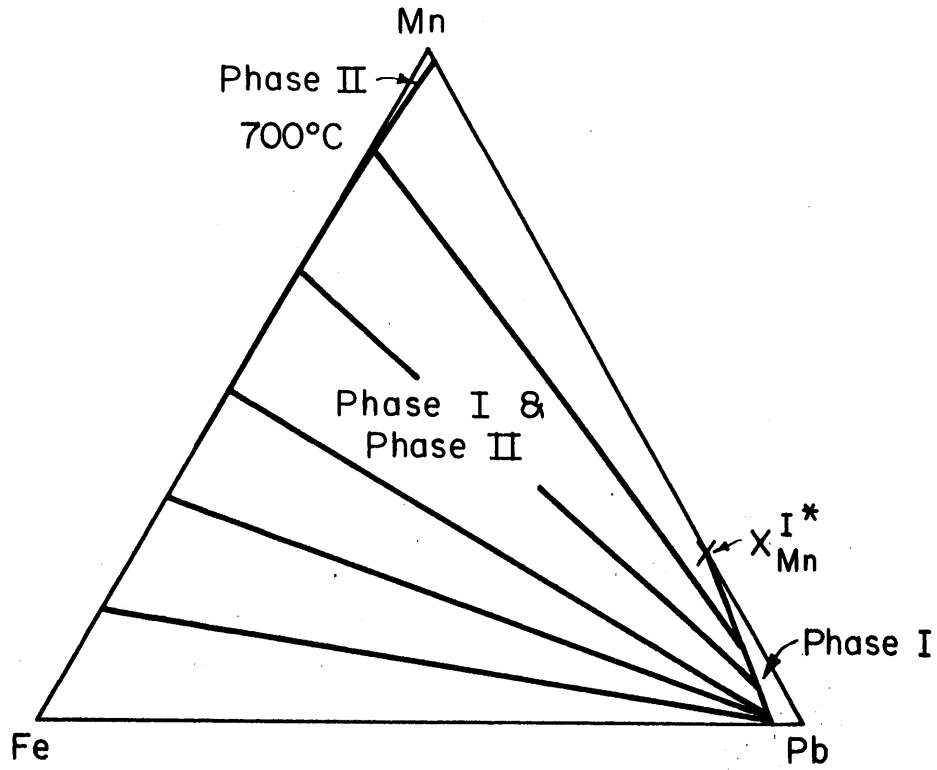


FIG. 38 SCHEMATIC MANGANESE-IRON-LEAD
TERNARY PHASE DIAGRAM FOR 700°C

APPENDIX III

CALCULATION OF AMOUNT AND COMPOSITION OF THE MANGANESE-LEAD

BATH CHARGE (MANGANESE-IRON STUDY) *

γ_{Mn}^I = activity coefficient of manganese in phase I (Pb-Mn)

γ_{Mn}^{II} = activity coefficient of manganese in phase II (Fe-Mn)

X_{Mn}^I = saturation composition of manganese at 700°C in Pb-Mn alloy
= 0.025 (from Mn-Pb study)

$$a_{Mn} = X_{Mn}^{II} \times \gamma_{Mn}^{II}$$

Assuming Henry's Law for Mn

$$a_{Mn} = \frac{X_{Mn}^I}{X_{Mn}^I} = X_{Mn}^{II} \cdot \gamma_{Mn}^{II} \quad (\text{activity same across tie line})$$

$$\therefore X_{Mn}^I = X_{Mn}^{II} \cdot \gamma_{Mn}^{II} \cdot X_{Mn}^I$$

Assume $\gamma_{Mn}^{II} = 0.8$ for a manganese iron alloy of 39 atomic percent

Mn ($X_{Mn}^{II} = 0.390$)

$$\therefore X_{Mn}^I = 0.390 \times 0.025 \times 0.8 = 0.0078$$

Volume of Pb necessary to cover coil

$$\begin{aligned} \pi r^2 h &= 3.14 \times 1^2 \times .75 \\ &= 2.35 \text{ in}^3 \end{aligned}$$

r = radius of crucible in inches
h = height necessary for Pb to
cover Fe-Mn coil (+)

* See Figure 38.

$$D = \frac{w}{V} = 10.645 = \frac{w}{(2.35)(2.54)^3}$$

$$w = 410 \text{ gms}$$

D = density of liquid Pb g/cm³

w = weight of Pb necessary
to cover coil and allow
sampling (gms)

Charge approximately 400 gms Pb.

How much Mn charged:-

$$X_{\text{Mn}} = 0.0078 = \frac{\frac{X}{54.93}}{\frac{400}{207.22} + \frac{X}{54.93}}$$

X = wt. of Mn in grams

$$X = 0.89 \text{ gms}$$

Charge approximately 0.5 grams in order to insure diffusion taking
place out of coil.

APPENDIX IV

CALCULATION OF THE FINAL COMPOSITION OF MANGANESE-IRON

ALLOY AFTER DIFFUSION

<u>Initial Fe-Mn Alloy</u>	<u>Initial Charge</u>
Wt. Fe - Mn = 15.7486 gms	Wt. Mn = 0.4700 gms
Wt.% Mn = 38.7 %	Wt. Pb = 400.1254 gms
Wt.% Fe = 61.3 %	Total Wt. = 400.5954 gms

1. At 705°C

CHEMICAL ANALYSIS OF Pb-Mn BATH

$$\text{Wt.\% Mn} = 0.183 \%$$

$$\text{Wt.\% Fe} = 0.011 \%$$

let X = the total wt. of Mn that has diffused out of the Mn-Fe alloy

$$\text{Wt.\% Mn} = 0.183 = \frac{X + 0.4700}{X + 400.6395}$$

Assumption:-

$$\text{Wt.\% Fe diffused} =$$

$$\frac{0.011}{100} \times 400.8954$$

$$= 0.0441 \text{ gms}$$

$$X = 0.26365$$

$$\text{Wt. Mn in coil} = 15.7486 \times 0.387 = 6.0947 \text{ gms}$$

$$\text{Wt. Mn in coil after diffusion} = 6.0947 - 0.2636 = 5.8311 \text{ gms}$$

$$\text{Wt. Fe in coil after diffusion} = 9.6539 - 0.0441 = 9.6098 \text{ gms}$$

$$\text{Wt.\% Mn in coil after diffusion} = 37.76\%$$

2. At 756.22°C

CHEMICAL ANALYSIS OF Pb-Mn BATH

$$\text{Wt.}\% \text{ Mn} = 0.215 \%$$

$$\text{Wt.}\% \text{ Fe} = 0.009 \%$$

$$\text{Wt.}\% \text{ Mn} = 0.215 = \frac{X + 0.4700}{X + 395.7911} \times 100 \quad \text{Total wt. bath(after sampling) = 395.7911}$$

$$X = 0.38177 \text{ gms Mn}$$

$$\begin{aligned} \text{Wt.}\% \text{ Mn in coil after diffusion} &= \frac{6.0947 - 0.38177}{(6.0947 - 0.38177) + 9.6098} \\ &= 37.284\% \end{aligned}$$

Similar calculations are made at subsequent temperatures.

APPENDIX V

EXPERIMENTAL DATA OF THE MANGANESE-IRON SYSTEM

<u>Alloy I(Coil)</u>	<u>Alloy II(Coil)</u>	<u>Alloy III(Coil)</u>	<u>Alloy IV(Powder)</u>
20.8 wt.%Mn	38.7 wt.% Mn	56.9 wt.% Mn	79.1 wt.% Mn
0.067 wt.%Si	0.25 wt.% Si	0.13 wt.% Si	0.036 wt.% Si
0.030 wt.%Al	0.030 wt.% Al		

<u>Initial Alloy</u>	<u>Temp. (°C)</u>	<u>Composition of Pb-Mn Bath (After Diffusion)</u>	<u>X_{Mn} in Fe-Mn (After Diffusion)</u>	<u>Potential (mv)</u>
I	752.66	0.032 Mn; 0.010 Fe*	0.2109	142.47
I	806.0	0.047 Mn; 0.008 Fe*	0.2074	147.40
I	849.99	0.058 Mn; 0.007 Fe*	0.2049	161.70
II	756.22	0.215 Mn; 0.009 Fe*	0.3766	60.23
II	807.0	0.282 Mn; 0.008 Fe*	0.3659	64.81
II	854.5	0.380 Mn; 0.008 Fe*	0.3497	69.69
III	758.25	0.0175‡	0.5348	32.89
III	806.25	0.0245‡	0.5079	33.75
III	857.50	0.0325‡	0.4738	37.05
IV	752.67	0.02575‡	0.7636	13.25
IV	801.25	0.0350 ‡	0.7024	16.35
IV	851.0	0.0450 ‡	0.6945	19.59

* Weight percent as determined by chemical analysis.

‡ Mole fraction manganese as determined from corresponding potentials of the lead-manganese study (chemical analyses of samples were not consistent).

APPENDIX VI

CALCULATED THERMODYNAMIC FUNCTIONS OF THE MANGANESE-IRON
SYSTEM (FIGURES SIGNIFICANT TO FOUR PLACES; EXTENDED FOR
CALCULATION PURPOSES)

1. Calculation of the Activity Coefficient Function of Manganese
in the Temperature Range 750° - 850°C

X_{Mn}	a_{Mn}	Temp. (°C)	γ_{Mn}	$\log \gamma_{Mn}$	$(1-X_{Mn})^2$	$\frac{\log \gamma_{Mn}}{(1-X_{Mn})^2}$
0.2049	0.0353	849.88	0.1724	-0.76346	0.6322	-.12076
0.2074	0.04195	806	0.2023	-0.694	0.6282	-1.1047
0.2109	0.03977	752	0.1886	-0.72446	0.6227	-1.1634
0.3497	0.2380	854	0.6806	-0.16711	0.4229	-0.3952
0.3659	0.2483	807	0.6786	-0.16839	0.4021	-0.4187
0.3766	0.2571	756.22	0.6827	-0.16577	0.3886	-0.4266
0.4738	0.4673	857.5	0.9863	-0.00599	0.2768	-0.0216
0.5079	0.4838	806.25	0.9525	-0.02114	0.2422	-0.0873
0.5348	0.4769	758.25	0.8917	-0.14978	0.2164	-0.2300
0.6945	0.6672	851	0.9607	-0.01741	0.0933	-0.1866
0.7350	0.7024	801.25	0.9556	-0.01972	0.0702	-0.2809
0.7636	0.7409	752.67	0.9703	-0.01309	0.0559	-0.2342

2. Calculation of the Activity Coefficient Function of Manganese from Plot of $\log \gamma_{Mn}$ vs. X_{Mn} (for two phase region boundary) 800°C

X_{Mn}	$\log \gamma_{Mn}$	γ_{Mn}	a_{Mn}	$\log \gamma_{Mn}/(1-X_{Mn})^2$
0.61	+ 0.001	1.002	0.611	+ 0.0006
0.64	- 0.020	0.955	0.611	- 0.154
0.67	- 0.040	0.9122	0.611	- 0.368

3. Calculation of the Activity Coefficient Function of Manganese from Plot of a_{Mn} vs. X_{Mn} (800°C)

X_{Mn}	a_{Mn}	γ_{Mn}	$\log \gamma_{Mn}$	$\log \gamma_{Mn}/(1-X_{Mn})^2$
0.70	0.650	0.9286	-0.03217	-0.3574
0.80	0.789	0.9863	-0.0059	-0.1496
0.90	0.899	0.9998	-0.00052	-0.052

4. Calculation of Activity Coefficient Function of Manganese when ($\alpha + \gamma$) Region is Taken into Account (800°C)

X_{Mn}	$\log \gamma_{Mn}/(1-X_{Mn})^2$	$\log \gamma_{Mn}$	γ_{Mn}	a_{Mn}
0.02	-1.301	- 1.301	0.05	0.001
0.05	-1.79	- 1.70	0.02	0.001

5. Calculation of the Activity, Activity Coefficient, and Activity Coefficient Function of Manganese at 800°C (standard state $a_{\beta_{\text{Mn}}} = 1$; $a_{\gamma_{\text{Fe}}} = 1$)

X_{Mn}	a_{Mn}	γ_{Mn}	$\log \gamma_{\text{Mn}}$	$(1-X_{\text{Mn}})^2$	$\log \gamma / (1-X_{\text{Mn}})^2$
0.000	0.000	0.0100	-2.000	0.1	-2.000
0.1000	0.00627	0.0627	-1.203	0.81	-1.485
0.2074	0.04195	0.2023	-0.694	0.6282	-1.1047
0.3659	0.2483	0.6786	-0.16839	0.4021	-0.4187
0.5079	0.4838	0.9525	-0.02114	0.2422	-0.0873
0.6000	0.6000	1.000	-0.000	0.16	0.00
0.7350	0.7024	0.9556	-0.01972	0.0702	-0.2809
0.8000	0.7878	0.9847	-0.0068	0.04	-0.170
0.9000	0.899	0.9988	-0.00052	0.01	-0.052
1.000	1.000	1.000	0.000	0.000	0.000

6. Calculation of the Excess Partial Molar Free Energy of Mixing of Manganese, the Partial Molar Free Energy of Mixing of Manganese and the Free Energy Function of Manganese at 800°C (standard state $a_{\beta_{\text{Mn}}} = 1$; $a_{\gamma_{\text{Fe}}} = 1$)

X_{Mn}	F_{Mn}^E (cal/mole)	$F_{\text{Mn}}^E / (1-X_{\text{Mn}})^2$	$\log a_{\text{Mn}}$	F_{Mn}^M
0.000	-9,820 cal/mole	-9,820 cal/mole	$-\infty$	$-\infty$ cal/mole
0.1000	-5,901 "	-7,291 "	-2.203	-10,813 "
0.2074	-3,401 "	-5,423 "	-1.377	-6,761 "
0.3659	-826.6 "	-2,056 "	-0.605	-2,969 "
0.5079	-103.8 "	-428.4 "	-0.314	-1,578 "
0.6000	0.00 "	0.00 "	-0.228	-1,120 "
0.7350	-96.80 "	-1,379 "	-0.153	-753.0 "
0.8000	-33.38 "	-834.25 "	-0.1036	-508.5 "
0.9000	-2.55 "	-255.0 "	-0.0462	-227.0 "
1.000	0.00 "	0.00 "	0.00	0.00 "

7. Calculation of the Activity Coefficient of Iron at 800°C Using the Gibbs-Duhem Equation and Figure 28 (standard state $a_{\text{Pb}} = 1$;

$$\log \gamma_{\text{Fe}} = -\log \gamma_{\text{Mn}} / (1 - X_{\text{Mn}})^2 X_{\text{Pb}} \cdot X_{\text{Mn}} + \int_{X_{\text{Mn}}=0}^{X_{\text{Mn}}} \log \gamma_{\text{Mn}} / (1 - X_{\text{Mn}})^2 dX_{\text{Mn}}$$

X_{Mn}	$\log \gamma / (1 - X_{\text{Mn}})^2$	$X_{\text{Mn}} \cdot X_{\text{Fe}}$	①	②	$\log \gamma_{\text{Fe}}$
0.000	-2.000	0.0	0.0	0.0	0.0
0.1000	-1.1047	0.09	-0.13370	-0.17425	-0.04055
0.2074	-1.1047	0.1644	-0.18161	-0.32195	-0.14034
0.3659	-0.4187	0.2320	-0.09714	-0.44249	-0.3535
0.5079	-0.0873	0.2499	-0.02182	-0.47633	-0.45451
0.6000	0.00	0.24	0.000	-0.47893	-0.47893
0.7350	-0.2809	0.1948	-0.05472	-0.50853	-0.45381
0.800	-0.170	0.16	-0.0272	-0.52293	-0.49573
0.900	-0.052	0.09	-0.00468	-0.52993	-0.52525
1.000	0.0	0.0	0.000	-0.53015	-0.53015

8. Calculation of γ_{Fe} , a_{Fe} , F_{Fe}^{E} and F_{Fe}^{M} at 800°C (standard state

$$a_{\text{Pb}} = 1; a_{\text{Fe}} = 1)$$

X_{Fe}	γ_{Fe}	F_{Fe}^{E}	a_{Fe}	$\log a_{\text{Fe}}$	F_{Fe}^{M}
1.0	0.1	0.0 cal/mole	0.1	0.0	0.0 cal/mole
0.9	0.9109	-199.0	0.8198	-0.0863	-423.6
0.7926	0.7239	-688.9	0.5738	-0.2413	-1,184
0.6341	0.4515	-1,695	0.2863	-0.5432	-2,666.6
0.4921	0.3339	-2,231	0.1643	-0.78436	-3,850
0.4000	0.3319	-2,351	0.1328	-0.8767	-4,304
0.2650	0.3517	-2,228	0.0932	-1.031	-5,059
0.200	0.3194	-2,434	0.0639	-1.1945	-5,863
0.100	0.2952	-2,578	0.0295	-1.5302	-7,512
0.000	0.2950	-2,603	0.000	$-\infty$	$-\infty$

9. Calculation of the Excess Molar Free Energy of Mixing and the Molar Free Energy of Mixing at 800°C (standard state $a_{\beta, \text{Mn}} = 1$;

$$a_{\text{Fe}} = 1)$$

$$F^E = X_{\text{Fe}} \int_{X_{\text{Mn}}=0}^{X_{\text{Mn}}} RT \log \gamma_{\text{Mn}} / (1 - X_{\text{Mn}})^2 dX_{\text{Mn}}; \quad F^M = \sum_i X_i F_i^M$$

X_{Mn}	X_{Fe}	2	F^E	$X_{\text{Fe}} \cdot F_{\text{Fe}}^M$	$X_{\text{Mn}} \cdot F_{\text{Mn}}^M$	F^M
0.000	1.000	0.0	0.0 cal	0.0	0.0	0.0 cal
0.1000	0.90	-0.17425	- 769.9 "	- 381	-1,081	-1,463 "
0.2074	0.7926	-0.32195	-1,253 "	- 938	-1,402	-2,341 "
0.3659	0.6341	-0.44249	-1,377 "	-1,691	-1,086.7	-2,778 "
0.5079	0.4921	-0.47633	-1,1507 "	-1,910	- 786.1	-2,696 "
0.6000	0.400	-0.47893	- 940 "	-1,722	- 671.98	-2,394 "
0.7350	0.265	-0.50853	- 661.5 "	-1,341	- 553.5	-1,894 "
0.800	0.200	-0.52293	- 513.4 "	-1,173	- 406.8	-1,579.6 "
0.900	0.100	-0.52993	- 260.1	- 751.2	- 204.3	- 955.5 "
1.00	0.000	-0.53015	0.0	0.0	0.0	0.0

10. Calculation of γ_{Fe} , F_{Fe}^E , a_{Fe} , F_{Fe}^M (for standard state $a_{\beta_{Mn}} = 1$; $a_{\alpha_{Fe}} = 1$) at 800°C (from integrated area difference Figures 28 and 29)

$$\log \gamma_{Fe} (a_{\beta_{Mn}} = 1; a_{\alpha_{Fe}} = 1) = \log \gamma_{Fe} (a_{\beta_{Mn}} = 1; a_{\gamma_{Fe}} = 1) - 0.0136$$

X_{Mn}	$\log \gamma_{Fe}$	F_{Fe}^E	a_{Fe}	$\log a_{Fe}$	F_{Fe}^M	γ_{Fe}
0.000	0.0	0.0	0.0	0.0	0.0	0.1
0.1000	-0.02695	- 132.3	0.8458	-0.0727	- 357.0	0.9398
0.2074	-0.12674	- 622.2	0.5920	-0.22768	-1,118	0.7469
0.3659	-0.33175	-1,628.6	0.2954	-0.52959	-2,599.7	0.4659
0.5079	-0.44091	-2,164.4	0.1783	-0.74885	-3,676	0.3623
0.6000	-0.46533	-2,284.3	0.1370	-0.86328	-4,238	0.3425
0.7350	-0.44021	-2,161	0.0962	-1.0168	-4,992	0.3629
0.800	-0.48213	-2,367	0.0659	-1.1811	-5,798	0.3295
0.900	-0.51165	-2,512	0.0308	-1.5115	-7,420	0.3079
1.000	-0.51385	-2,523	0.000	$-\infty$	$-\infty$	0.3063

11. Calculation of the Excess Molar Free Energy of Mixing and the Molar Free Energy of Mixing at 800°C (standard state $a_{\beta, \text{Mn}} = 1$;

$$F^E = X_{\text{Fe}} \int_{X_{\text{Mn}}=0}^{X_{\text{Mn}}} RT \log \gamma_{\text{Mn}} / (1-X_{\text{Mn}})^2 dX_{\text{Mn}} \quad (2)$$

X_{Mn}	X_{Fe}	(2)	F^E cal/mole	$X_{\text{Fe}} \cdot F_{\text{Fe}}^M$ cal/mole	$X_{\text{Mn}} \cdot F_{\text{Mn}}^M$ cal/mole	F^M
0.0	1.0	0.0	0.0	0.0	0.0	0
0.1000	0.9	-0.16065	- 709.8	- 321.3	-1,081	-1,403
0.2074	0.7926	-0.30835	-1,199.7	- 885.4	-1,402	-2,288
0.3659	0.6341	-0.42889	-1,335	-1,649	-1,087	-2,735
0.5079	0.4921	-0.46273	-1,118	-1,809	- 786.1	-2,595
0.6000	0.4000	-0.46533	- 913.7	-1,695	- 671.98	-2,367
0.7350	0.2650	-0.49493	- 643.8	-1,323	- 553.5	-1,876
0.800	0.200	-0.50933	- 500.1	-1,160	- 406.8	-1,566
0.900	0.100	-0.51633	- 253.5	742	- 204.3	- 946
1.000	0.00	-	0.0	0.0	0.0	0

APPENDIX VII

DATA AND CALCULATED ACTIVITIES FROM THE SOLID ELECTRODE CELL

<u>Composition Alloy (Wt. % Mn)</u>	<u>Temp. °C</u>	<u>Potential (mv)</u>	<u>a_{Mn}</u>
20.6*	752	138.45	0.0438
20.6	805	142	0.0464
20.6	840	144.05	0.050
38.5*	752	75.9	0.1795
38.5	805	83.32	0.171
38.5	840	84.66	0.1715
59.83‡	752	21.39	0.617
59.83	805	23.10	0.610
59.83	840	23.68	0.611
82.50‡	752	13.70	0.734
82.50	805	13.30	0.750
82.50	840	12.05	0.779

* Coil Composition Analyzed by Chemical Analyses.

‡ Casting Composition Calculated from Weights Charged.